Fakultät für Medizin

Klinik und Poliklinik für Innere Medizin III

Tumor immunosurveiliance: Innate immune activation as a mechanistic prerequisite for efficient immune checkpoint blockade in cancer immunotherapy

Alexander F. G. Wintges

Vollständiger Abdruck der von der Fakultät für Medizin der Technischen Universität München zur Erlangung des akademischen Grades eines

Doktors der Naturwissenschaften (Dr. rer. nat.)

genehmigten Dissertation.

Vorsitzender: Prof. Dr. Percy A. Knolle

Prüfer der Dissertation:

1. Prof. Dr. Christian Peschel

2. Prof. Dr. Dirk Haller

Die Dissertation wurde am 25.04.2018 bei der Fakultät für Medizin der Technischen Universität München eingereicht und durch die Fakultät für Medizin am 11.10.2018 angenommen.

Dedicated to Laura and Paul

Index

1 Introduction

1.1 Malignant melanoma

1.1.1 Manifestation of malignant melanoma

The skin is the human body's largest organ and represents the first barrier for pathogens, noxious substances and other infectious agents that contact and invade our body. It is, furthermore, a shield against heat, injury and radiation and consists of various layers. The upper layer, the so called epidermis, that consists of squamous cells, basal cells and melanocytes, is the site where malignant alterations occur and skin cancer develops (Bleyer, 2002).

In contrast to more frequent skin cancer entities such as basal and squamous cell carcinomas, which in the majority of cases do not spread to distant organs, the rarer malignant melanoma is capable of invading nearby tissues and further metastasizing. Its formation is not exclusively restricted to the skin but can also rarely occur in mucosal tissues, the intestine or the eye (McGuire, 2016). Apart from genetic risk factors, the principal non-genetic risk factor is exposure to ultraviolet radiation. That, however, can be either beneficial as non-burning sun light exposure is associated with a reduced risk for melanoma or detrimental as sunburn doubles the risk of developing a malignant disease (Gandini et al., 2005).

In the last 30 years, the incidence rate of metastasized malignant melanoma has tripled thus contributing to the majority of skin cancer-related deaths (Aamdal, 2011). It is a highly aggressive and metastatic form of cancer and has been defined as a heterogeneous disease. Tumor growth commences in the lowest epidermis layer and is followed by tumor dissemination as a multistage process. Furthermore, melanoma represents the most common cancerous disease among young women and the second most common cancer among young men aged 20 to 30 (Siegel, Miller, & Jemal, 2017).

1.1.2 Therapeutic approaches to malignant melanoma

There are curative treatments for early stage melanoma. Several therapies are standard of care when treating advanced melanoma. These include, for example, surgery to remove primary lesions as well as cytotoxic approaches such as chemotherapy or radiotherapy that kill the cancer cells and stop them from dividing and growing. Furthermore, targeted therapy, such as angiogenesis inhibitors, signal transduction inhibitors and oncolytic viral therapy are also used. (Bajetta et al., 2002; Bastiaannet, Beukema, & Hoekstra, 2005; Luke, Flaherty, Ribas, & Long, 2017). However, despite all efforts and early diagnosis, patients with a metastatic disease still have a poor prognosis. The 5-year survival rate among these patients is 10 – 15 % and their median overall survival amounts to less than one year (Pollack et al., 2011). In recent years, improved knowledge of cancer pathophysiology and a better understanding of the immune system's role in tumor control and its microenvironment have led to the development and approval of several immunotherapies as novel therapeutic approaches.

1.2 Tumor immunotherapy

1.2.1 Basic principles of immunotherapy

Immunotherapies are treatments that can either induce, enhance or suppress an immune response. Activating immunotherapies have been designed to elicit and amplify immune responses whereas suppressive immunotherapies attenuate and suppress these.

The basis for immunotherapeutic approaches against cancer is the principal ability of the immune system to recognize tumor cells as a threat to the organism's integrity, to discriminate between foreign and self and the subsequent activation and proliferation of cytotoxic T-cells that play a central role in eradicating malignant cells. Besides cell-based immunotherapies that focus on modifying immune cells *in vitro* and *in vivo*, immunomodulators such as cytokines, chemokines and interleukins are used to stimulate and enhance immune responses.

For years, melanoma has been one of the rare solid tumors for which, apart from classic chemotherapy, a form of immunotherapy has been standard of care. Despite the fact that various tumor entities such as melanoma elicit strong immune responses evident due to the infiltration of tumor infiltrating lymphocytes (TILs) into primary lesions, tumors have the ability to evade detection and elimination by the immune system (Swann &

Smyth, 2007). This process is termed tumor immune evasion and can be subdivided into two mechanisms. On the one hand, triggering of immune tolerance, on the other hand, evolving resistance to killing by cytotoxic T cells or other activated effector cells (Drake, Jaffee, & Pardoll, 2006). By the time tumors have become clinically detectable, they have already manipulated their microenvironment with the release of tumor-derived soluble factors like chemokines and cytokines (Swann et al., 2008) and thus evade the immune response mounted by the host. Immunotherapeutic approaches are intended to successfully overcome this tumor-mediated immune suppression.

1.2.2 Immunotherapeutic approaches for malignant melanoma

The first successful immune-based cancer therapies that demonstrated a clinical benefit comprised treatment with interferon-α in the adjuvant setting and high doses of immune-stimulating interleukin-2 (IL-2) in advanced melanoma (Atkins et al., 1999; Floros & Tarhini, 2015). Moreover, the combination of a high-dose IL-2 therapy and therapeutic vaccination with gp100, a cell surface protein expressed on melanoma cells that can serve as antigen, further improved the objective response rate (ORR) significantly (Schwartzentruber et al., 2011). Nevertheless, cytokine-based therapies as well as treatment with cytotoxic drugs have been characterized by generally low objective response rates (approximately 10-20% of patients) and no significant increase in overall survival (Mackiewicz, 2012).

However, in the last decade, immunotherapy has transitioned from the cytokine-based treatment to the antibody-mediated blockade of immune checkpoints. Monoclonal antibodies directed against different so-called immune checkpoints such as the cytotoxic T-lymphocyte-associated antigen-4 (CTLA-4) and the programmed cell-death protein 1 (PD-1) have revolutionized the treatment of unresectable or metastatic melanoma as well as other cancer entities by achieving durable clinical responses and prolonging patient survival with the hope of a cure for an increasing proportion of patients.

1.2.3 Immune checkpoints and their therapeutic potential in tumor therapy

Endogenous antitumor immunity relies on the ability of T cells to selectively recognize peptide antigens, kill antigen-expressing cells, to control additional components of the immune system and to mediate immunological memory. The intensity of a T cell-

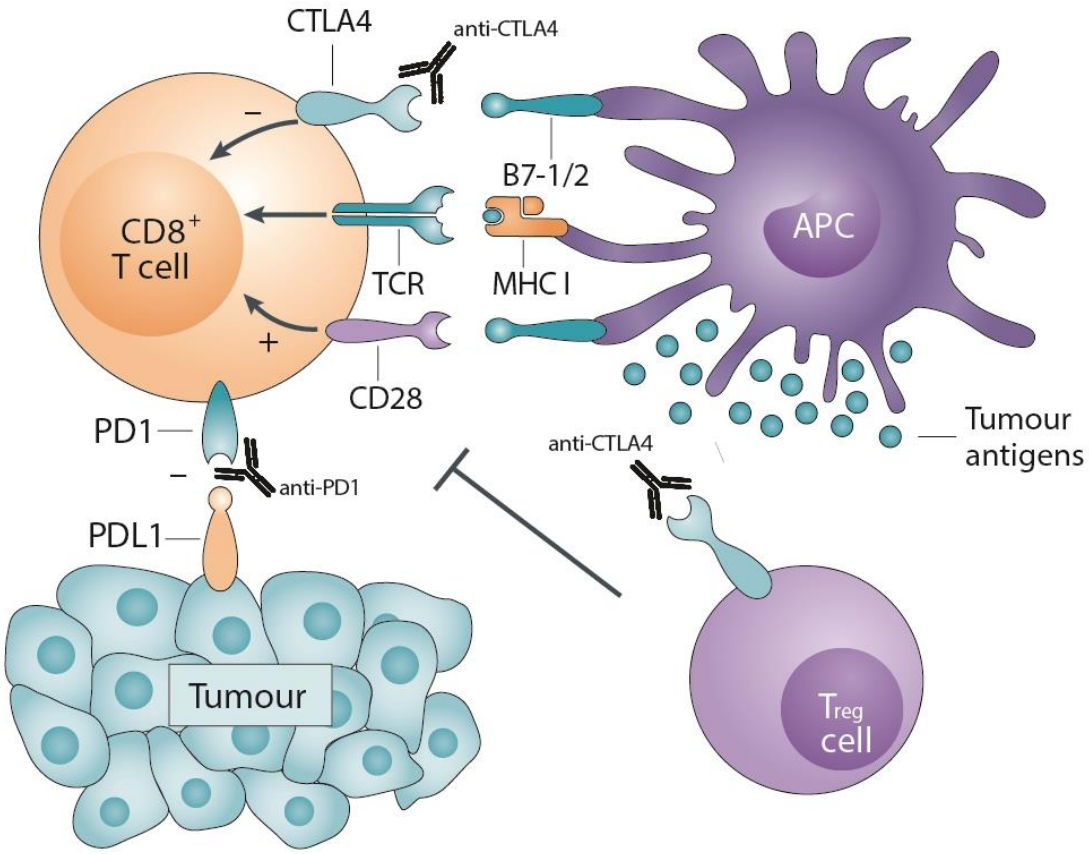

Figure 1.1: Scheme of stimulatory and inhibitory interactions between immune cells and / or tumor cells mediated by immune checkpoints. Depicted are interactions between immune checkpoints and their ligands as well as their cellular effects. **A)** CTLA-4 pathway inhibition: T cells get activated and proliferate into effector T cells by interaction of the TCR with an MHC-I bound antigenic peptide presented to the T cell by an APC. The co-stimulatory molecule CD28 is required to stabilize TCR downstream signaling, however CTLA-4 competes for the same ligands, CD80 or CD86 (B7 molecules) and dampens the immune response upon binding to prevent excessive immune responses. Inhibition of CTLA-4 with monoclonal antibodies precludes inhibition and therefore allows upregulation of T cell activation. **B)** PD-1/PD-L1 pathway inhibition: Activated T cells express PD-1 that interacts with either one of its ligands PD-L1 or PD-L2. Whilst PD-L2 is predominantly expressed on APCs, PD-L1 is expressed on many cell types, including tumor cells and immune cells. This interplay induces an inhibitory stimulus leading to T cell inactivation and anergy. Blocking of either PD-1 or its ligands with monoclonal antibodies abrogates this inhibitory stimulus, resulting in a more potent antitumor immune response. **C)** Treg cells are a T cell subpopulation capable of suppressing immune responses. Blocking of CTLA-4 on Treg cells inactivates and depletes this inhibitory subpopulation and enhances immune responses.

mediated immune response, initiated after antigen recognition by the T cell receptor, is regulated by the balance of costimulatory and inhibitory signals, so called immune checkpoints (L. Chen & Flies, 2013). Under physiological conditions, these inhibitory

signals are necessary to keep up self-tolerance and prevent excessive immune reactions. The expression of immune checkpoint proteins is often dysregulated in cancer and its microenvironment (Pardoll, 2012). In various cancer entities, tumor-infiltrating T lymphocytes express high levels of negative costimulatory markers (Ahmadzadeh et al., 2009), therefore suggesting a tumor-derived mechanism involved in antitumor suppression (Zou & Chen, 2008). Agonists of costimulatory signals as well as antagonists of inhibitory signals, the latter referred to as checkpoint blockade, turned out to be an attractive therapeutic target for tumor immunotherapy.

1.2.4 Blockade of cytotoxic T lymphocyte associated antigen-4

Cytotoxic T-lymphocyte-associated antigen 4 (CTLA-4) was the first immune checkpoint receptor used for therapeutic purposes. It is a member of the CD28/B7 immunoglobulin superfamily and is exclusively expressed on effector and regulatory T cells where it fulfills its delicate task of limiting the extent of early T cell activation. Under physiological conditions, CTLA-4 thus prevents overly intense immune responses in healthy individuals such as autoimmunity (Robert et al., 2011). CTLA-4 counterbalances the costimulatory receptor CD28 that stabilizes and enhances the signaling cascade of T cell activation after an antigen is recognized by the T cell receptor. CD28 and CTLA-4 compete for the same ligands: CD80 and CD86 (Azuma et al., 1993; Linsley et al., 1991). While the precise underlying mechanisms are subject of controversial debate, a theory exists that CTLA-4 inhibits the activation of T cells by competitive inhibition of CD28 in the binding to CD80 and CD86 because of its greater affinity for both ligands (Linsley et al., 1994). Direct inhibitory signals on T cells have also been postulated (Parry et al., 2005; Schneider et al., 2002). Activation of effector T cells as well as the inhibition of regulatory T cells are essential factors for the therapeutic success of CTLA-4 checkpoint blockade (Pardoll, 2012). Preclinical studies in mouse models determined a significant increase in the antitumor immune response due to monoclonal antibody-mediated CTLA-4 checkpoint blockade (Leach, Krummel, & Allison, 1996). However, this has only been observed for immunogenic tumors that elicit a spontaneous basal immune response. Barely immunogenic tumors did not respond to monotherapy with anti-CTLA-4 immune checkpoint blockade although to the combination with a cytokine secreting GM-CSF transduced cell vaccine (van Elsas, Hurwitz, & Allison, 1999). In this study, pre-established tumors were found to be eradicated in 80% of the animals receiving combination treatments whereas monotherapy had only marginal effects suggesting a potential synergism of tumor vaccines and checkpoint inhibitors that can boost immunity and, most importantly, could prevent tumor escape from newly–released or de novo

generated immune responses. Further preclinical studies support the role of combining cancer vaccines and immune checkpoint blockade to enhance the efficacy of each other. In this context, anti-CTLA-4 antibodies can reduce inhibitory signaling on activated T cells (Kwon et al., 1997) and further interfere with T_{reg} cells, thus altering the intratumoral T cells to T_{reg} cells ratio towards a favorable balance (Quezada, Peggs, Curran, & Allison, 2006). Moreover, anti-CTLA-4 therapy can increase and maintain the vaccine-induced stimulation of CTLs and their homing to the tumor (Wada et al., 2013).

Based on these preclinical findings, ipilimumab, a fully humanized anti-CTLA-4 antibody was approved for treatment of advanced malignant melanoma by the US-American and European regulatory authorities in 2010 and 2011. An improved overall survival of 3.5 months compared to treatment with the melanoma specific peptide vaccine gp100 has been demonstrated in a pivotal study (Hodi et al., 2010). Ipilimumab-mediated CTLA-4 blockade resulted in prolonged activation of T cells, further proliferation of T cells and ultimately in the amplification of the T cell-mediated immune response, altogether contributing to an enhanced T cell-driven antitumor immune response (Peggs, Quezada, Korman, & Allison, 2006; Robert & Ghiringhelli, 2009). Although treatment with ipilimumab was the first therapeutic approach to achieve an improved overall survival of patients with metastasized malignant melanoma, the fact that approximately 20 % of these patients showed a durable clinical response for more than 5 years, which had never been achieved with any prior treatment, appeared even more impressive (Schadendorf et al., 2015). This ongoing immune reaction and the associated tumor remission achieved even long after completion of the comparatively short therapy phase (4 doses over a period of 10 weeks) support the concept that immune-based therapies can reprogram the immune system and therefore keep tumors in check long after therapy has been completed. Besides this small percentage of patients showing a remarkable response to therapy with ipilimumab, the majority of patients could not substantially benefit from sole CTLA-4 blockade (Hodi et al., 2010). However, the mechanisms that underlie this inter-patient heterogeneity are not fully understood yet and need to be further clarified.

1.2.5 The role of PD-1 in checkpoint blockade-mediated immunotherapy

Another major immune checkpoint receptor is the programmed cell death protein 1 (PD-1). Whilst CTLA-4 is considered to inhibit initial T cell activation, the physiological role of PD-1 is the limitation of the T cell effector function in peripheral tissues in order to prevent excessive immune reactions. After binding to its ligand, PD-1 inhibits several proteins

with kinases function that are necessary for T cell activation (Freeman et al., 2000). PD-1 has a broader expression pattern compared to CTLA-4 as it is not exclusively expressed on effector and regulatory T cells (Francisco et al., 2009) but also on B cells (Velu et al., 2009), natural killer cells (NK cells) (Terme et al., 2011) and monocytes (Freeman et al., 2000). Two ligands for PD-1, PD-1 ligand 1 (PD-L1) and PD-1 ligand 2 (PD-L2) have been described and are further termed B7-H1 and B7-H2 (Freeman et al., 2000; Latchman et al., 2001). PD-L1 is expressed on B cells, T cells, macrophages, DCs but also tumor cells. In contrast, PD-L2 is expressed mainly on activated macrophages and DCs (Kirkwood et al., 2012).

High expression levels of PD-L1 either on carcinoma cells themselves or on myeloid cells in the tumor microenvironment are related to an impaired overall survival in patients with renal cell carcinoma (R. H. Thompson et al., 2004). On the one hand, overexpression of PD-L1 and PD-L2 on tumor cells can result from constitutive activation of oncogenic signaling pathways like the anaplastic lymphoma kinase (ALK) in certain lymphomas (Marzec et al., 2008). Moreover, tumor cells upregulate PD-L1 as direct adaption to IFN-γ detection that is released in the dynamic process of a tumor specific immune response (Taube et al., 2012).

Besides an increased PD-L1/2 expression in tumors and their microenvironment, the augmented expression levels of PD-1 on non-functional, exhausted T cells in chronic viral infection and cancer also represents an attractive target for antibody-mediated checkpoint blockade. Previous studies in a mouse model demonstrated an increased antitumor immune response by antibody-mediated inhibition of PD-1 either alone or in combination with GM-CSF secreting tumor cell lines (Blank et al., 2004; B. Li et al., 2009). Phase III clinical trials with the humanized anti-PD-1 antibody nivolumab revealed significant therapeutic responses in patients with nonsquamous, squamous and non-small-cell lung cancer (K. J. Harrington et al., 2017; Horn et al., 2017). In addition, nivolumab administration resulted in long-term clinical benefit and increased relapse-free survival in patients suffering from advanced melanoma (Weber et al., 2017). Furthermore, nivolumamb was approved by the FDA in 2014 for application in a wide range of solid tumors such as melanoma and renal cell carcinoma and may even become recommended first-line therapy for non-small cell lung cancer.

An approach that combined PD-1 and CTLA-4 checkpoint blockade demonstrated an increase in the percentage of infiltrating T cells and a reduction in the numbers of Tregs and myeloid cells within B16 melanoma tumors (Curran, Montalvo, Yagita, & Allison,

2010). Moreover, the combined blockade of both inhibitory pathways synergized in the therapy of malignant melanoma as 50 % of the patients developed a clinical response (Ott, Hodi, Kaufman, Wigginton, & Wolchok, 2017).

Similar to the experiences achieved with anti-CTLA-4, the data from various phase II and III clinical trials suggest a long-term response whereas many patients apparently show no benefit from treatment with the anti-PD-1 monoclonal antibody. Concurrently, new hope for a broader response to this promising immunotherapy arises from the premature development of synergistic combination therapies. Such therapy approaches comprise the combination of PD-1 blockade with either chemotherapy or radiotherapy in patients suffering from NSCLC. The combination of chemotherapy with anti-PD-1 blockade revealed an increased ORR whereas checkpoint blockade enhanced the response initiated by RT to systemic antitumor responses (Deng, Liang, Burnette, et al., 2014; Langer et al., 2016). Furthermore, a phase III clinical trial of melanoma patients receiving combined nivolumab with ipilimumab treatment demonstrated complimentary activity of both checkpoint inhibitors resulting in enhanced survival and an increased ORR (Larkin, Hodi, & Wolchok, 2015). In addition, several phase I and II clinical trials are currently evaluating second and third generation immune-oncology drugs to overcome resistance and to improve ORR. Among others, these include inhibitory compounds such as TIM-3, LAG-3 and IDO or costimulatory antibodies CD40, CD137 and ICOS (Dempke, Fenchel, Uciechowski, & Dale, 2017).

1.2.6 Resistance Mechanisms to Immune-Checkpoint Blockade in Cancer

Despite the significant success achieved with checkpoint-mediated immunotherapy in cancer treatment, the majority of patients fails to respond to immune checkpoint blockade or has to stop treatment because of the development of immune-related adverse events. This strong inter-individual variation in the clinical response to checkpoint inhibitors such as anti-CTLA-4 has not yet been fully elucidated and thus remains a major challenge. However, several resistance mechanisms comprising T-cell exhaustion (Fuertes Marraco, Neubert, Verdeil, & Speiser, 2015), the overexpression of caspase-8 (Schimmer, 2004) and a different mutational load as well as the subsequent formation of neoantigens (Liontos, Anastasiou, Bamias, & Dimopoulos, 2016) have been made accountable for the high degree of inter-patient heterogeneity. Thus leaving the questions of how the development of a synergistic combination therapy can overcome this problem open.

Tumor associated antigens, so called neo-antigens, can be recognized by the immune system resulting in the destruction of tumor cells expressing them. It is assumed that the expression of such new epitopes is a consequence of newly acquired mutations that can be caused by DNA damage and EGFR mutation (D. S. Chen & Mellman, 2013). In recent years, genetic mutation analysis of tumor samples has been used to determine mutations that can actually give rise to antigens recognizable by T cells. So-called neoantigens can then be applied as active cancer vaccines. In this context, a previous study investigated the role of tumor-specific neoantigens and changes in the tumor microenvironment in response to anti-CTLA-4 mediated checkpoint blockade in pretreated tumor biopsies. The clinical benefit was significantly associated with the overall mutational and neoantigen load as well as the expression of cytolytic markers by tumor infiltrating lymphocytes in the immune microenvironment (Van Allen et al., 2015). In addition, whole exome and RNA sequencing has been applied to identify cancer-specific neoantigens for the subsequent generation of peptide or RNA vaccines for active immunotherapy. Personalized RNA vaccines were designed to encode 10 individual neoantigens per person and all patients developed a T cell response to multiple neoantigens upon application that achieved a clinical response in the combination with PD-1 mediated immune checkpoint blockade (Sahin et al., 2017). Furthermore, another study used synthetic peptides encoding 20 neoantigens as immunogens that led to a complete response when combined with PD-1 blockade (Ott, Hu, et al., 2017).

Moreover, a recent report has postulated a potential link between the two distinct pathways of anti-CTLA-4-mediated immune checkpoint blockade and high expression profiles of antiviral defense genes in patients with metastasizing malignant melanoma. A gene array analysis of tumor biopsies demonstrated that patients expressing increased levels of genes involved in antiviral immunity such as RIG-I within whole tumor lysates benefited from anti-CTLA-4-mediated checkpoint blockade by developing a durable clinical response (Chiappinelli et al., 2015). It has been suggested that high basal expression levels of endogenous retroviral transcripts can activate and increase the expression of anti-viral defense genes resulting in a favorable therapy response. Furthermore, it is supposed that genetic changes as well as increases in ERVs and viral defense genes could be applied as biomarkers to predict therapy outcome by immune checkpoint inhibitors and other immunomodulatory approaches. However, the underlying mechanism by way of which nucleic acid receptor signaling affects the efficacy of checkpoint blockade has to be further elucidated.

1.3 Mechanisms of anti-tumor immunity

1.3.1 Immune cells involved in the defense against tumors

The most essential role of our immune system is to protect our body from invading pathogens by inducing a protective immunity and preventing autoimmunity against self-tissues. This is achieved via a complex network of organs, tissues and effector cells comprising antigen-presenting cells, T and B cells as well as NK cells whose functions are the initiation, differentiation and triggering of the effector phase and finally the termination of an immune response.

Each T and B lymphocyte expresses only a single antigen-specific receptor. Due to individual somatic recombination of the receptor encoding genes a practically infinite repertoire of specific receptors is created by gene rearrangement. B cells are primarily responsible for humoral immunity. Upon antigen recognition they secrete antibodies termed immunoglobulins that are capable of opsonizing pathogens and, moreover, binding antigens and inactivating them.

In contrast to immunoglobulins, T lymphocytes recognize antigens only when they are displayed on the surfaces of infected cells or presented by antigen-presenting cells. Moreover, T lymphocytes can be subdivided into T helper (T_H) cells and cytotoxic T cells. T_H cells are characterized by the costimulatory molecule CD4 whereas cytotoxic T cells express CD8 on their surface. Helper T cells are activated when antigen, bound to MHC Class II molecules, is recognized whereas cytotoxic T cells require a strong interaction of their T cell receptor with a peptide-bound MHC class I molecule. Upon activation naïve T_H cells differentiate into various subsets of effector cells and trigger the release of distinct cytokine sets, depending on their subtype, which influences the activity of various immune cells (Glimcher & Murphy, 2000). In addition, T_H cells are essential for mediating and maximizing the capacities of an adaptive immune response. T_H1 cells induce the production of IFN-γ which in turn boosts the killing efficacy of macrophages and enhances proliferation of cytotoxic T cells. Furthermore, T_H2 cells improve humoral immune responses due to the secretion of cytokines such as IL-4, IL-5 and IL-13 leading to B cell proliferation, enhanced antibody production and antibody class switching. T_H17 cells also mediate protection against extracellular bacteria and fungi by secreting IL-17 (L. E. Harrington et al., 2005; LeibundGut-Landmann et al., 2007). The role of $CD4^+$ helper T cells in anti-tumor immunity is not yet fully understood. However, they provide cytokines for the differentiation of naïve $CD8^+$ T cells, so that these cells can differentiate

into effector and memory T cells. Moreover, T helper cells, specific to tumor antigens, can secrete TNF-α and IFN-γ that increase the expression of MHC-I on tumor cells (Burkholder et al., 2014).

In contrast, regulatory T (T_{reg}) cells represent an inhibitory subpopulation of T_H cells competent in suppressing immune responses and thereby maintaining self-tolerance and immune homeostasis. This subpopulation is characterized by the expression of CD25 and the transcription factor forkhead box p3 (foxp3) apart from CD4 (Vignali, Collison, & Workman, 2008). Increased numbers of T_{reg} cells in peripheral blood and the TME are commonly found in patients with invasive and metastatic cancer entities (Fehervari & Sakaguchi, 2004).

Cytotoxic T cells (CTLs) induce cell death of damaged, dysfunctional and viral infected cells or pathogens. In response to a particular pathogen, CTLs undergo a process called clonal selection. Only certain lymphocyte populations are selected to become functional and clonally expand. These activated effector cells are then released into the system where they bind to cells expressing the distinct antigen as counterpart to their specific receptor and induce lysis or apoptosis of these cells. Once an infection has been fended off most effector cells die and are cleared by phagocytes, nevertheless, a few survive and remain as memory cells. These cells can quickly differentiate into effector cells on a de novo encounter with the same antigen and therefore fulfill the task of immunological memory.

CTLs can deploy three major mechanisms to kill and destroy malignant cells. The first is the secretion of TNF-α, IFN-γ and other cytokines, which can facilitate anti-viral and anti-tumor effects. The second is the destruction of tumor cells via Fas/FasL interaction. Fas ligand is produced by activated $CD8^+$ T cells and can bind to its receptor, Fas, which is expressed on the surface of viral infected cells as well as on tumor cells. Binding causes trimerization of Fas molecules resulting in the concentration of signaling molecules and the subsequent induction of apoptosis in the target cell by activation of the caspase cascade (Lettau, Kabelitz, & Janssen, 2015). Moreover, CTLs are able to produce and release cytotoxic granules containing proteins with lytic function including granzymes and perforin. Perforin can form a pore in the membrane of the target cell which in turn allows the granzyme molecules to penetrate the tumor cell and induce apoptosis by cleavage of proteins due to their proteolytic function.

Natural killer cells (NK cells) are involved in rapid immune responses against viral infected cells and also respond to tumor formation. They can recognize cells affected by cellular and genomic stress typically found in cancer and initiate cell lysis independent on activation by antibodies or the presence of MHC-I (Vivier et al., 2011). The recognition of MHC-I molecules on cellular membranes provides inhibitory signals to NK cells; NK cells thus respond in particular to the absence of MHC-I which has been observed in many tumors. Furthermore, distinct tumors also express proteins such as MIC and ULB that can serve as ligands for the NKG2D receptor on NK cells. However, tumors have developed strategies to escape NK cell-mediated lysis by blocking the NKG2D receptor via secretion of specific ligands (Handgretinger, Lang, & Andre, 2016; Kohrt et al., 2014).

1.3.2 Pattern recognition receptor families

1.3.2.1 Recognition of microbial patterns by the immune system

The basis of every immune response is the activation of the innate immune system by pattern recognition receptors (PRRs). These germline-encoded receptors recognize the presence of microbial intruders by binding so called pathogen-associated molecular patterns (PAMPs). These conserved molecular structures are only present in pathogens but not in healthy host cells. This way, the immune system is capable of identifying hazardous situations and discriminating between self and foreign. Among the most important PRRs are classic membrane-bound toll-like-receptors (TLRs), C-type lectin receptors (CLRs) as well as members of the cytoplasmic receptor family such as NOD-like-receptors (NLRs), RNA-helicases such as RIG-I-like helicases (RLHs), AIM-2-like helicases (ALHs) and the Cyclic GMP-AMP synthase (cGAS) (Sun, Wu, Du, Chen, & Chen, 2013; Takeuchi & Akira, 2010).

1.3.2.2 Membrane-bound receptors

The most prominent member of the classic membrane-bound receptors is the family of TLRs. Activation of TLRs leads to the recruitment of adaptor proteins and the subsequent induction of inflammatory responses by signal transduction via the NF-kB pathway and other transcriptional events such as the expression of costimulatory molecules and the production of inflammatory cytokines (Medzhitov, Preston-Hurlburt, & Janeway, 1997). Until today, 13 different members of the TLR family have been described (Akira, 2009).

Many of these are conserved in mice and humans, however, TLR8 and TLR10 are non-functional in mice and TLR11 to TLR13 have disappeared from the human genome.

TLRs are expressed on the membranes of either epithelial cells or on cells and tissues with immunological function. These include, in particular, cells involved in innate immunity such as dendritic cells, macrophages, natural killer cells and other adaptive immunity cells like B and T lymphocytes. In addition, they are expressed on various epithelia like the gastro intestinal (GI) tract, the lung, the skin and the spleen (Delneste, Beauvillain, & Jeannin, 2007). However, their expression profiles vary within the different expression sites.

Furthermore, the TLR family can be divided into different subgroups according to their cellular distribution. TLR1, 2, 4, 5, 6 and 11 are located on the cell surface and thus recognize lipids, proteins and lipoproteins as part of microbial and fungal membranes. In contrast, TLR3, 7, 8 and 9 are expressed on intracellular vesicles such as endosomes and lysosomes. Due to their localization, this subpopulation predominantly detects nucleic acids like bacterial-derived DNA by their conserved structures such as frequent unmethylated CpG motifs. Furthermore, this subpopulation of TLRs, in particular TLR9 which recognizes bacterial and viral DNA and CpG oligonucleotides, TLR3 which senses double-stranded RNA and TLR7 and 8 which detect single-stranded RNA, occupy a key role in the recognition of viral nucleic acids (Takeuchi & Akira, 2010).

Detection of both viral DNA or RNA by respective TLRs, triggers intracellular signaling pathways that lead to the induction of either IFN via the TRIF-dependent pathway or the MyD88-dependent dissemination of NFκB into the nucleus where it activates transcription and the subsequent induction of inflammatory cytokines (Kawai & Akira, 2010). Secretion of IFN by infected cells inhibits viral replication of the infected cell itself as well as in neighboring uninfected cells through the induction of antiviral proteins by IFN-stimulated genes (ISGs).

1.3.2.4 Detection of nucleic acids by RIG-I like helicases

The identification of RLHs, that are present in various cells of the immune system but also in the cytosol of almost all somatic cells, represents essential progress in understanding of endogenous viral defense. Members of the RLH family are the retinoic acid inducible gene I (RIG-I), melanoma differentiation-associated protein 5 (MDA-5) and the laboratory of genetics and physiology 2 (Lgp2). Recognition of RNA, for instance viral or tumor derived RNA, by RIG-I takes place in the cytosol, whereas endosomal localization is required for the identification and the discrimination between self and foreign by TLRs (Schmidt, Endres, & Rothenfusser, 2011).

RIG-I and MDA-5 turned out to be decisive for the detection of human pathogen viruses. RIG-I preferentially binds short dsRNA molecules whereas MDA-5 selectively binds long dsRNA and thus can detect various viral strains (Kato et al., 2006; Takeuchi & Akira, 2007). The exact molecular property of the viral PAMP, which allows MDA-5 to distinguish between viral RNA and host self-RNA in the cytosol, is not known until today. It has been shown that uncapped 5´-triphospat RNA (3pRNA), a viral RNA modification that occurs in eukaryotic cells where it is hidden by the 5´capstructure is exclusively detected by RIG-I. Such 3pRNA can be produced by *in vitro* transcription or in a synthetically induced manner (Hornung et al., 2006; Schlee et al., 2009) and can, therefore, mimic the effects of naturally occurring viral RNA. 3pRNA selectively activates RIG-I and can be used as pharmacological reagent for immune stimulation.

A unique feature of viral detection is the fact that the characteristic protein-sugar-lipid modification, which often serves as recognition pattern for fungi or bacteria, does not exist in viruses as these solely consists of host cellular components. Therefore, the innate immune system employs specific viral PAMPs like viral capsids, methylation, an uncapsulated 5´triphospate end in viral RNA or the production of double-stranded RNA for the recognition of viral infections. Moreover, aberrant localization of RNA in the cytosol is classified as a danger signal and thus followed by the induction of an immune response.

Sensing of a viral infection is followed by the induction of an innate immune response and accompanied by the production of antiviral cytokines of the group of IFN-I (IFN-α/-β) and IFN-III (IFN-λ) that can be formed in somatic cells as well as in specialized cells of the immune system (Levy, Marie, & Durbin, 2011). Detection of viral structures by PRRs furthermore involves the production of proinflammatory cytokines that can either induce apoptosis in viral infected cells or initiate inflammatory responses that recruit cells

from the innate immune system to the site of infection and optimize the molecular conditions for immune responses mediated by the adaptive immune system (Nakanishi, Yoshimoto, Tsutsui, & Okamura, 2001).

In addition, cancer as a genetic disease arises by an evolutionary process where somatic cells acquire multiple mutations. Therefore, cancer cells share properties comparable to those of viruses as both arise from host cells. For this reason, similar defense mechanisms are applied to fend off uncontrolled expansion of tumor cells as are employed in anti-viral immunity. For instance, aberrant localized tumor-derived nucleic acids that are released upon tumor cell death can be detected by the innate immune system and facilitate an IFN-I driven immune response finally resulting in tumor eradication (Dunn et al., 2005).

1.3.2.5 RIG-I mediated induction of apoptosis

Until recently, knowledge about the function of RIG-I was restricted to the induction of IFN-I and proinflammatory cytokines. However, by targeted activation of RIG-I in tumor cells an essential role of RIG-I in anti-tumor immunity and a RIG-I-dependent signaling pathway for apoptosis induction by an immunogenic variant of cancer cell death leading to growth inhibition of pre-established tumors has been described.

In this context, a previous report revealed that RIG-I and MDA-5 ligation in both somatic- and tumor cells triggers two distinct and functionally independent signaling pathways. One results in the release of IFN-I by both tumor and host cells, the other leads to the induction of pro-apoptotic BH3-only proteins and subsequent apoptosis of malignant cells (Besch et al., 2009). This effect was primarily driven by the transcriptional induction of Noxa but was independent of p53 induced IFN-I. In addition, apoptotic signaling triggered by RIG-I and MDA-5 led to the induction of caspase-9, an essential mediator of the mitochondrial apoptosis pathway in melanoma cells. Pro-caspase-9 was further cleaved by the effector caspase-3 and this cleavage was accompanied by cytochrome c release from mitochondria, another critical event in mitochondrial apoptosis. In contrast to the massive cell death induction in melanoma cells, nonmalignant cells evade induction of apoptotic cell death by upregulating anti-apoptotic proteins such as Bcl-2 whereas this mechanism was found to be lost in melanoma cells. A follow-up study revealed that the susceptibility to RIG-I-mediated intrinsic apoptosis was not restricted to melanoma cells but also found in a preclinical model of pancreatic cancer (Duewell et al., 2014). It was further suggested that this kind of tumor cell death is immunogenic as

dying tumor cells exhibited characteristic features of immunogenic cell death by translocation of calreticulin to the outer membrane as well as the release of HMGB1. RIG-I-triggered tumor cell death furthermore led to the activation of DCs, in particular CD8α$^+$ DCs, capable of cross-presenting tumor-associated antigens to naïve T cells mediated by tumor derived IFN-I.

In addition, another study observed that *in vivo* delivery of 3pRNA contributes to overall antitumor activity of RIG-I and MDA-5 by activating NK cells capable of eradicating pre-established tumors (Poeck et al., 2008).

1.3.2.6 Detection of tumor associated antigens by dendritic cells

Upon recognition and internalization, the antigen is processed and digested into small peptides containing epitopes and presented to T cells by major histocompatibility complex (MHC) molecules at the cell surface (Dalod, Chelbi, Malissen, & Lawrence, 2014; Rossi & Young, 2005). The activation of cytotoxic T cells by presentation of an exogenous antigen bound to MHC class-I molecules is referred to as cross-presentation (den Haan, Arens, & van Zelm, 2014). Sensing of an antigen leads to a phenotypic transformation and ultimately to the activation and maturing of dendritic cells. This in turn is accompanied by the upregulation of MHC molecules and co-stimulatory factors like CD80 and CD86 which trigger CD28 on T cells (Brzostek, Gascoigne, & Rybakin, 2016).

Previous studies have suggested these three signaling classes as being crucial for the subsequent fate of T cells as they appear to be required for effector T-cell generation and thus move DC to the center of adaptive immunity (Joffre, Nolte, Sporri, & Reis e Sousa, 2009). Immature DCs are insufficient in antigen presentation because they lack an efficient costimulatory signaling function. Therefore, naïve T cells only receiving signal 1 enter a state of inactivity either by anergy, induction of tolerance or diversion into a regulatory cell fate (Dhodapkar, Steinman, Krasovsky, Munz, & Bhardwaj, 2001; Joffre et al., 2009; Shortman & Heath, 2001). The underlying mechanism of this regulation has been determined by studies showing that maturation of DCs and the subsequent release of a potent immune response is primarily achieved by recognition of pathogen-derived microbial patterns (Medzhitov & Janeway, 1997). Endogenous inducible danger signals like pro-inflammatory cytokines can also serve as mediators for the transition of DCs to immunogenic APCs (Belardelli & Ferrantini, 2002). In addition, dendritic cell-intrinsic IFN-I signaling has been shown to be of particular importance for the generation of antigen-

specific T-cell responses against growing tumors by facilitating tumor-specific T cell priming and the subsequent accumulation of $CD8\alpha^+$ T DCs in the tumor (Diamond et al., 2011; Fuertes et al., 2011). Previous studies demonstrated that DCs are capable of sensing and processing tumor derived antigens from either living or dying tumor cells and further cross-present these to T cells resulting in tumor rejection by the induction of a T cell-mediated immune response suggesting DCs as a potential target for cancer immunotherapy.

1.3.2.7 Maturation of dendritic cells by immunogenic cell death

Cancer cell death can be either immunogenic or non-immunogenic depending on the initiating stimulus. Immunogenic cell death (ICD) is associated with changes in the cell surface and a spatial and temporal release of immunogenic damage-associated molecular patterns (DAMPs) capable of inducing an immune response (Garg, Martin, Golab, & Agostinis, 2014). However, preclinical cancer models in mice have demonstrated that the nature of cell death influences the *in vivo* immunogenic potential of DCs loaded with apoptotic tumor cells (Goldszmid et al., 2003; Hatfield et al., 2008).

Dying or dead cancer cells can exhibit an immune stimulatory potential by their ability to elicit adaptive immune responses mediated by DCs which ultimately result in tumor eradication (Kroemer, Galluzzi, Kepp, & Zitvogel, 2013).This includes the release of defined DAMPs that can act as potent danger signals. Furthermore, ICD is accompanied by the induction of reactive oxygen species (ROS) and endoplasmatic reticulum (ER) stress (D. V. Krysko et al., 2012). There are at least three types of signals elicited by dying tumor cells that interact with DCs, including the “find me”, “eat me” and “don´t eat me” signals (Ravichandran, 2011). Apoptotic cells release molecules that function as “find me” signals including ATP and passively released high-mobility group box 1 (HMGB1). Calreticulin (ecto-CRT) and phosphatidylserine are membrane-bound and therefore surface-exposed molecules that serve as “eat me” markers for phagocytes thus supporting detection and uptake of dying cells (Kepp et al., 2014). In addition to these stimulatory signals, negative regulators like lactoferrin and CD47 serve as “don´t eat me” signals for the prevention of phagocytosis (Chao et al., 2010). Moreover, studies in mouse models demonstrated that ICD-undergoing cancer cells also function as very potent Th1-driving anticancer vaccines (Guo et al., 2017). Therefore, creating highly immunogenic antigenic tumor cell cargo by combining the potential of ICD inducers with other immunogenic modalities can even further improve immunotherapy of cancer.

1.3.2.8 Downstream signaling of RLHs

Activation of RIG-I and MDA-5 involves the potent release of IFN-I (Goubau et al., 2014b; Hornung et al., 2006) and furthers the secretion of proinflammatory cytokines e.g. IL-6 and TNF-α (Kato et al., 2006).These essential molecules are mainly produced by cells of the innate immune system like DCs and macrophages but also fibroblasts. Concurrent secretion of IFN-I and proinflammatory cytokines is responsible for the inhibition of viral replication and the induction of an adaptive immune response. The mitochondrial antiviral signaling protein (MAVS) serves as an adaptor protein for the RIG-I- and MDA-5-mediated signaling cascade by activating the transcription factors interferon regulating factor 3 and 7 (IRF3; IRF7) which are necessary for the production of IFN-I and further the nuclear factor 'kappa-light-chain-enhancer' of activated B-cells (NF-κB) which induces proinflammatory cytokines and chemokines. Activation of NF-κB is further regulated via the adaptor proteins caspase-recruitment-domain-protein 9 (CARD9) and B-cell lymphoma 10 (BCL-10) (Poeck et al., 2010).

Another key pyrogen during an infection besides IL-6 and TNF-α is IL-1β. This cytokine triggers the generation of fever and the induction of an adaptive immune response as well as the recruitment of leucocytes to the site of infection (Yu & Finlay, 2008). Due to these diverse biological functions, a multi-protein complex, the so-called inflammasome, closely regulates the secretion of IL-1β. The central effector protein of the inflammasome is caspase-1, which catalyzes the cleavage of the inactive precursor pro-IL-1β and pro-IL-18 into the biologically active cytokines IL-1β and IL-18. The name of each inflammasome is based on its respective receptor. Currently three different inflammasomes have been described, which play an important role for the clearance of viruses: the NLRP3-inflammasom, the AIM2-inflammasom and the RIG-I inflammasome (Franchi et al., 2014; Poeck et al., 2010; Pothlichet et al., 2013).

1.3.2.9 Cytosolic DNA as danger signal

In addition to aberrant cytosolic RNA sensing, detection of cytosolic DNA is also perceived as a danger signal and thus initiates an immune response upon recognition. A source of cytosolic DNA can be genetic material from viral genomes or replication intermediates during viral infection. The detection of DNA is facilitated by different sensors including the membrane-bound TLR9 receptor, which recognizes CpG motif containing nucleotides within the endosome, as well as the recently discovered cytosolic DNA sensors Absent in Melanoma-2 (AIM2) and cGAS (Atianand & Fitzgerald, 2013; Fernandes-Alnemri, Yu, Datta, Wu, & Alnemri, 2009; Rathinam & Fitzgerald, 2011). Activation of AIM2 leads to the formation of the AIM-2 inflammasome complex whereas activation of cGAS induces an innate immune response comparable to the recognition of cytosolic RNA via RIG-I by producing IFN-I and proinflammatory cytokines.

1.3.2.10 Detection of cytosolic DNA via the cGAS/STING pathway

cGAS is one of several DNA-binding proteins functioning upstream of its adaptor protein, the stimulator of interferon gene (STING). Upon recognition and binding of double-stranded DNA (dsDNA), cGAS catalyzes the formation of cyclic guanosine monophosphate–adenosine monophosphate (cGAMP) from ATP and GTP (Sun et al., 2013). The STING protein is located on the endoplasmatic reticulum where it recognizes and binds cGAMP with a higher affinity compared to its ligands cyclic di-guanylate monophosphate (c-di-GMP) and cyclic-di-adenylate monophosphate (c-di-AMP), which have a similar structure as cGAMP (Burdette et al., 2011).

Upon ligand binding, STING activates TANK-binding kinase 1 (TBK1) which triggers the phosphorylation of IRF-3 and subsequent transcription of IFN-β and associated genes (Tanaka & Chen, 2012). Furthermore, STING coordinates the activation of STAT, thus inducing certain interferon stimulating genes (ISG) and chemokines such as CCL2 and CCL20 (Burdette et al., 2011; H. Chen et al., 2011) and is assumed to activate NF-κB transcription via the activity of the inhibitor of kappa B kinase (IKK) (Tanaka & Chen, 2012).

1.3.2.11 The role of STING in viral infection and immunotherapy

By its ability to elicit a strong IFN-I response upon ligand binding, STING occupies a crucial role in controlling infections from DNA viruses such as herpes simplex virus 1 (HSV-1) (Schoggins & Rice, 2011). Recent studies further demonstrated the importance of STING signaling in sensing of retroviruses like HIV-1 (Gao et al., 2013). Besides its role in antiviral immunity, STING agonist have been shown to be potent adjuvants in therapeutic vaccination approaches (X. D. Li et al., 2013). Additionally, STING signaling appears to be a promising target for the development of new strategies in cancer therapy because of its critical role in innate immune sensing of immunogenic tumors and the subsequent priming of $CD8^+$ T cells against tumor antigens (Woo et al., 2014).

It is furthermore involved in spontaneous anti-tumor responses by sensing tumor derived DNA as well as IFN-β release and the activation of host antigen-presenting cells by signaling via cGAS/STING and interferon regulatory factor 3 (IRF3). Moreover, cGAS and STING seem to be crucial in immunotherapeutic approaches as mice deficient in either one of these genes lost the ability to mount an efficient antitumor immune response induced by the combination of PD-1-mediated immune checkpoint blockade with direct targeting of the cGAS/STING pathway (H. Wang et al., 2017). In contrast, monotherapy with anti-PD-1 did not inhibit tumor growth. (Ueha et al., 2015).

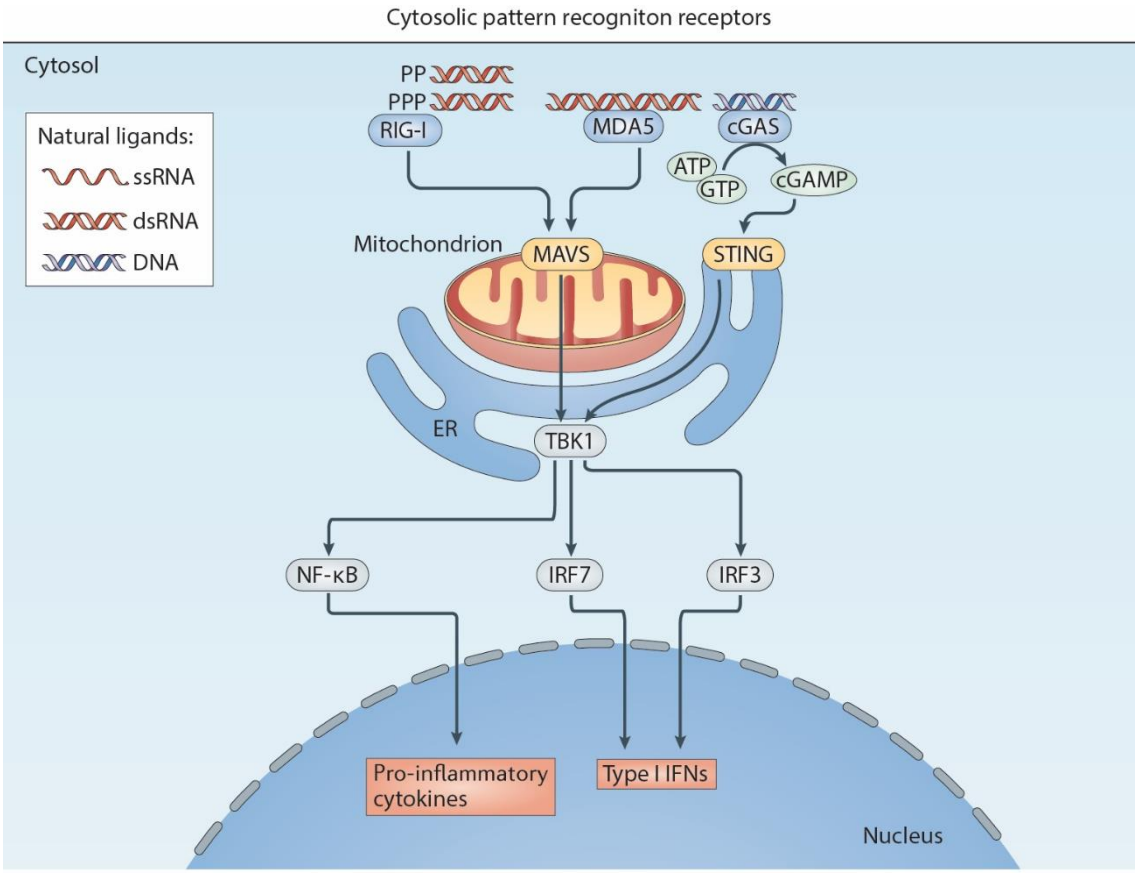

Figure 1.2: Overview of cytosolic pattern recognition receptor signaling pathways and their respective target transcription factors. This schematic overview is reduced to receptors, adaptor molecules and the main transcription factors. Adapted from (Junt & Barchet, 2015).

1.3.2.12 Implications of STING and RIG-I agonists in cancer immunotherapy

In recent years, intense research on cells of innate and adaptive immunity and the pattern recognition receptors expressed on their surface have broadened the understanding of the central role of PRRs in immunotherapy. Specific PRR ligands serve as attractive immune modulators. An advantage in the use of specific ligands is their ability to induce a precise immune response by mimicking a bacterial or viral infection. In addition, activation of PRRs is an appropriate adjuvant for vaccination strategies due to their ability to selectively activate professional APCs and the subsequent antibody release and induction of cellular immunity.

Previous studies demonstrated that intratumoral application of modified cyclic dinucleotides (CDNs) can trigger systemic and tumor specific immune responses in mice and men that result in the regression of primary injected tumors as well as systemic metastasis (Corrales et al., 2015). Moreover, a vaccination approach with a GMCSF

transduced STING agonist in a preclinical mouse model led to reduced tumor growth in several cancer entities *in vivo*. Tumor regression was further accompanied by tumor infiltration by CTLs and high expression levels of PD-L1 in the tumor microenvironment. Combining vaccination with anti-PD-1-mediated checkpoint blockade resulted in tumor regression and prevented further tumor growth in a re-challenge experiment (Fu et al., 2015). Furthermore, direct targeting of PRRs elicits a Th1-mediated immune response and the ensuing potent IFN-I driven defense mechanisms against intracellular pathogens. Moreover, this PRR-mediated stimulation of adaptive immunity supports immunological defense against tumor cells (C. K. Tang et al., 2013).

Due to their ability to induce either tumor cell death as well as efficient cross priming, RIG-I ligands represent promising immune stimulants and can furthermore be utilized for the generation of new adjuvants in the use of cancer vaccines (Liu et al., 2016). A previous study demonstrated the successful use of RIG-I agonist as vaccine adjuvants in a murine influenza model. Application of 3pRNA in combination with influenza hemagglutinin, serving as an antigen, resulted in antibody production and activation of CTLs and further protected mice against a lethal influenza challenge (Beljanski et al., 2015; Hochheiser et al., 2016). Moreover, RIG-I has recently been shown to be activated in tumor and host cells by small noncoding RNAs that are translocated from the nucleus in the cytosol after irradiation and to lead to the induction of an IFN-β driven immune response (Ranoa et al., 2016).

Besides their function in facilitating anti-tumor effects, PRRs have also been found to promote cancer progression. Chemically induced epidermal carcinogenesis by a polycyclic aromatic hydrocarbon leads to the release of DNA into the cytosol, which is subsequently sensed by STING leading to the induction of proinflammatory cytokines and the attraction of inflammatory cells which then causes a state of chronic inflammation that further promotes tumorigenesis (Ahn et al., 2014). Moreover, a previous report revealed that direct targeting of RIG-I in a preclinical model of breast cancer fails to induce a therapeutic response and additionally enhances tumor growth, formation of metastasis and leads to therapy resistance (Nabet et al., 2017).

Altogether, several important aspects seem to affect the efficiency of PRR activation in immunotherapy including the tumor microenvironment, the cell specificity of response as well as the nature of agonists and tumor immunogenicity. In addition, the role activation of tumor and host intrinsic PRR signaling has for checkpoint-mediated immunotherapy and how activation of one respective compartment differs from another remains ill-

defined. Furthermore, the current knowledge of PRRs in immunotherapy is almost completely based on preclinical studies highlighting the importance of follow-up studies to further elucidate the impact of PRRs on cancer therapy in humans.

1.4 Objectives

Targeting the immune checkpoint CTLA-4 with the monoclonal antibody ipilimumab turned out to be an effective tumor immunotherapy in both mice and men. However, its success depends on a preexisting T-cell response which limits its therapeutic potential to patients with spontaneous presence of T cells in the tumor microenvironment.

In addition, high expression levels of various antiviral defense genes including DDx58, which encodes the cytosolic RNA receptor RIG-I, have been linked to durable clinical responses to CTLA-4 blockade in melanoma patients, suggesting a potential link between these two distinct pathways. Yet, little is known about how RIG-I signaling in the tumor / host impacts on the efficacy of anti-CTLA-4 checkpoint blockade.

To address how activation of the RIG-I pathway in tumor and/or host immune cells within the tumor microenvironment may affect the efficacy of CTLA-4 blockade, this work was designed to answer the following questions:

(1) Do tumor and / or host RIG-I signaling influence the therapy efficacy of CTLA-4-mediated immune checkpoint blockade?
(2) If so, what are the signaling and adapter proteins and the cellular and molecular effector mechanisms involved?
(3) What is the role of RIG-I-induced immunogenic tumor cell death in the efficacy of anti-CTLA-4 immunotherapy?

2 MATERIALS AND METHODS

2.1 Materials

2.1.1 Technical equipment

Accu jet pro	Brand, Wertheim, Germany
Balance (Si-64)	Denver Instruments, Bohemia, USA
Cat RM5	CAT, Ballrechten-Dottingen, Germany
Cell culture CO_2 incubator	Binder, Tuttlingen, Germany
Cell culture laminar flow HERASafe KS	Thermo Fisher Scientific, Walham, USA
Centrifuge 5417 R	Eppendorf, Hamburg, Germany
Centrifuge 5810 R	Eppendorf, Hamburg, Germany
FACSAria II, FACSCanto II	Becton Dickinson, San Jose, USA
Innova 4000 Incubator Shaker	New Brunswick Scientific, New Jersey, USA
INTAS ADVANCED ECL Imager	INTAS Science Imaging
LightCycler 480 II	Roche, Mannheim, Germany
Microscope Axiovert 40 C	Zeiss, Jena, Germany
Mithras LB940 multilabel plate reader	Berthold, Bad Wildbad, Germany
MyCycler Thermal Cycler System	Biorad, Berkeley, USA
Nanodrop ND-1000	NanoDrop, Wilmington, USA
Polymax 204	Heidolph, Schwabach, Germany
Refrigerators (4°C, -20°C, -80°C)	Siemens, München, Germany
Tecan Sunrise	Tecan Group, Männedorf, Switzerland
Thermomixer comfort	Eppendorf, Hamburg, Germany
Vacusafe Vaccum Pump	Integra, Biebertal, Germany
Vortex Genie 2	Scientific Industries, Bohemia, USA
Water bath WB14	Memmert, Schwabach, Germany

2.1.2 Chemicals, reagents and buffers

Albumin Fraktion V	Roth, Karlsruhe, Germany
Aqua	Braun, Melsungen, Germany
Chloroform	Sigma Aldrich, St. Louise, USA
Dimethyl sulfoxide (DMSO)	Sigma Aldrich, St. Louise, USA
Dulbecco's PBS (1x)	Sigma Aldrich, St. Louise, USA
Ethylenediaminetetraacetic acid (EDTA)	Promega, Madison, USA

FastDigest BpiI	Thermo Fisher Scientific, Walham, USA
Filtrated Bovine serum albumine (FBS)	PAN, Aidenbach, Germany
G-Dex RBC Lysis Buffer	intron, Sangdaewon-Dong, Korea
Isoflurane (Forene®)	Abbott, Zug, Switzerland
Lipofectamine 2000	invitrogen, Carlsbad, USA
Paraformaldehyde (PFA)	Fisher Scientific, Schwerte, Germany
Percoll (density 1.129 g/ml)	GE Healthcare, Uppsala, Schweden
Pierce RIPA Buffer	Thermo Fisher Scientific, Walham, USA
Plasmid-Safe DNase	Biozym Scientific, Oldendorf, Germany
Ponceau S solution	Sigma Aldrich, St. Louise, USA
T4 DNA Ligase	New England Biolabs, Ipswich, USA
TRIzol Reagent	Thermo Fisher Scientific, Walham, USA
Trypan blue (0.4%)	gibco life technologies , Carlsbad, USA
Trypsin (0.05%)	gibco life technologies , Carlsbad, USA
TWEEN 20	Sigma Aldrich, St. Louise, USA

ELISA coating buffer

0.2 M sodium phosphate

in H_2O

pH 6.5

ELISA assay diluent

10% FCS

in PBS

pH 7.0

ELISA wash buffer

0.05% Tween 20

in PBS

Lämmli-Buffer

0.5 M Tris/HCL

25% Glycerol

10% β-Mercaptoethanol

5 % SDS

Bromphenol blue

H_2O

Running Buffer 10x

30 g Tris pure

144 g Glycerin

20% SDS

1l H_2O

Stripping – Buffer
62.5 mM Tris/HCL
20% SDS
β-Mercaptoethanol
in H_2O
pH 6.8

TBS 10x
24 g Tris pure
80 g NaCl
in 800 ml H_2O
pH 7.4

TBST 10x
24 g Tris pure
80 g NaCl
2.5 ml Tween
in 800 ml H_2O
pH 7.4

Transfer Buffer
480 mM Tris
390 mM Glycerin
10 % SDS
in H_2O

LB-medium
10 g NaCL
10 g Trypton
5 g Yeastextract
1l H_2O

2.1.3 Cell culture materials, reagents and media

β-Mercaptoethanol	gibco life technologies, Carlsbad, USA
Dulbecco's modified Eagle´s medium (DMEM), high glucose	gibco life technologies, Carlsbad, USA
Fetal calf serum (FCS)	PAN Biotech, Aidenbach. Germany
In vivo-jetPEI	polyplus, Illkirch-Graffenstaden, France
L-glutamine 200mM	gibco life technologies, Carlsbad, USA
MEM-NEAA (non-essential amino acids)	gibco life technologies, Carlsbad, USA
Minimum Essential Medium Eagle	gibco life technologies, Carlsbad, USA
Nuclease-Free Water	Promega, Madison, USA
OptiMEM + GlutaMAX	gibco life technologies, Carlsbad, USA
Penicillin / Streptomycin (100x)	gibco life technologies, Carlsbad, USA
Phosphate buffered saline (PBS)	Sigma Aldrich, St. Louise, USA
Roswell Park Memorial Institute (RPMI) 1640 medium	gibco life technologies, Carlsbad, USA

RPMI complete medium
10% FCS
2 mM L-glutamine
100 IU/ml penicillin
100 µg/ml streptomycin
1 % β-mercaptoethanol
in RPMI 1640

DMEM complete medium
10% FCS
2 mM L-glutamine
100 IU/ml penicillin
100 µg/ml streptomycin

Cryo medium
90% FCS
10% DMSO

Blocking antibodies:

Description	**Isotype**	**Clone**	**Distributor**
Anti-CTLA4	Syrian Hamster IgG	9H10	BioXCell
Anti-PD1	Rat IgG2a	RMP1-14	BioXCell
Anti-CD4	Rat IgG2b	GK1.5	BioXCell
Anti-CD8α	Rat IgG2b	2.43	BioXCell
Anti-NK1.1	Rat IgG2a	PK136	BioXCell

Disposable plastic materials for cell culture experiments were purchased from Becton Dickinson (Heidelberg, Germany), Braun (Melsungen, Germany), (Eppendorf (Hamburg, Germany), Falcon (Heidelberg, Germany), Hartenstein (Würzburg, Germany) Nunc (Rochester, USA), Sarstedt (Nümbrecht, Germany), Thermo Scientific (Walham, USA) or TPP (Trasadingen, Switzerland), VWR (Ismaning, Germany).

2.1.4 Oligonucleotides and other stimuli

5-Azacytidine	Sigma Aldrich, St. Louise, USA
Etoposide	Sigma Aldrich, St. Louise, USA
ISD	Sigma Aldrich, St. Louise, USA
LPS	invivogen, San Diego, USA

Necrostatin	Selleckchem, Houston, USA
Nigericin sodium salt	Sigma Aldrich, St. Louise, USA
Recombinant murine TNF-α	PeproTech, Rocky Hill, USA
Shikonin	Sigma Aldrich, St. Louise, USA
SMAC mimetic 164	ApeXBio, Hsinchu City, Taiwan
SMAC mimetic LCL-161	Roche, Mannheim, Germany
Staurosporine	Sigma Aldrich, St. Louise, USA
z-VAD FMK	invivogen, San Diego, USA

Listing of all oligonucleotides used in this work:

Description	**Nucleotide sequence (5' --> 3')**
5´triphosphate RNA	UCAAACAGUCCUCGCAUGCCUAUAGUGAGUCG
ISD	TACAGATCTACTAGTGATCTATGACTGATCTGTACATGATCTACA

2.1.5 Kits

RNA isolation, reverse transcription, qRT-PCR

RNeasy mini isolation kit	Qiagen, Hilden, Germany
Super Script II reverse transcriptase kit	invitrogen, Carlsbad, USA
qPCR Core kit for SYBR Green	eurogentec, Seraing, Belgium
Universal ProbeLibrary	Roche, Mannheim, Germany

Cytokine ELISA sets (Ready-SET-Go!)

IL-1β murine	invitrogen, Carlsbad, USA
IL-6 murine	invitrogen, Carlsbad, USA
IL-12p70 murine	invitrogen, Carlsbad, USA
IFN-γ murine	invitrogen, Carlsbad, USA
TNF-α murine	invitrogen, Carlsbad, USA

Cytokine ELISA antibodies

Description	Antibody type	Clone	Distributor
Rat anti-mouse IFN-α (Mab)	Capture Ab	RMMA-1	PBL
Anti-IFN-α (polyclonal)	Detection Ab		PBL
Rat anti-mouse IFN-β (Mab)	Capture Ab	RMMB-1	PBL
Anti-IFN-β (polyclonal)	Detection Av		PBL
Goat anti-rabbit IgG HRP (Pab)	Enzyme		Abcam

Protein determination and Western Blot detection kits

Pierce BCA Protein Assay Kit	Thermo Fisher Scientific, Walham, USA
ECL Select Western Blotting Detection Reagent	GE Healthcare, Buckinghamshire, Great Britain
SuperSignal West Pisco Chemiluminescent Substrate	Thermo Fisher Scientific, Walham, USA

Cell death staining and intracellular staining kits for flow cytometry

CaspGlow Flourescein Active Caspase-3 staining kit	invitrogen, Carlsbad, USA
CellTiter-Glo Luminescent Cell Viability Assay Kit	Promega, Madison, USA
Annexin V Apoptosis Detection Kit	Thermo Fisher Scientific, Walham, USA
FIX & PERM Cell	Thermo Fisher Scientific, Walham, USA

Fixation & Cell Permeabilization Kit

APO-BRDU Kit	Becton Dickinson, San Jose, USA
Bio-Plex Cell Lysis Kit	Biorad, München, Germany

Nucleic acid purification systems

Wizard SV Genomic DNA Purification System	Promega, Madison, USA
MEGAshortscript T7 Transcription Kit	Thermo Fisher Scientific, Walham, USA

2.1.6 FACS antibodies

Description	Isotype	Clone	Distributor
anti-CD3	Rat IgG2b, κ	17A2	biolegend
anti-CD4	Rat / IgG2b, κ	GK1.5	ebioscience
anti-CD11b	Rat IgG2b, κ	M1/70	biolegend
anti-CD11c	Armenian Hamster IgG	N418	ebioscience
anti-CD8a	Rat / IgG2a, κ	53-6.7	biolegend
anti-CD45	Rat IgG2b, κ	30-F11	biolegend
anti-CD64	Mouse IgG1, κ	X54-5/7.1	biolegend
anti-CD80 (B7-1)	Armenian Hamster IgG	16-10A1	biolegend
anti-CD86 (B7-2)	Rat / IgG2a, κ	GL1	ebioscience
anti- CD103	LOU/M IgG2a, κ	M290	BD Pharmigen
anti-FOX3	Rat IgG2b, κ	MF-14	biolegend
anti-GranzymeB	Rat / IgG2a, κ	NGZB	ebioscience
anti-IFNγ	Rat / IgG1a, κ	XMG1.2	biolegend
anti-Ly6C	Rat IgG2c, κ	HK1.4	biolegend

anti-mouse H-Kb bound to SIINFEKL	Mouse IgG1, κ	25-D1.16	biolegend
anti-MHC II (I-A/I-E)	Rat IgG2b, κ	M5/114.15.2	biolegend
anti-NK1.1	Mouse IgG2a, κ	PK136	biolegend
anti-PD-L1	Rat IgG2b, κ	10F.9G2	biolegend

2.1.7 CRISPR/Cas9 Single guide RNA target sequence

DDX58 (RIG-I)	5′-GGCTGATGAGGATGATGGAGCGG-3′
TMEM173 (STING)	5′-CAGTAGTCCAAGTTCGTGCG-3′
IRF3	5′-GCATGGAAACCCCGAAACCG-3′
IRF7	5′-CTACGACCGAAATGCTTCCA-3′
Casp-3	5′-CGGGGTACGGAGCTGGACTG-3′
MLKL	5′-GATGCAGTTGCAAATTAGCG-3′

2.1.8 Quantitative real-time PCR primer

2.1.8.1 ERV mRNA primer sequence

eMLV spliced fwd	5′-CCAGGGACCACCGACCCACCG-3′
eMLV spliced rev	5′-TAGTCGGTCCCGGTAGGCCTCG-3′
MMTV spliced fwd	5′-AGAGCGGAACGGACTCACCA-3′
MMTV spliced rev	5′-TCAGTGAAAGGTCGGATGAA-3′
xMLV fwd	5′-TCTATGGTACCTGGGGCTC-3′
xMLV rev	5′-GGCAGAGGTATGGTTGGAGTAG-3′
pMLV / mpMLV common fwd	5′-CCGCCAGGTCCTCAATATAG-3′
pMLV rev	5′-AGAAGGTGGGGCAGTCT-3′

mpMLV rev	5′-CGTCCCAGGTTGATAGAGG-3′
GLN fwd	5′-TGTGTAAGTCCAGACGCAG-3′
GLN rev	5′-CCAACCTACTCCAAAAACAG-3′
IAP fwd	5′-AAGCAGCAATCACCCACTTTGG-3′
IAP rev	5′-CAATCATTAGATGCGGCTGCCAAG-3′
MMERVK fwd	5′-CAAATAGCCCTACCATATGTCAG-3′
MMERVK rev	5′-GTATACTTTCTTCTTCAGGTCCAC-3′
MusD / EnTII common fwd	5′-GTGCTAACCCAACGCTGGTTC-3′
MusD rev	5′-CTCTGGCCTGAAACAACTCCTG-3′
ETnII rev	5′-ACTGGGGCAATCCGCCTATTC-3′
Mervl Pol fwd	5′-ATCTCCTGGCACCTGGTATG-3′
Mervl Pol rev	5′-AGAAGAAGGCATTTGCCAGA-3′
Actin fwd	5´-CACACCCGCCACCAGTTCG-3′
Actin rev	5´-CACCATCACACCCTGGTGC-3′
IFNβ rev	5´-ATAAGCAGCTCCAGCTCCAA-3′
IFNβ fwd	5´-GCAACCACCACTCATTCTGA-3′

2.1.8.2 TIL mRNA primer sequence

mIFNG1 fwd	5′-ATCTGGAGGAACTGGCAAAA-3′
mIFNG1 rev	5′-TTCAAGACTTCAAAGAGTCTGAGG-3′
mGZMB fwd	5′-TGCTGCTCACTGTGAAGGAA-3′
mGZMB rev	5′-TTACCATAGGGATGACTTGCTG-3′
mCCL5 rev	5′-TGCCCACGTCAAGGAGTATTT-3′
mCCL5 fwd	5′-TCGAGTGACAAACACGATGC-3′

mPerforin fwd	5′-CAAGGTAGCCAATTTTGCAGC-3′
mPerforin rev	5′-GGCGAAAACTGTACATGCGAC-3′
mICOS fwd	5′-GCACTGGAGGAGAAGACTGC-3′
mICOS rev	5′-GAAGACAAAGACACGGCAGAA-3
mLAG3 fwd	5′-CCGGGCCATAGAGGAGAT-3′
mLAG3 rev	5′-AGCAGTCCCAGAAGCAAAAA-3′
mHAVCR2 fwd	5′-TTTTCAGGTCTTACCCTCAACTG-3′
mHAVCR2 rev	5′-CATAAGCATTTTCCAATGACCTT-3′
mPDCD1 fwd	5′-TGCAGTTGAGCTGGCAAT-3′
mPDCD1 rev	5′-GGCTGGGTAGAAGGTGAGG-3′

2.1.9 Western blot antibodies

2.1.9.1 Western blot primary antibodies

Target (m)	**Isotype**	**Clone**	**Distributor**
RIG-I	Rat IgG2a	SS1A	Enzo
RIPK1	Mouse IgG2a	38/RIP	BD
RIPK3	Rabbit IgG	Polyclonal	ProSci
Caspase-8	Rabbit IgG1	Polycloncal	Cell Signaling
MLKL	Rat IgG	3H1	Merck Millipore
pMLKL	Rabbit IgG	Polycloncal	Cell Signaling
β-Actin	Rabbit IgG	13E5	Cell Signaling

2.1.9.2 Western blot HRP-linked secondary antibodies

Target (m)	Isotype	Clone	Distributor
Mouse IgG	Horse IgG	Polyclonal	Cell Signaling
Rabbit IgG	Goat IgG	Polyclonal	Cell Signaling
Rat IgG	Goat IgG	Polyclonal	Cell Signaling

2.1.10 Software

Adobe Illustrator CS3	Adobe System, San Jose, USA
Endnote X7	Thompson Reuter, Carlsbad, USA
FlowJo V10	Tree Star, Ashland, USA
Microsoft Office 2016	Microsoft, Redmond, USA

2.2 Animal experimentation

2.2.1 Mice

Female C57Bl/6j and BALB/c mice were purchased from Janvier labs. Mice genetically deficient in MAVS, IFNaR1, Batf3, STING (Tmem173/STING$^{gt/gt}$) and CD11c-DTR transgenic mice have been described previously (Hildner et al., 2008; Jung et al., 2002; Muller et al., 1994; Sauer et al., 2011; Seth, Sun, Ea, & Chen, 2005). CD11c-DTR, IFNaR-deficient mice, MAVS deficient mice and Batf3 deficient mice were kindly provided by Prof. D. Busch (Department of Medical Microbilology, Klinikum Rechts der Isar, Technical University Munich, Germany) and Prof. U. Kalinke (TWINCORE, Department for Experimental and Clinical Infection Research, Hannover, Germany) and Prof. Dr. K. Hildner (Department for Pneumology and Immunology, Erlangen, Germany). Mice genetically deficient in STING were purchased from The Jackson Laboratory. Mice were 6 to 12 weeks of age at the onset of experiments and maintained in specific pathogen free conditions. Wild-type and genetically deficient mice included in the same experiments were co-housed for at least four weeks before onset of experiments or were bred as littermates. All animal studies have been approved by the local regulatory agency (Regierung von Oberbayern, Munich, Germany).

2.2.2 Isolation of tumor-infiltrating leukocytes

Mice were anesthetized and sacrificed by cervical dislocation. Subcutaneous tumors were removed using forceps and surgical scissors and minced into small pieces. Tumor slices were pressed through a 100 µm nylon strainer to disintegrate tissue structure and further homogenized by repeated pipetting. The tumor cell suspensions were then washed in complete RPMI medium and purified on a 30 % Percoll gradient (500 G, 15 minutes, 4°) to eliminate dead cells and tumor cell debris and further to separate tumor-infiltrating lymphocytes from denser cell populations such as tumor cells. For lymphocyte purification, the cell pellets were suspended in 4 ml of 40% Percoll and layered onto 4 ml of 80% Percoll, then centrifuged (2.200 rpm, 20°C, 30 min) and the interphase containing the leucocyte fraction was extracted, washed in PBS and kept in RPMI complete medium on ice for subsequent experiments.

2.2.3 Isolation of lymph node cells

Mice were sacrificed by cervical dislocation after anaesthetization with isoflurane. Tumor-draining inguinal lymph nodes were resected with forceps and surgical scissors. For disintegration of tissue structure, lymph nodes were mashed through a 100 µm cell strainer. The single cell solutions were centrifuged (400 G, 5 minutes, 4°) and re-suspended in complete RPMI and kept on ice for subsequent experiments.

2.2.4 Measurement of cytokine concentrations in tumor tissue

For the determination of proinflammatory cytokine and IFN-I concentrations in whole tumor tissue, mice were subcutaneously inoculated with B16.OVA cells as indicated in chapter 2.2.7. When tumors became palpable, 3pRNA or the vehicle control was injected into the right-sided tumors. 24 h later, bilateral tumor tissue was removed and snap-frozen in liquid nitrogen. Frozen tumors were mechanically disrupted using a precooled mortar and pestle. The shredded tissue was then suspended in Bio-Plex™ Cell Lysis Buffer and vortexed for 30 seconds. Homogenized tissue lysates were spun down at 20.000 G for 30 min at 4°C, and supernatants were kept for further analysis.

2.2.5 Immunostimmulation of mice

2.2.5.1 Selective activation of cytosolic pattern recognition receptors

Double-stranded in vitro-transcribed 5' triphosphate RNA (3pRNA) was used as defined RIG-I stimulus and was generated as previously described (Poeck et al., 2008). Also, single-strand oligonucleotides for Interferon Stimulatory DNA (ISD), a specific ligand for STING signaling, were purchased from Sigma-Aldrich and annealed by heating to 75 °C for 30 minutes and subsequent re-cooling to room temperature. Either 25 µg 3pRNA or 50 µg ISD were mixed with 3.5 µl *in vivo*-jetPEI® - a liposomal transfection reagent - in a volume of 50 µl 5% glucose solution. The reaction mixture was then incubated for 15 min at RT to allow the formation of stable complexes ensuring protection against enzymatic degradation and subsequently an effective *in vivo* delivery by intratumoral injection. Stimulants were injected into the right-sided flank tumor when subcutaneous tumors were palpable and reached an average size ranging 50 mm^3 to 75 mm^3. Treatment was repeated twice in an interval of three days.

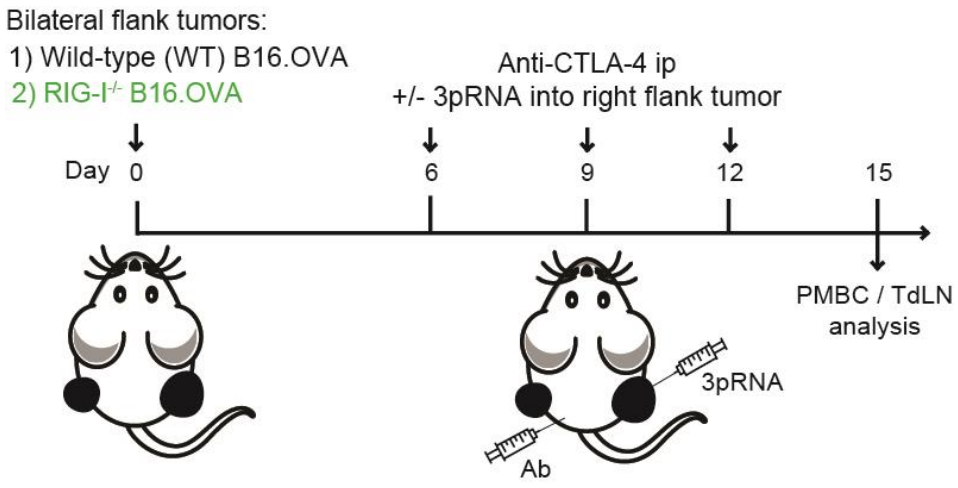

Figure 2.1: Treatment scheme. Mice were implanted with either wild-type (WT) or RIG-I-deficient (RIG-$I^{-/-}$) B16.OVA cells in each flank; right-sided tumors were induced with more B16.OVA cells to facilitate a faster growth dynamic in comparison to left. Anti-CTLA-4 or isotype control antibodies were administered intraperitoneally (ip). Some mice were repeatedly injected with the RIG-I ligand 3pRNA into the right-sided ('local') tumor.

2.2.5.2 Immune checkpoint blockade

To assess the immunotherapeutic potential of monoclonal antibody-mediated checkpoint blockade by itself or in combination with particular PRR ligands *in vivo,* distinct monoclonal blocking antibodies were applied systemically by intraperitoneal injection. For investigation of the role of either CTLA-4 or PD-1 in a model of malignant melanoma, 200 µg of the respective blocking antibody were injected in a volume of 400 µl PBS intraperitoneally. Animals in the control groups received the adequate isotype antibodies. Treatment was carried out according to the protocol applied for immunostimmulation and boosted by two additional injections of 100 µg antibody respectively.

2.2.5.3 Tumor irradiation

In some experiments, radiotherapy was used as an inducer of tumor cell death. Tumor cells were inoculated as described in chapter 2.2.6 and irradiated when tumor volumes reached an average size from 50 mm^3 and 75 mm^3. The mice were initially anesthetized by intraperitoneal injection of an anesthetic mixture containing 1.0 mg/kg midazolam, 0. 5 mg/kg medetomidine and 0.1 mg/kg fentanyl, fixated under a lead shield to restrict irradiation to tumor tissue and irradiated once with 20 Gy as described previously (Deng, Liang, Xu, et al., 2014). Irradiation was combined with anti-CTLA-4 checkpoint blockade. The blocking antibody or the appropriate isotype controls were administered intraperitoneally on day 6, 9 and 12. Tumor growth and overall survival were assessed daily.

2.2.5.4 Acazytidine treatment

To assess the basal activation of tumor intrinsic RIG-I signaling by continuous low-level detection of ERVs within tumor cells, the mice were inoculated subcutaneously with B16.OVA WT cells or the respective RIG-I deficient clone and treated with intratumoral injections of the DNA methyltransferase inhibitor 5-acazytidine with a concentration of 5 µg in 50 µl PBS. Treatment was applied on 5 consecutive days and the therapy cycle repeated after 3 days. The 5-azacytidine treatment was additionally combined with anti-CTLA-4 checkpoint blockade. Blocking antibodies or the appropriate isotype control antibody were injected intraperitoneal on day 6, 9 and 12 and mice monitored for tumor growth and ongoing survival every day.

2.2.6 Depletion of immune cell subsets

For closer examination of defined immune cell subsets and their impact on therapy outcome, mice received monoclonal depleting antibody injections intraperitoneally. To deplete either T cells or NK cells, 100 µg of monoclonal antibodies targeting anti-CD8α (clone 2.43), anti-CD4 (clone GK1.5) or NK1.1 (clone PK136) were administered two days before onset of tumor challenge followed by injection of 50 µg antibody twice a week throughout the experiment. For determination of depletion efficiency, whole blood was obtained by a buccal bleed, processed as outlined in chapter 2.4.4, stained for respective markers and analyzed by FACS.

2.2.7 Tumor experiments

In order to assess local and systemic therapy effects and to determine continuous survival a bilateral flank tumor model was established. Mice were shaved at the site of injection and Ovalbumin-transduced B16 melanoma cells (B16.OVA) as well as respective CRISPR KO clones were injected as described in the following. 2.4 x 10^5 B16.OVA cells, in a volume of 50 µl PBS, were injected subcutaneously into the right flank and 0.8 x 10^5 into the left flank. Successful tumor cell delivery between two skin layers was ensured by formation of a bleb. The identical procedure was applied for 4T1 mamma carcinoma cells and C26 colon carcinoma cells. For experiments with non-immunogenic B16.F10 cells, mice were inoculated subcutaneously with 1 x 10^5 cells in both flanks, whereas 1 x 10^6 cells were injected into the right sided flank and 5 x 10^5 cells into the left flank for studies with PancO2 pancreatic adenocarcinoma and EL4 lymphoma cell lines,. Therapy was started when tumors reached an average size ranging from 50 mm^3 to 75 mm^3 and was applied as indicated in chapter 2.2.5. Tumor volumes were measured daily and animals were euthanized when showing signs of distress or when the maximum tumor diameter exceeded 15 mm according to standard legal procedure (responsible state office Regierung von Oberbayern). For analysis of tumor-infiltrating lymphocytes, cytokine concentration in whole tumor tissue, histology experiments and intratumoral TUNEL assays, 5 x 10^5 cells were inoculated in both flanks respectively. For re-challenge experiments, mice were injected with 5 x 10^5 B16.OVA cells in a volume of 200 µl PBS intravenously into the tail vain. Animals were sacrificed on day 18 after tumor cell inoculation and superficial pulmonary pseudo-metastases were counted.

The length (the longest dimension) and width (the distance perpendicular to the length) of each tumor was measured with a Vernier caliper and calculated using the formula for an ellipsoid volume: volume (mm^3) = $\frac{\pi}{6}$ x [(length + width)/2]^3

2.3 Cell culture

2.3.1 B16 melanoma cell line

B16.F10 murine melanoma cells and the B16 melanoma cell line expressing the chicken egg white protein ovalbumin (OVA) were kindly provided by Prof. Marcel R.M. van den Brink (New York, USA). This B16 melanoma cell line of C57BL/6 background was created by transfecting the parental B16.F10 cell line with a cDNA encoding the ovalbumin gene (Linardakis et al., 2002). All B16 cell lines and respective CRISPR Cas KO clones were cultured in complete DMEM medium. Cell density, signs for cell death and microbial contaminations were checked repeatedly by light microscopy. Tumor cells were regularly transferred to new culture flasks by aspirating culture medium, washing the adherent cells with PBS and further detaching them with 1% trypsin-EDTA solution at 37°C in an incubator. Trypsin was inactivated by adding serum-containing complete RPMI and cells were re-seeded after a single washing step with complete RPMI medium. Possible mycoplasmatic contaminations were excluded by frequently repeated testing.

2.3.2 Additional cancer cell lines

Other tumor cell lines used for this work were cultured as stated below and used for *in vivo* assays as indicated in chapter 2.2.7. 4T1 cells, C26 cells, EL-4 cells, PancO2 cells and L929 cells were a kind gift from Prof. M. Schnurr (Department for Clinical Pharmacology, Klinikum der Universität München, Germany), Prof. J. Ruland (Department of Clinical Chemistry and Pathobiochemistry, Klinikum Rechts der Isar, Technical University Munich, Germany), Prof. D. Busch (Department of Medical Microbilology, Klinikum Rechts der Isar, Technical University Munich, Germany) and Prof. Marcel R.M. van den Brink (Memorial Sloan Kettering Institute, New York, USA).

Tumor cell line	Tissue	Morphology	Culture Properties	Strain	Culture medium
4T1	mammary gland	epithelial	adherent	BALB/cfC3H	cRPMI
C26	colon	fibroblast	adherent	BALB/c	cRPMI
EL-4	T lymphocyte	lymphoblast	suspension	C57BL/6N	cDMEM
L929	connective tissue	fibroblast	adherent	C3H/An	cDMEM
PancO2	pancreas	fibroblast	adherent	C57BL/6N	cDMEM

2.3.3 Cell maintenance

2.3.3.1 General culture conditions and testing for cell viability

All cell lines used for this study were cultured in incubators at 37°C, 5% CO_2/air mixture and 95% atmospheric humidity using pretreated disposable tissue culture flasks. Manipulations of all in vitro assays and reagents were carried out using sterile techniques and performed under a laminar flow hood. To determine viability and cell numbers for plating, *in vivo* assays and transfection reactions, cells were tested by trypan blue exclusion using a Neubauer hemocytometer. A feature of dying cells is a decreased membrane integrity that allows the absorption of the dye. In contrast, trypan cannot penetrate living cells, thus dead cells can be excluded under the light microscope due to their blue intracellular staining. To determine the density per ml of a single cell suspension the following formula was used:

$$\text{Cells (per ml)} = \text{mean cell count} \times \text{dilution factor} \times 10^5$$

2.3.3.2 Long term storage and liquid nitrogen recovery

For optimal long-term storage, cells were kept in liquid nitrogen. The growth medium was removed from culture flasks and the cells washed with PBS. Cells were then detached with trypsin and enzyme activity was stopped by adding FBS containing growth medium. After a single washing step, supernatant was discarded and the cell pellet re-suspended in freezing medium to a density of 2×10^6 cells per ml. Cryovials were placed in a freezing

container to guarantee a 1°C/min cooling rate which is required for optimal cryopreservation of cells. After freezing for 24h, vials were transferred into liquid nitrogen for long-term storage.

For gentle recovery, cells were removed from storage and quickly thawed in a temperature controlled water bath at 37°C. 9 ml of pre-warmed culture medium were added to 1 ml of cell-containing freezing medium and centrifuged at 400g for 5 min at 4°C. The supernatant was removed, the cell pellet re-suspended in fresh growth medium and transferred to a cell culture flask.

2.3.4 Stimulation of tumor cells *in vitro*

To analyze the induction of tumor cell death and its nature by defined immune stimulants *in vitro*, various tumor cell lines were transfected with either nucleic acids, 5-azacytidine or defined cell death inducers. Nucleic acid transfection was carried out as described in the following. Oligonucleotides and the transfection reagent were prepared in two separate reaction mixtures. 3 µg of RNA or 6 µg of DNA were adjusted to a volume of 10 µl by adding OptiMEM medium. Twice the volume of Lipofectamin 2000, as used for 3pRNA or ISD, was utilized and adjusted to 10 µl with OptiMEM medium. Both reaction mixtures were mixed thoroughly and incubated at RT for 15 minutes for complexation. 20 µl of the master mix was applied directly into the cell culture medium and incubated at 37°C for the indicated time.

5-azacytidine was dissolved in complete medium at concentrations between 10 µM and 1 mM. 24h before onset of experiments, cells were seeded into appropriate culture plates to allow settling. For stimulation, medium was aspirated and replaced by stimulation medium, incubated at 37°C for 24 hours and subsequently analyzed for gene expression and the induction of cancer cell death. In order to assess the nature of tumor cell death, pre-seeded cells were incubated with specific cell death inducers. For the induction of apoptosis, cells were either incubated with 100 µM etoposide for 6 hours or 20 ng/ml TNF-α and 100 nM SM-164 for 4 hours depending on the cell line. To initiate necroptosis, cells were pretreated for 30 minutes with 20 ng/ml of the pan-caspase inhibitor Z-VAD FMK before the induction of cell death with either 20 ng/ml TNF-α and 100 nM SM-164 for 4 hours or 2.5 µmol of Shikonin for 12 hours. Appropriate controls were prepared using Z-VAD FMK and Necrostatin-1, a defined inhibitor for TNF-α-induced necroptosis. After stimulation, cells were subsequently analyzed by immune blotting, FACS analysis or ATP release.

2.3.5. Histological analysis

2.3.5.1 Preparation of whole tumor tissue

Tumor samples were fixed in 10% neutral-buffered formalin solution for a minimum of 48 hours, dehydrated under standard conditions and embedded in paraffin. Serial 2µm-thin sections prepared with a rotary microtome were collected for histological and immunohistochemical analysis. Hematoxylin-Eosin (H.-E.) staining was performed on deparaffinized sections with Eosin and Mayer's Haemalaun according to standard protocols.

2.3.5.2 Immunohistochemical staining procedure and evaluation

Slides were deparaffinized in xylene and rehydrated with alcohol washes of decreasing concentration (100%, 96%, 70%). After heat-induced antigen retrieval, unspecific protein and peroxidase binding was blocked with 3% hydrogen peroxide and 3% goat (cleaved Caspase 3) or 3% rabbit (CD8) serum. Immunohistochemistry was performed with a Dako autostainer using antibodies against CD8a (clone GHH8) and cleaved Caspase 3 (Asp175). Antibodies were detected by using the Dako Envision-HRP rabbit labeled polymer for cleaved Caspase 3 and a biotinylated secondary rabbit anti-rat antibody incubated with Streptavidin Peroxidase for CD8. Antibody binding was visualized with diaminobenzidine (DAB) giving a brown precipitate. Counterstaining was performed using hematoxylin and slides were dehydrated by applying alcohol washes of increasing concentration (70%, 96%, 100%) and xylene and were finally coverslipped using Pertex® mounting medium. Stained slides were scanned with an automated slide scanner and evaluated by using the Aperio Imagescope software. Immunohistochemical stainings were evaluated by documenting the percentage of tumor tissue covered by CD8 positive cells for localization (tumor periphery vs. central part of the tumor tissue). For cleaved caspase 3, the number of positive cells within 5 low power fields (435.000 μm^2) as well as a set of 5 high power fields of view, so called hot spot areas, was evaluated in tumor periphery and central part of the tumor.

2.4 Immunological methods

2.4.1 Flow cytometry

Fluorescent activated cell sorting (FACS) is a specialized form of flow cytometry and a common laboratory technique applied for counting cells or microscopic particles from heterogeneous suspensions. It is also used to examine the expression levels of cell surface and intracellular molecules, to assess purity of isolated cell subpopulations and to analyze cells and particles according to size and volume. Moreover, cells can be sorted by FACS analysis according to specific properties. Before staining, a single cell suspension needs to be prepared from cell culture or tissue samples. Cellular antigens of interest can be visualized and detected by binding fluorochrome-conjugated antibodies. The cell suspension is aspirated into the flow cell were it is hydrodynamically focused by the sheath fluid stream, causing the cells to pass through a tiny nozzle and past a laser beam one-by-one. Incoming light is either absorbed by the cell or scattered from it. When a fluorochrome is excited with the corresponding excitation wavelength light is re-emitted as fluorescence if the cell either contains a naturally fluorescent substance or if one or more fluorochrome-conjugated antibodies are attached to surface or intracellular structures of the cell. Scattered light of cells passing through the laser beam can be either detected as forward scatter (FSC) or side scatter (SSC) depending on the cells size and shape. The FS correlates with the relative cell size whereas the SSC depends on the granularity of the cell. Forward and side scattered light as well as the fluorescence signals are split into defined wavelengths and channeled through various filters and mirrors that block certain wavelengths whilst transmitting others.

2.4.1.1 Multicolor flow cytometry

Flow cytometry analysis was performed with a FACSCanto II and cell sorting with a FACSAria II. The FACSCanto II is equipped with a set of three different lasers. A blue argon-ion laser illuminates cells at a wavelength of 488 nm and therefore supports the detection of the fluorochromes: fluorescein isocyanate (FITC), phycoerythrin (PE) and peridinin chlorophyll protein (PerCP) as well as the Cy7-coupled tandem-dye PE-Cy7. The second red diode laser excites fluorochromes at 633 nm including allophycocyanin (APC) and the tandem-dye APC-Cy7. The third laser, a violet diode laser with an excitation at 405 nm allows the application of the fluorescent dyes Pacific Blue and Pacific-Orange amongst other dyes. Various fluorophores used for flow cytometry share the same emission spectra which can cause spectral overlap when used in the same

assay. This ‘spillover’ of light to photodetectors used for the detection of other dyes can compromise data acquisition. Therefore, a selected combination of appropriate fluorophores was composed for 8-color analysis to minimize spectral overlap.

2.4.1.2 Analysis of cell surface antigens

To analyze cell surface antigens, cells or tissue lysates were prepared according to the respective assay and re-suspended in PBS supplemented with 3% FCS. Up to eight fluorochrome-conjugated monoclonal antibodies directed against antigens of interest were added with a concentration of 1.25 µl/ml and the cells subsequently incubated for 30 minutes at 4°C. After two washing steps with PBS, cells were either re-suspended in PBS supplemented with FCS for subsequent analysis, fixated with 0.5% PFA for intermediate storage or suspended in fixation buffer for staining of intracellular antigens. All staining procedures were carried out in the dark to minimize light exposure. For analysis, flow cytometry data can be illustrated in two ways. On the one hand, surface antigens can be expressed as percentage of cells staining positive for the fluorochrome-coupled antibody directed against the investigated antigen or as mean fluorescence intensity (MFI). The MFI is directly calculated by the flow cytometer as the amount of cell-bound fluorescent dye and thus reflects the expression levels of the antigen of interest.

2.4.1.3 Analysis of intracellular antigens

In some experiments, cells were stained for intracellular antigens such as IFN-γ and the transcription factor FOXP3. Therefore, extracellular antigens were stained as described above (chapter 2.4.1.2). By incubating the cells for 30 minutes at 4°C with the fixation/permeabilization buffer, extracellular bound fluorochrome-coupled antibodies were fixated and the cell membranes permeabilisized to allow antibodies to penetrate the cell. After washing the cells twice with washing buffer, 2.5 µl/ml of the respective antibody was added and the cells incubated at 4°C for at least 1 hour or overnight. Finally, cells were washed twice with PBS supplemented with FCS and subsequently analyzed.

2.4.2 Apoptosis staining

In order to determine apoptosis induction by certain stimulants *in vitro*, cells were stained with the Annexin V and 7-AAD apoptosis detection kit. This assay combines staining of phosphatidylserine (PS) by Annexin V and labeling of nuclear DNA with 7-AAD and therefore allows determination of diverse apoptosis stages. During apoptosis the asymmetric cell membrane structure is lost. Thus PS, which is located on the cytoplasmic membrane of viable cells, is more frequently expressed on the outward membrane. Viable cells with an intact cell membrane are negative for both stainings, whereas early apoptotic cells are positive for PS staining but negative for 7-AAD. Late apoptotic cells and secondary necrotic cells stain positively for both markers. The manufacturer's protocol was modified for staining and carried out as follows:
Cell death was induced with defined stimulants. Supernatant and cells were collected in a 15 ml falcon tube, spun down and washed once with PBS. After an additional washing step with Annexin V Binding Buffer, cell suspensions were stained in Annexin V Binding Buffer by adding 50 µl/ml of each antibody and incubated for 15 minutes at RT in the dark. Samples were diluted 1:4 by adding the appropriate amount of Annexin V Binding Buffer and subsequently analyzed by flow cytometry.

2.4.3 Active Caspase-3 staining

To further characterize the nature of tumor cell death *in vitro*, cleaved caspase-3 was stained according to the manufacturer's protocol. In brief, 5 x 10^4 cells were seeded in a non-tissue treated 24 well culture plate 24 hours prior to stimulation. Apoptosis was induced with distinct stimuli and a negative control prepared by using the specific pan-caspase inhibitor Z-VAD-FMK at a concentration of 20 nM. For analysis, the FITC-conjugated specific Caspase-3 inhibitor DEVD-FMK was directly applied into the culture medium and incubated for 60 minutes at 37°C. Cells were washed from the plate with cold PBS by repeated pipetting. After centrifugation at 3000 g for 5 minutes, the supernatant was discarded and the cell pellet washed twice with PBS. Surface staining with additionally antibodies was applied as indicated in chapter 2.4.1.2 and cells were subsequently analyzed by FACS.

2.4.4 MHC class I tetramer staining

To quantify the systemic T cell response specific for a given antigen, venous blood was drawn from a buccal bleed and collected in a heparinized vacutainer to ensure proper single-cell dissociation. Whole blood was treated with erythrocyte lysis buffer to enrich the lymphocyte fraction and to further reduce background by erythrocytes. Osmotic lysis was stopped by adding FBS containing medium and centrifuged at 400 g for 5 min. The supernatant was aspirated and process repeated once or twice as needed. After washing the cell suspension twice with PBS, staining with commercial purchased MHC class I OVA tetramers was carried out according to the manufacturer's protocol. In brief, 6 µl/ml MHC class I tetramers and additional antibodies for surface staining (2.5 µl/ml) were applied to the cells and incubated at RT for 30 minutes. After two washing steps, cells were suspended in PBS supplemented with 0.5% formaldehyde and were stored at 4°C protected from light for a minimum of 1 hour prior to analysis by FACS.

TRP-2 MHC-I tetramers were kindly provided by Prof. D. Busch and generated using the method developed by (Altman et al., 1996). For each sample, 0.4 µg of purified biotinylated TRP-2 monomers were tetramerized by adding 60 ng of both APC and PE fluorescently-labeled streptavidin in FCS containing PBS and incubation for at least 60 minutes at 4°C in the dark. Leucocytes from whole blood were purified as stated above and FC receptor blocking (5 µl/ml) and Amin staining (1 µl/ml) were applied in PBS and incubated for 20 minutes at 4°C. Cells were washed once with FACS buffer and the MHC tetramer reagent added to the cells and incubated at RT for 30 minutes. After a single washing step, additional antibodies were applied for extracellular surface staining and incubated at 4°C for 30 min. After washing with PBS, cells were fixated by adding 0.5% PFA containing PBS and were analyzed by FACS.

2.4.5 TUNEL assay

Terminal deoxynucleotidyl transferase dUTP nick end labeling (TUNEL) was used for the detection and quantification of apoptotic DNA fragmentation. Tumor cells were extracted from tumors as described in chapter 2.2.2 without further lymphocyte enrichment by density centrifugation. Cell pellets were suspended in 1% paraformaldehyde in PBS at a concentration of 1 x 10^6 cells/ml and kept on ice for 1 hr. After centrifugation at 300 g for 5 min, the supernatant was discarded and the cells were washed twice with PBS. Pellets were suspended in precooled 70% ethanol and stored at -20 °C in the freezer for at least 18 hours prior to staining. For TUNEL analysis, the samples were centrifuged at 300 g

for 5 min and ethanol carefully removed by aspiration. Cells were washed twice with wash buffer and re-suspended in DNA Labeling Solution.

Component	**Volume**
Reaction Buffer	10.00 µl
TdT Enzyme	0.75 µl
Br-dUTP	8.00 µl
Distilled H_2O	32.25 µl

Samples were incubated at 37°C for 60 min and re-suspended by gently shaking every 15 min. At the end of the incubation time, rinse buffer was added and the cells were centrifuged at 300 g for 5 min. Cells were rinsed twice and the cell pellet was re-suspended in 100 µl antibody staining solution and incubated at RT for 30 min protected from light. In addition, 500 µl PI/RNase staining buffer was added to each sample and incubated for another 30 min in the dark at RT before analysis by flow cytometry.

Component	**Volume**
FITC-Labeled Anti-BrdU	5.00 µl
Rinsing Buffer	95.00 µl

2.4.6 Enzyme-linked immunosorbent assay

A highly sensitive and selective method for the detection and quantification of a particular antigen of interest is the enzyme-linked immunosorbent assay (ELISA). Binding the antibody to an analyte subsequently converts a colorless reporter molecule into a colored or luminescent reagent. To investigate the cytokines from murine tumor cell lysates, respective supernatants or whole tumor tissue lysates, a so-called sandwich ELISA was performed. Cytokines, captured by plate-bound antibodies are incubated with a secondary biotinylated antibody bound to a streptavidin molecule conjugated to a peroxidase. The peroxidase enzyme catalyzes the oxidation of tetramethylbenzidine (TMB) with hydrogen peroxide into a blue fluorochrome. All cytokines, except IFN-α and IFN-β were detected with commercially available ELISA kits according to the

manufacturers' protocol. Samples were applied undiluted or diluted 1:10 to 1:1000 depending on the sample type.

A modified protocol was applied for IFN-α and IFN-β measurement: For coating of ELISA detection plates, a capture antibody binding the particular cytokine was diluted in coating buffer (5 µg/ml) and applied to each well. The plates were then incubated on a shaker overnight at 4°C, washed three times and subsequently incubated again with blocking buffer for 3 hour at RT to prevent unspecific binding. After washing the plates several times with washing buffer, the standard protein dilution and samples were applied onto the plates and again incubated overnight at 4°C. The top standard for the IFN-α ELISA was set at 2000 pg/ml and for IFN-β at 2200 pg/ml. All samples were applied undiluted. For detection, the respective antibody was applied in an assay diluent at a concentration of 620 ng/ml and incubated for 3h at RT. After extensive washing, horseradish peroxidase-conjugated F(ab´)2 fragments (15 µg/ml) were added for 3h at RT. After several washing steps, a buffer containing tetramethylbenzidine and hydrogen peroxide served as substrate for the horseradish peroxidase. The enzymatic reaction was stopped by adding sulfuric acid to each well. All ELISA assays were read-out at a wavelength of 450 nm with correctional subtraction at 590 nm.

2.4.7 Cell Viability Assay

The CellTiter-Glo® Luminescent Cell Viability Assay was used for determination of cell viability in culture based assays. Based on the principal that metabolically active cells produce ATP, this assay enables the quantification of viable cells by generating a luminescent signal proportional to the amount of ATP present in the culture medium upon artificially induced cell lysis. Therefore, cell density was adjusted to 12.5 x 10^4 cells/ml and 100 µl per well were seeded in a 96-well plate 24 hours before stimulation. Cells were treated as indicated in chapter 2.3.4. For analysis, 50 µl of supernatant was aspirated and 50 µl of CellTiter-Glo® reagent added. Plates were incubated on an orbital shaker for 15 min at RT for optimal cell lysis and to stabilize the luminescent signal. 95 µl of supernatant were transferred to an opaque-walled 96-well plate and luminescence was measured at an integration time of 1 second per well.

2.5 Molecular biology methods

2.5.1 Isolation of cytoplasmic RNA

To examine RIG-I-dependent changes on gene expression levels in whole tumor tissue after 3pRNA treatment or anti-CTLA4-mediated checkpoint blockade, total cellular RNA was extracted using the RNeasyMini Kit (Qiagen). Therefore, mice were sacrificed and whole tumor tissue was resected and processed as described in chapter 2.2.2 without further purification of tumor cells. Tumor lysates were washed twice with cold PBS and the supernatant carefully removed. Then cell pellets were re-suspended in 300 µl of Trizol and immediately frozen in liquid nitrogen. After thawing on ice, 120 µl of chloroform was added and mixed by inverting the tube several times and incubated at room temperature for 5 minutes. After centrifugation for 15 min at 4°C at maximum speed, the aqueous upper phase was carefully removed, mixed with an equal volume of 100% ethanol and transferred into an RNeasy spin column. After centrifugation at 10.000 g for 20 seconds, the nucleic acids retained in the filter and the flow-through was discarded. Disintegrated DNA and phenol/chloroform residuals were removed in three consecutive washing steps. First, 700 µl of RW1 washing buffer was added and the samples were centrifuged at 10.000 g for 20 seconds. Then 500 µl of RPE buffer were added and probes centrifuged at 10.000 g for 20 seconds. This step was repeated once. Then the RNeasy spin columns were placed into new collection tubes and centrifuged for 1 minute at maximum speed to remove remaining washing buffer. The retained RNA was re-suspended in 30 µl RNase free water and eluted from the filter membrane by centrifugation at maximum speed for 1 minute. Total RNA was either applied for reverse transcription or stored at -80°C for further analysis.

2.5.2 Reverse transcription

Complementary DNA (cDNA) is produced by synthesis of DNA from an RNA template via reverse transcription and can be used directly as a template for polymerase chain reaction (PCR). The annealing mix for reverse transcription was composed of the following: 100 ng Random Primer and 10 mM dNTP mix in RNase free water. 1 µl of previously isolated total RNA was mixed with 11.0 µl of the reaction assay to a final volume of 12 µl. Samples were incubated at 65°C for 5 minutes and then 4.2 µl of first-strand buffer substituted with 0.1 M DTT was added to the probes. After incubation at 25°C for 2 minutes, 0.8 µl of superscript II enzyme was added to each sample and again incubated at 25°C for 10 minutes. Probes were then heated to 42°C for another 50

minutes. In order to prevent interference of the reverse transcriptase with subsequent PCR steps the samples were heated to 70°C for 15 minutes to denaturize the enzyme. cDNA was diluted 1:10 by adding nuclease free water and stored at -80°C for subsequent experiments.

2.5.3 Polymerase chain reaction

2.5.3.1 Functional principle

Polymerase chain reaction is a technique which facilitates the amplification of a specific DNA sequence, a so called template, in a diverse mixture of nucleic acids such as genomic DNA or synthesized cDNA. An optimal reaction requires a thermoresistant DNA polymerase enzyme and a sequence-specific primer pair, which are homologue to the template´s ends. The amplification process is characterized by three repetitive steps. Initially, the DNA double strand is separated in a thermal process (denaturation). In a second step, the primers hybridize with their homologue target sequence on the DNA templates (annealing). In a final step, DNA is synthesized beginning at the primers (elongation). In every following amplification cycle, newly synthesized DNA fragments serve as additional matrices themselves. Thus, multiple amplification rounds provide an exponential accumulation of DNA sequences. Conventional PCR does not allow for a quantification of the initial DNA amount as a linear interval of amplification efficacy is required for this purpose, which, however, gradually declines with every cycle due to exhaustion of reagents and enzyme. Nevertheless, this problem is overcome by quantitative real-time PCR which allows for simultaneous measurement of synthesized DNA in the reaction assay during PCR.

2.5.3.2 Quantitative real-time PCR

Quantitative real-time PCR (qRT-PCR) is a molecular biological assay that is based on the polymerase chain reaction. It is used to amplify and quantify a specific target DNA molecule during the PCR in real time after each amplification cycle. A non-specific fluorescent dye e.g. the asymmetric cyanine dye SYBR Green, is added to the PCR samples. This fluorochrome preferentially intercalates with double-stranded DNA.
Thus the increasing amount of synthesized DNA during PCR leads to a proportional increase in fluorescence intensity which can be measured after each cycle with an appropriate detector. The fluorescence intensity is adjusted according to the number of amplification cycles. To draw a final conclusion of quantitative mRNA expression of the

target gene, the measured copy numbers are normalized to match the copy numbers of a reference gene. A reference or housekeeping gene is typically a ubiquitously expressed gene whose expression is not altered by the experimental manipulations and is additionally measured in every sample. In this work, actin, a multi-functional protein, responsible for the formation of microfilaments, was used as reference gene. All qRT-PCR assays were performed using a qPCR Core Kit for SYBR Green and primers were designed with the help of the Universal ProbeLibrary Assay Design Center (Roche). The following protocol was applied for each assay:

Component	**Volume**	**Final concentration**
10x reaction buffer	5 µl	1x
$MgCl_2$	3.5 µl	3.5 mM
dNTP mix	2 µl	200 µM
Forward primer	5 µl	100 nM
Reverse primer	5 µl	100 nM
HotGoldStar	0.25 µl	0.025 U/µl
Diluted SYBR	1.5 µl	
Water, PCR-grade	22.75 µl	
cDNA	5 µl	

After preparation of the experimental assay in a 96-well plate at RT, all samples were amplified and analyzed on a LightCycler 480 II system using LightCycler 480 II Software 1.5.0 SP4. The thermocycler was programed using the following parameters:

Cycles	**Component**	**Targert temperature**	**Hold time**
1	Pre-Incubation	95 °C	10 min
40	Denaturation	95 °C	15 s
	Annealing	60 °C	20 s
	Elongation	72 °C	40 s
1	Cooling	40 °C	30 s

2.5.4 Quantification of total protein by BCA

In order to determine and adapt the total protein content of either western blot or tumor tissue lysates for further assays, the BCA Protein Assay was applied. This colorimetric assay is based on the reduction of Cu^{2+} to Cu^{1+} by protein in alkaline medium and the subsequent colorimetric switch due to the interaction of the cuprous cation and bicinchonic acid. For analysis in a 96-well format, samples were diluted 1:10 with PBS and a BSA standard series was set up in a working range of 20-2000 µg/ml. The working reagent was prepared in a ratio 1:50 and 25 µl of standard and sample were applied in a single well respectively. 200 µl of the working reagent (sample to working reagent ratio 1:8) was added to each well and mixed thoroughly on a plate shaker for 30 second. The plate was then incubated at 37 °C for 30 minutes, cooled to RT afterwards and the absorbance was measured at 562 nm on a plate reader.

2.5.5 Western Blot analysis

2.5.5.1 Preparation of Western Blot samples

B16.OVA melanoma cells were seeded 24h prior to stimulation in non-tissue treated 6-well plates and stimulated as indicated in chapter 2.3.4. After stimulation, cells were harvested on ice. Therefore, the supernatant was discarded and the cells washed off the culture plate with precooled PBS by repeated pipetting, they were then centrifuged and washed once again with PBS. The supernatant was aspirated and the cell pellet re-suspended in RIPA buffer substituted with proteinase inhibitor, DTT, NaF, β-Glycoside and Na_3VO_4. Tissue lysates were stored on ice for 30 minutes and centrifuged for 15 min at 12.000 rpm at 4°C afterwards. The supernatant was removed thoroughly and transferred into a fresh tube. Protein concentration was determined by BCA and adjusted to 25 µg/µl in 4x Lämmli buffer. Samples were subsequently heated to 95°C for 5 minutes, placed on ice for 1 minute afterwards and spun down at maximum speed. Supernatants were either applied on a gel for subsequent gel electrophoresis or stored at -80°C for later analysis.

2.5.5.2 SDS-PAGE and Western Blotting

Protein separation was carried out by sodium dodecyl sulfate polyacrylamide gel electrophoresis (SDS-PAGE), a method used to separate molecules and proteins depending on their molecular weight and electrical charge. Single-percentage gels ranging from 7.5% to 15% were used depending on the size of the target protein. SDS-PAGE was run at 70 V for 45 minutes to stack proteins followed by 1 hour at 130 V to separate proteins according to their size. To make the proteins accessible to antibody detection, the gel was transferred to a nitrocellulose membrane by electroblotting at a current of 0.2 A per gel for 1.5 hours. Uniformity and overall effectiveness of the transfer was checked by staining the membrane with Ponceau S. Before blocking, the membrane was washed with TBST and subsequently blocked for 15 minutes at RT with either 5 % non-fat milk or 5 % bovine serum albumin (BSA) in TBST, depending on the respective primary antibody. Incubation with the primary antibody was carried out overnight at 4°C on a roll mixer. After three additional washing steps with TBST, each lasting at least 10 minutes, the secondary antibody coupled with horse-radish-peroxidase (HRP) was applied to the membrane in TBST at room temperature for 1.5 hours. After washing the membrane three times, signals were visualized using Pierce ECL western blotting substrate on the INTAS science imaging system.

2.5.6 CRISPR Cas9 genome editing

2.5.6.1 Functional principle

The clustered regularly interspaced short palindromic repeats (CRISPR)/Cas9 are an adaptive antiviral immune system component of bacteria and prokaryotic cells. It has been adapted as an inexpensive and efficient genome editing tool for targeted DNA modification and is used for a wide range of applications. This includes both knock-in and knock-out genetic engineering of distinct model organisms, pooled library screening and further gene therapy. For a targeted endogenous knock-out, an RNA-guided DNA nuclease Cas9 enzyme and a single guide RNA (sgRNA) are required for efficient base-pairing and cleaving. sgRNAs are chimeric noncoding RNAs that consist of a 20 nt base-pairing sequence, complementary to targeted genomic sequences and an protospacer adjacent motif (PAM). This PAM is an essential targeting component required for successfully binding and cleaving the target sequence as it enables distinction of bacterial self from non-self DNA and thus prevents the CRISPR locus from being targeted and destroyed. The Cas9 enzyme checks foreign DNA and cleaves it when it is

complementary to the 20 base-pair spacer region of the sgRNA. Therefore, both the Cas9 nuclease and the complementary sgRNA have to form a complex that binds the cognate genomic DNA sequence via Watson-Crick base-pairing and induces a double strand break (DSB) at a predictable position within the target site which is repaired by indel-forming of non-homologous end joining.

2.5.6.2 CRISPR design

sgRNA sequences were selected from the Broad GPP genome-wide Brie Library (Adgene) and checked for genomic matches or near-matches to reduce off-target effects. Guide sequences consist of a 20 nucleotide protospacer sequence upstream of a PAM. The reverse complementary strand for each sgRNA was determined and modified by adding a PAM. Therefore, sgRNAs were customized by adding a CACC nucleotide sequence before the guiding sequence and an AAAC sequence before the reverse complement. If the first position of the complement oligo was not a G, a G nucleotide was added after the CACC sequence and a C at the 3´end of the reverse complement strand to enhance the expression from the U6 promotor of the pSpCas9(BB)-2A-GFP plasmid (pX458, Addgene plasmid ID 48138). This plasmid was selected as it includes GFP as a selectable marker.

2.5.6.3 CRISPR cloning

2.5.6.3.1 Oligonucleotide annealing and phosphorylation

The previously synthesized oligonucleotides were re-suspended in highly purified double distillated water (ddH_2O) to a final concentration of 100 µM and were added to a reaction mix of 5 µl prepared for each guide and its respective reverse complement. Annealing was carried out in a thermocycler by incubating samples at 37°C for 30 minutes followed by heating at 95°C for 5 minutes and then ramping down to 25°C at 5°C per minute. Afterwards, oligonucleotides were diluted 1:200 in ddH_2O to a final concentration of 50 nM.

Component	Volume	Final concentration
10 x T4 Ligation Buffer	0.5 µl	1x
sgRNA	0.5 µl	100 µM
sgRNA rc	0.5 µl	100 µM
T4 Polynucleotide Kinase (PNK)	0.5 µl	10.000 U/ml
ddH_2O	3 µl	

2.5.6.3.2 Golden gate cloning

Golden Gate assembly was used for ligation of the annealed oligonucleotides into the pX458 plasmid, kindly gifted by Feng Zhang. 10 µl of mastermix per reaction were prepared and 6 repetitive cycles of 37 °C for 5 minutes and 20 °C for 5 minutes were run in a thermocycler to obtain digestion and ligation in a single reaction.

Component	Volume	Final concentration
pX458 vector	0.5 µl	100 ng/µl
10 x tango buffer	0.5 µl	1 x
annealed oligos	1 µl	50 nM
DTT	0.5 µl	10 mM
ATP	0.5 µl	10 mM
T4 DNA ligase	0.5 µl	20.000 U/ml
FD BpiI restricton enzyme	0.5 µl	
H_2O	5.5 µl	

2.5.6.3.3 Plasmid-Safe

To prevent ligation of residual DNA fragments into the cloning vector and thus false positive results and high backgrounds, Plasmid-Safe was applied to the samples. Plasmid-Safe is an ATP-dependent DNase that selectively removes contaminating bacterial chromosomal DNA from plasmid and vector preparations. 2 µl of master mix was, therefore, added to the ligation mixture and incubated on a thermocycler for 30 minutes at 37°C followed by an additional 30 minutes at 70°C.

Component	Volume	Final concentration
Ligation mixture	5.5 µl	
10 x Plasmid-Safe Buffer	0.75 µl	1 x
ATP	0.75 µl	10 mM
Plasmid-Safe exonuclease	0.5 µl	10.000 U/ml

2.5.6.3.4 Bacterial transformation

Bacterial transformation was then performed to allow for the replication of the plasmid in competent E. coli bacterial cells. 2 µl of ligation mixture were transferred into 20 µl of chemically competent E. coli Stbl cells and incubated on ice for 20 minutes. After heating the reaction mixture to 42°C for 30 seconds, the probes were cooled on ice for 2 minutes. 100 µl of Super Optimal broth with Catabolite repression medium (SOC medium) was then added to each tube and the samples incubated on a thermocycler for 30 minutes at 37°C. The reaction mixture was subsequently transferred onto lysogeny broth (LB) agar plates containing 100 µg/ml ampicillin using sterile glass beads and incubated at 37°C overnight.

2.5.6.4 Plasmid DNA Isolation and purification by mini-prep

Two to three colonies were picked using sterile pipet tips and incubated in 10 ml of LB culture medium for 16 hours on an orbital shaker. 5 ml of bacterial culture were collected for subsequent analysis and centrifuged at 10.000 g for 5 minutes to pellet bacteria. The SN was removed and the cell pellet thoroughly re-suspended in 250 µl resuspension solution. 250 µl of Cell Lysis Solution was added, inverted several times and incubated for approximately 5 minutes until the solution cleared. After adding 350 µl of Alkaline Protease Solution, the tubes were inverted and incubated for 5 minutes at RT. Protease activity was neutralized by adding 350 µl of neutralization solution and subsequently centrifuged at maximum speed for 10 minutes at RT. The supernatant was transferred to a spin column by decanting and centrifuged at maximum speed for 1 minute at RT. The flow-through was discarded and the column washed by adding 750 µl washing solution and an additional centrifugation step was applied. Washing was repeated with 250 µl of washing solution and followed by 2 minutes of centrifugation. The membrane was spun dry and plasmid DNA eluted in 100 µl of nuclease free water. Each colony was sequenced by Sanger sequencing using a U6 promoter forward primer.

2.5.6.5 Transfection of CRISPR/Cas9 constructs into cells of interest

CRISPR/Cas9 constructs of sequence-verified colonies were selected for transfection into B16.OVA melanoma cells. For transfection, B16.OVA melanoma cells were thawed and passaged until they reached a logarithmic growth phase. 24 hours prior to transfection, cells were seeded in a density of 1.25 x 10^5 cells per ml into tissue treated 6-well culture plates. Complexation was prepared in two separate reaction mixtures. In the first reaction mixture, 2 µg of plasmid DNA was adjusted to a volume of 100 µl with OptiMEM. In the second mixture, twice the volume of Lipofectamine 2000 was used than was applied for DNA and further adjusted to 100 µl by OptiMEM. Both reaction mixtures were combined and incubated for 15 minutes at room temperature. For transfection, half of the culture medium was replaced by fresh, preheated growth medium. In addition, 200 µl of complexation reaction were applied per well and incubated for 6 hours at 37°C. To stop transfection, the culture medium was completely removed and a preheated medium was added carefully to the cells. Cells were cultured for up to 72 hours and transfection efficiency checked every day with fluorescence microscopy.

2.5.6.6 Fluorescence Activated Cell Sorting of Transfected Cells

Cells were prepared for sorting by FACS when approximately 10% to 20 % of the cells became GFP positive, as indicated in chapter 2.3.4 without further staining and filtered through a 50 µm strainer. Cell-sorting was performed with a FACSAria II and a single GFP positive cell was re-seeded to each well of a 96-well flat bottom plate including 100 µl of culture medium per well. Clones were incubated at 37°C for 7 to 14 days depending on the doubling time of the respective clone and transferred to the next larger size of culture dish when cells reached a confluency of approximately 80%. Validation of gene-deficient CRISPR/Cas9 clones was verified by immunoblotting and the appropriate functional assay.

2.6 Statistical analysis

For the comparison of multiple experiments, all the data is calculated as geometric mean values. The variance of mean values is indicated as standard error of the mean (SEM). Statistical significance of single data sets was assessed with the independent two-tailed Student's t-test. For multiple statistical comparisons of repetitive experiments, the one-way ANOVA test with Bonferroni post-test was used. In tumor growth experiments, the inter-group comparison of mean tumor volumes was calculated on the day the first mouse within a respective treatment group succumbed to tumor growth progression.

Comparison between the four treatment groups for a given tumor genotype was calculated on the day that the mean tumor volume analysis in the 'isoytpe' control group was terminated and One-way ANOVA was used to adjust for multiple testing. The comparison of the treatment response of different tumor genotypes to a given treatment modality was calculated on the day that the mean tumor volume analysis in the given treatment group was terminated; the independent two-tailed Student's t-test was used. Overall survival was analyzed using the Log-rank test. Significance level was set at P values < 0.05, $p < 0.01$ and $p < 0.001$ and was then indicated with an asterisk (*, ** and ***). All statistical calculations were performed using Prism (GraphPad Software) and graphical design was done with Adobe Illustrator.

3 Results

3.1 Impact of tumor intrinsic RIG-I signaling on efficacy of anti-CTLA-4 checkpoint blockade

3.1.1 RIG-I-deficient tumor cells are incapable in mounting an IFN-I response

To address the role of tumor or host intrinsic RIG-I signaling for anti-CTLA-4-mediated checkpoint blockade, we took advantage of the novel biochemical method of CRISPR/Cas9 genome editing and generated a RIG-I deficient B16 melanoma cell line expressing the model antigen OVA (B16.OVA). To prove knockout efficacy, we analyzed cell lysates of distinct CRISPR KO clones using western blot and found that various cell clones no longer expressed RIG-I at the protein level **(Figure 3.1 A)**. Direct activation of RIG-I with its specific ligand *in vitro* transcribed 5'-triphosphorylated RNA (3pRNA) triggers a strong IFN-I release and is moreover capable of inducing a form of immunogenic cell death in several tumor cell lines **(Figure 3.1 B-D and 3.23 C)** (Besch et al., 2009; Duewell et al., 2014). We observed that RIG-I-deficient B16 tumor cells (RIG-I$^{-/-}$ B16.OVA) failed to mount an IFN-I response by analyzing the supernatant of 3pRNA-transfected cells by ELISA. Furthermore, gene deficient clones were resistant to RIG-I-mediated cell death upon *in vitro* stimulation with 3pRNA **(Figure 3.1 B-D)**.

These results demonstrated that we effectively knocked out RIG-I in a murine melanoma cell line which gave us the opportunity to investigate the role of tumor intrinsic RIG-I signaling in subsequent experiments.

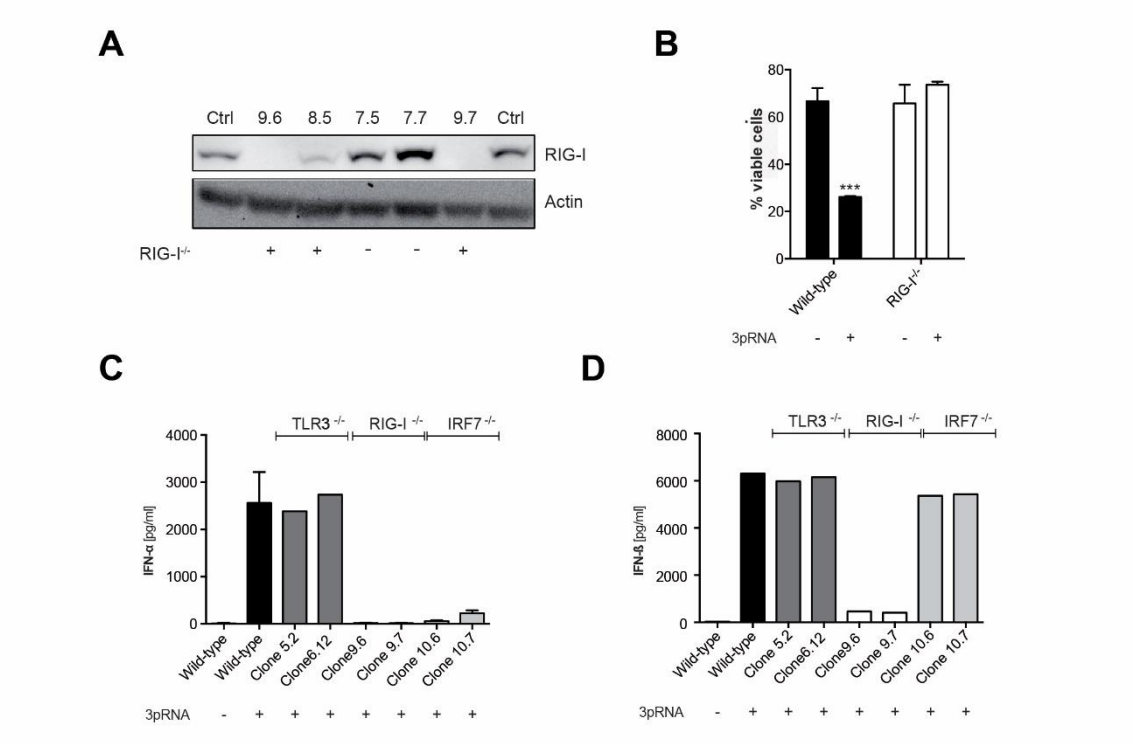

Figure 3.1: RIG-I deficient tumor cells are incapable in mounting an antiviral-immune response. (A) Western blot of different B16.OVA clones after CRISPR/Cas9-mediated *DDX58* (RIG-I) deletion. The RIG-I deficient (RIG-I-/-) clone 9.6 was used for subsequent experiments. **(B-D)** Different B16.OVA clones were transfected with 3pRNA *in vitro* using Lipofectamin 2000. **(B)** After 48h, cell viability was assessed by Annexin V and 7-AAD staining. **(C, D)** ELISA was used to determine release of IFN-I . Error bars give the mean ± S.E.M. of triplicate samples.

3.1.2 Tumor cell intrinsic RIG-I signaling promotes anti-CTLA-4-mediated systemic antitumor immunity

In order to investigate the impact of tumor-intrinsic RIG-I signaling on anti-CTLA-4 immune checkpoint blockade *in vivo*, we designed a bilateral flank tumor model. This gave us the opportunity to investigate local antitumor effects by intratumoral 3pRNA application into the right-sided (injected) tumor and to further observe systemic therapy effects on the left sided (distant) tumor by local 3pRNA application as well as intraperitoneal anti-CTLA-4 antibody administration. Furthermore, this model allowed us to examine possible synergistic abscopal effects arising from combining both therapeutic approaches.

As previous studies demonstrated only a slight or even no treatment effect from monotherapy with anti-CTLA-4 blocking antibodies in non-immunogenic tumor entities (Hurwitz, Yu, Leach, & Allison, 1998; van Elsas et al., 1999), we choose the immunogenic B16.OVA tumor model for further experiments. To investigate tumor growth and survival, wild-type BL6/J mice were inoculated with either wild-type (WT) B16.OVA cells or the previously designed RIG-I$^{-/-}$ B16.OVA cell line. When tumors became palpable, treatment was applied by either injecting *in vitro* transcribed 3pRNA into the right sided tumor or intraperitoneal administration of the anti-CTLA-4 monoclonal antibody or the combination of both treatments. Animals of the control group and the 3pRNA monotherapy group were further injected with an appropriate isotype control. Treatment was repeated three times at an interval of three days followed by further analysis on day 15.

Furthermore, systemic anti-CTLA-4 monotherapy also resulted in tumor growth delay in mice bearing wild-type B16.OVA tumors. Treatment effects of systemic anti-CTLA-4 administration were significantly impaired in mice inoculated with RIG-I$^{-/-}$ tumors, indicating that effective anti-CTLA-4 treatment crucially relies on tumor cell intrinsic RIG-I signaling **(Figure 3.2 B)**. Regarding variations in anti-CTLA-4-mediated growth delay between local and distant tumors, we hypothesized that this might be attributable to different tumor volumes and the resulting growth dynamics in our model.

Furthermore, therapeutic targeting of RIG-I by 3pRNA application into the right-sided flank tumor of mice bearing wild-type tumors led to a complete regression of the respective tumor. In addition, we observed improved tumor growth control in these mice reflected in a delayed progression of the contralateral (distant) tumor. Interestingly, local 3pRNA-induced tumor regression seemed to be largely independent of tumor intrinsic RIG-I signaling as mice bearing RIG-I$^{-/-}$ B16.OVA tumors maintained the ability to reject the local tumor to a certain extent, suggesting additional mechanisms, independent of tumor intrinsic RIG-I signaling, are involved in local tumor control **(Figure 3.2 A)**. However, systemic therapy effects were crucially dependent on tumor cell-intrinsic RIG-I signaling as distant RIG-I$^{-/-}$ B16.OVA tumors were characterized by a rapid tumor outgrowth independent of therapy.

Moreover, by combining local RIG-I activation with systemic anti-CTLA-4 blockade, a synergistic therapy effect emerged as outgrowth of distant non-injected tumors was held in check due to significant growth control of these tumors, resulting in long term survival in most of the treated animals **(Figure 3.2 A-C)**. This effect also relied on tumor intrinsic RIG-I signaling as tumors in mice bearing RIG-I$^{-/-}$ B16.OVA tumors showed rapid

outgrowth comparable to monotherapy with 3pRNA resulting in a survival disadvantage of these animals.

Additionally, long-term surviving animals remained tumor-free and gained antitumor immunological memory as they developed immunity against a subsequent intravenous re-challenge with WT B16.OVA cells **(Figure 3.2 D)**.

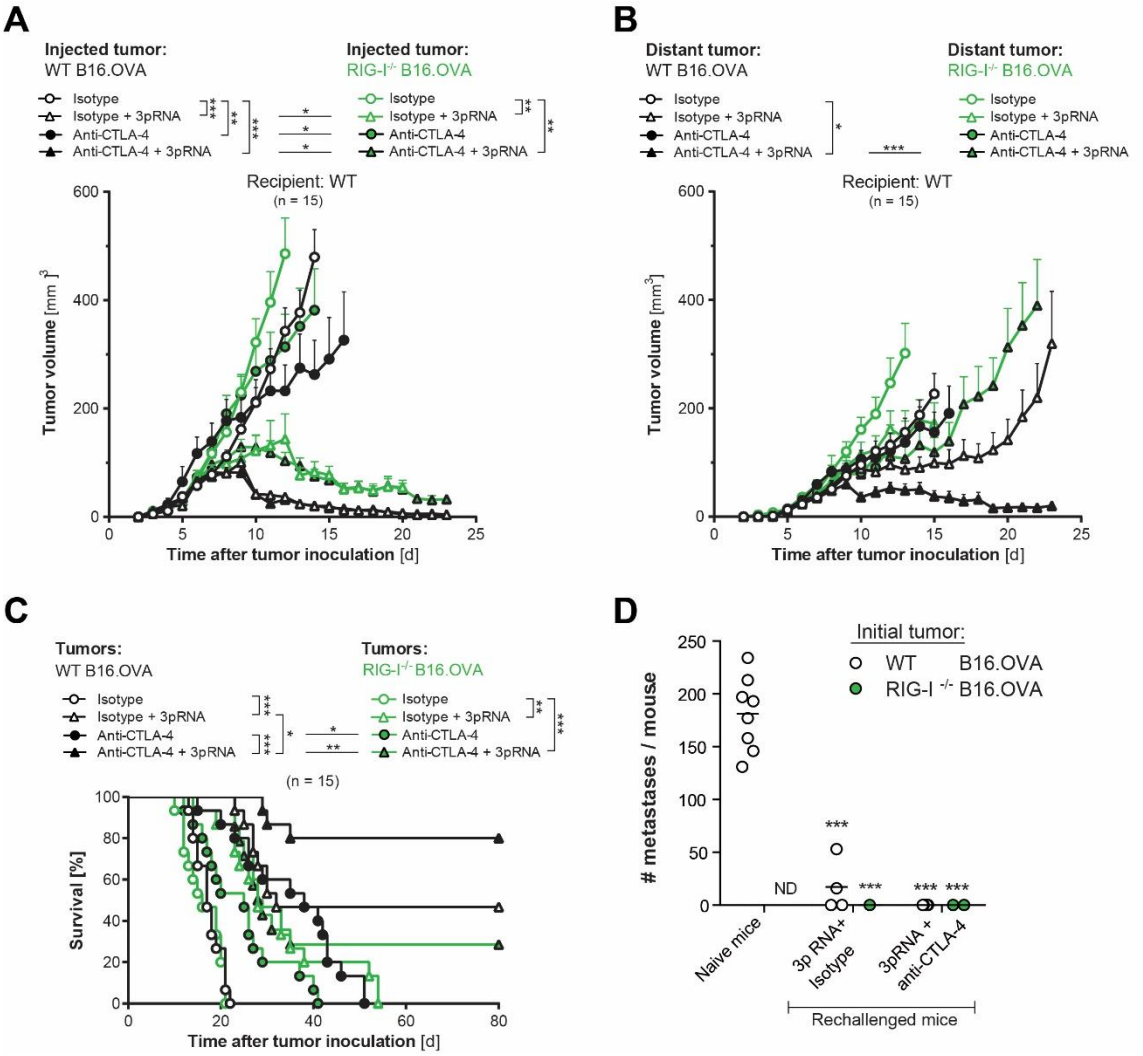

Figure 3.2 Tumor cell intrinsic RIG-I signaling promotes anti-CTLA-4-mediated systemic antitumor immunity. (A-B) Tumor growth of mice bearing either WT or RIG-I-/- B16.OVA tumors that were treated with 3pRNA or anti-CTLA-4. All tumor growth curves show mean tumor volume ± S.E.M. of n = 15 individual mice and were pooled from three independent experiments. **(C)** Overall survival of treated mice bearing either WT or RIG-I-/- B16.OVA tumors. **(D)** Long-term surviving animals were re-challenged iv with WT B16.OVA cells and formation of pulmonal pseudometastases was analyzed 14 days later. Naive mice were used as control group for successful tumor induction. ND, not determined. All data was pooled from at least two independent experiments.

These results indicate that effective anti-CTLA-4 mediated anticancer immunity crucially relied on tumor intrinsic RIG-I signaling and is dispensable for local tumor control mediated by a synthetic RIG-I agonist. However, local and selective RIG-I ligation enhances the therapeutic effectiveness of anti-CTLA-4-mediated immunotherapy on systemic tumors.

3.2 RIG-I activation enhances cross-presentation of tumor-associated antigen by CD103+ dendritic cells and the subsequent cross-priming of CD8+ T cells

3.2.1 Induction of tumor cell death by 3pRNA *in vivo* is dependent on tumor intrinsic RIG-I signaling

Having demonstrated that tumor intrinsic RIG-I signaling is substantial for the induction of tumor cell death *in vitro* we furthermore wanted to assess the role of therapeutic RIG-I activation *in vivo*. For this purpose, whole tumor tissue was harvested 24 hours after a single intratumoral injection with 25 µg 3pRNA, it was further processed to single cell suspensions and analyzed for apoptotic DNA fragmentation via a TUNEL assay. 3pRNA administration resulted in a fast induction of tumor cell death in the injected tumor. However, apoptosis induction was restricted to the injected flank tumor and further dependent on tumor cell-intrinsic RIG-I signaling **(Figure 3.3)**. It appeared that distant non-injected wild type tumors showed a significant difference in the percentage of TUNEL positive cells when compared to RIG-I deficient tumors.

Thus, we demonstrated that tumor intrinsic RIG-I signaling clearly influences 3pRNA induced cell death both *in vitro* and *in vivo*.

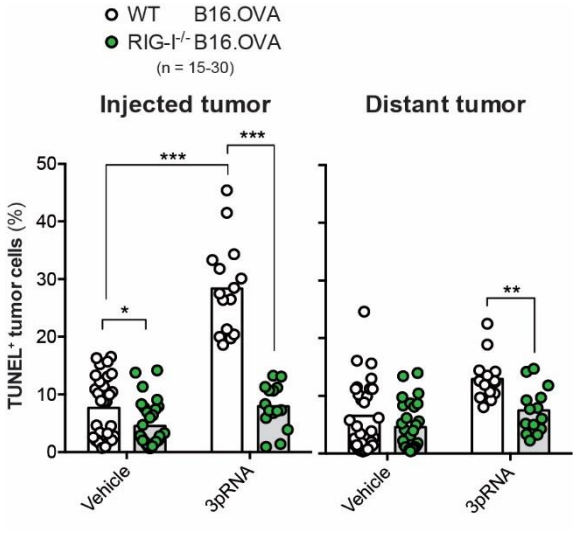

Figure 3.3: Induction of tumor cell death by 3pRNA *in vivo* is dependent of tumor cell-intrinsic RIG-I signaling. WT mice bearing bilateral WT or RIG-I$^{-/-}$ B16.OVA tumors were treated with a single, one-sided intratumoral 3pRNA administration or its vehicle in vivo-jetPEI. 24 h later, the frequency of apoptotic tumor cells was analyzed by terminal deoxynucleotidyl transferase dUTP nick end labeling (TUNEL).

3.2.2 Intact tumor intrinsic RIG-I signaling is required for effective cross-presentation

Tumor cell death is accompanied by tumor cell disintegration and the possible subsequent release of tumor-associated antigens. DCs occupy a central role in innate immunity due to their ability to sense and process tumor-derived antigens. Thereby, DCs link innate and adaptive immunity by displaying processed antigens on their surface which in turn results in cross-priming of CD8$_+$ T cells and the subsequent induction of a tumor antigen specific CTL response (Berard et al., 2000). In our previous experiments, we had shown that RIG-I ligation by 3pRNA induces tumor cell death both *in vitro* and *in vivo,* hypothesizing that this might lead to increased tumor antigen release, necessary for efficient cross-priming of CD8$_+$ cytotoxic T cells by DCs.

To address this, we started by assessing the role of tumor-intrinsic RIG-I ligation for DC activation and its potential for effective cross-priming of CD8$_+$ T cells. As CD103$_+$ migratory DCs, a subpopulation of CD8α-like DCs, have previously been shown to occupy an important role in the transport of melanoma-associated antigens to draining lymph nodes and also to be decisive for the related efficient cross-presentation of either self or foreign skin-associated antigens to CD8$_+$ cytotoxic T cells (Bedoui et al., 2009; Salmon et al., 2016), we focused our efforts on this specific DC subpopulation.

For analysis of OVA cross-presentation and DC activation status, we analyzed DCs within tumor-draining lymph nodes for the expression of the immune dominant ovalbumin-derived peptide SIINFEKL bound to MHC class I to quantify OVA specific antigen presenting cells as well as for other markers by FACS on day 15 after tumor induction. This approach revealed enhanced cross-presentation of the OVA immune dominant peptide epitope SIINFEKL by CD103+ DCs in the context of MHC-I during monotherapy with either 3pRNA or anti-CTLA-4 or the combination of both treatments, which in turn critically relied on tumor cell-intrinsic RIG-I signaling **(Figure 3.4 A)**. Enhanced cross-presentation was spatially restricted to the lymph node draining the 3pRNA-injected tumor **(Figure 3.4 A–B)**. Although cross-presentation was found to be dependent on tumor intrinsic RIG-I signaling, the expression of the co-stimulatory molecule CD86 on activated CD103+ DCs was not affected by any treatment in both local or distant tumor draining lymph nodes **(Figure 3.4 C–D)**.

These data suggests that tumor intrinsic RIG-I signaling is mandatory for efficient cross-presentation of tumor-associated antigens by CD103+ DCs. Moreover, the maturation status of CD103+ DCs appears to be independent of tumor intrinsic RIG-I signaling.

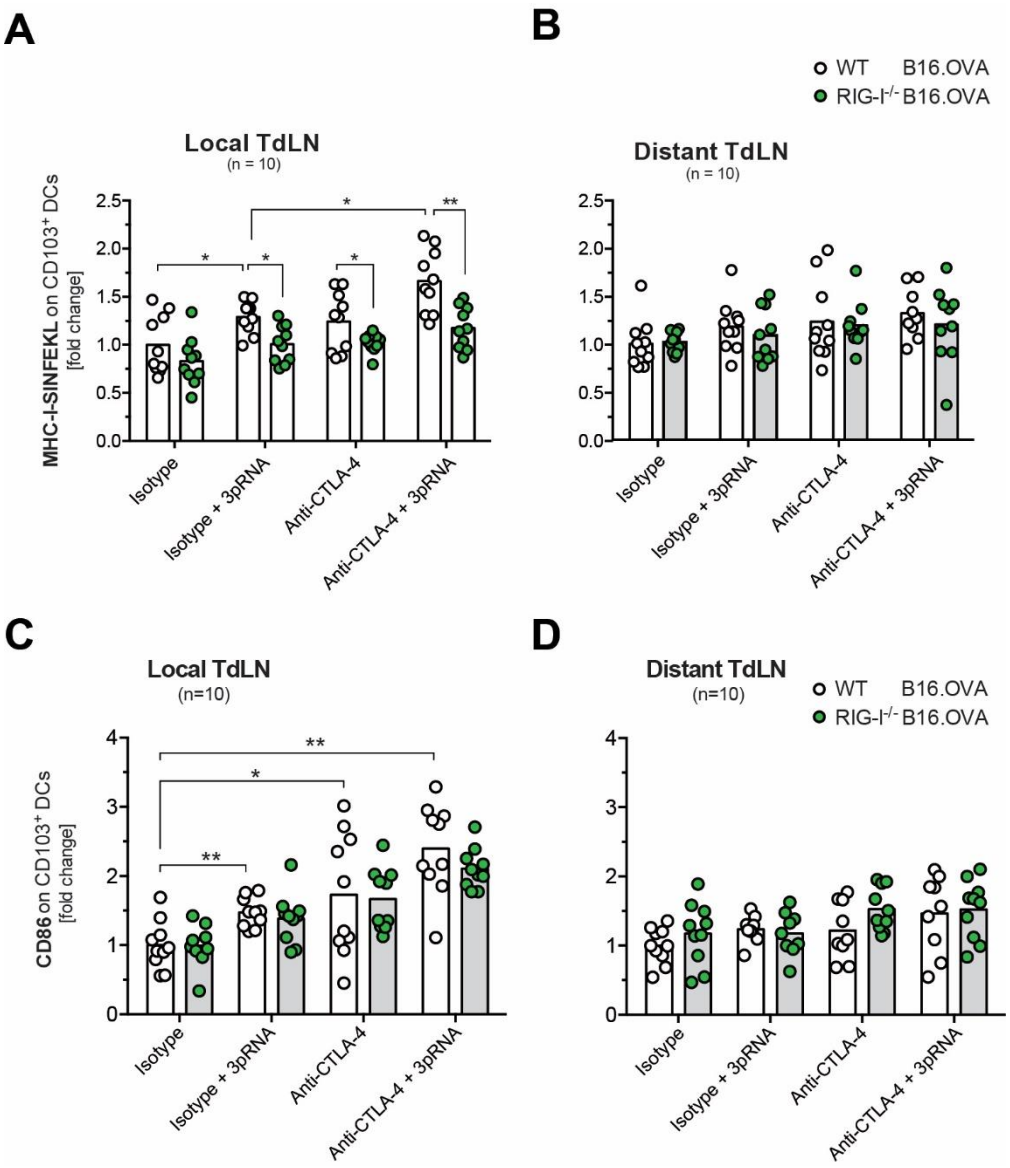

Figure 3.4: Intact tumor intrinsic RIG-I signaling is required for effective cross-presentation. Mice were implanted with either WT or RIG-I-/- B16.OVA cells in each flank. The RIG-I ligand 3pRNA was injected into the right-sided tumor; anti-CTLA-4 antibody was administered ip. Analyses were performed on day 15 after tumor induction. **(A-B)** Cross-presentation of the processed OVA peptide-epitope SIINFEKL in the context of MHC-I on CD103+ DCs in the lymph node draining the 3pRNA-injected tumor (TdLN) and the draining lymph node of contralateral, non-injected tumors. **(C-D)** CD86 expression on CD103+ DCs in tumor-draining lymph nodes. Data is normalized to gene expression in isotype-treated mice bearing WT B16.OVA tumors (control) and give mean ± S.E.M. of n = 10 individual mice that were pooled from two independent experiments. An asterisk without brackets indicates comparison to the WT control group.

3.2.3 CD8α-like DCs are mandatory for local and systemic tumor control in response to therapy

Having demonstrated the crucial role of CD103+ DCs for efficient cross-presentation, we were interested in how the lack of this DC subpopulation would influence therapy efficiency *in vivo*. Therefore, we used our bilateral flank tumor model in mice genetically deficient of the transcription factor Batf3 (Batf3$^{-/-}$). These mice lack CD8α-like DCs including the subset of CD103+ DCs. Thus, KO mice are not capable of processing and cross-presenting tumor-derived antigens. As a direct consequence, treatment by either local RIG-I activation or anti-CTLA-4 checkpoint blockade failed to induce expansion of OVA specific CTLs in Batf3-deficient mice **(Figure 3.5 D)**. Consistently, Batf3$^{-/-}$ mice treated with 3pRNA showed a rapid tumor outgrowth of distant tumors. Interestingly however, local tumors were kept in check although a complete tumor regression was not achieved **(Figure 3.5 A-B)**. Moreover, mice systemically treated with anti-CTLA-4 checkpoint blockade did not respond to therapy as further reflected in reduced survival **(Figure 3.5 C)**. The inability of both monotherapies to keep tumor growth in check was also reflected in significantly reduced combined treatment efficacy in Batf3-deficient mice. However, the combination of both treatments led to local as well as systemic tumor control and thus enhanced survival independent of a systemic T cell immune response, suggesting additional DC- and thus Batf3-independent antitumor mechanisms such as anti-CTLA-4 antibody-mediated depletion of pro-tumorigenic regulatory T cells to mediate antitumor immunity (Simpson et al., 2013).

This data further emphasizes the importance of CD8α+ DCs, especially the subset of CD103+ DCs for anti-CTLA-4 mediated checkpoint blockade and RIG-I-mediated T cell-based antitumor immunity.

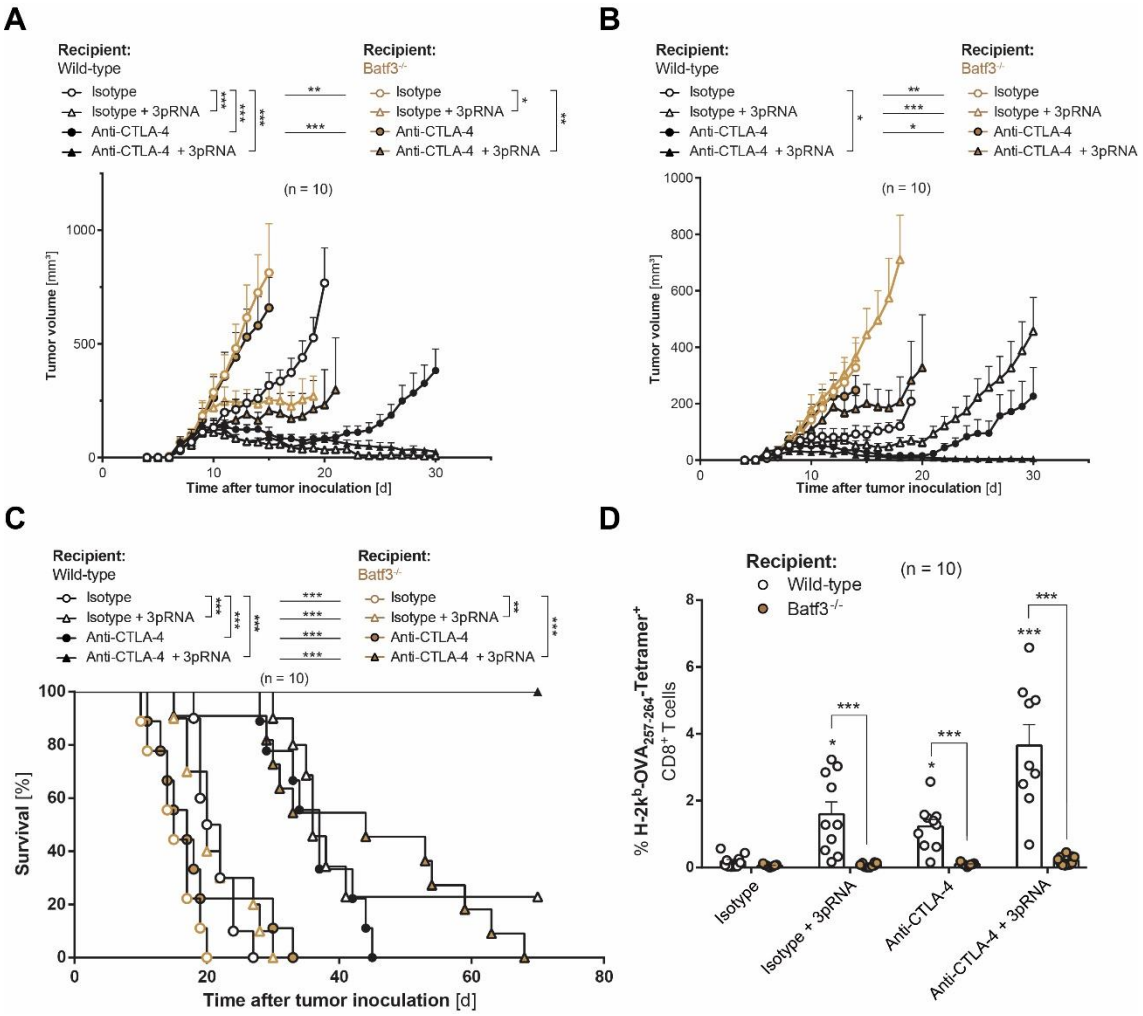

Figure 3.5: CD8α+ DCs are mandatory for tumor control in response to therapy. (A-B) Tumor growth of WT and Batf3-deficient (Batf3-/-) mice bilaterally inoculated with WT B16.OVA cells. Mice were repeatedly treated with anti-CTLA-4 +/- intratumoral 3pRNA. All tumor growth curves show mean tumor volume ± S.E.M. of n = 10 individual mice and were pooled from two independent experiments. **(C)** Overall survival of tumor-bearing mice and **(D)** the frequency of H-2Kb-SIINFEKL Tetramer+ CD8+ T cells in peripheral blood on day 15 after tumor induction were determined.

3.2.4 Tumor intrinsic RIG-I signaling is a prerequisite for the formation of a systemic T cell-mediated immune response

Effective cross-presentation is the basis for clonal expansion of antigen specific CTLs. In line with our previous findings showing a distinct role of tumor-intrinsic RIG-I signaling on cross-presentation of tumor-associated antigens, we were interested if this would translate into a systemic T cell-mediated immune response.

We, therefore, performed an MHC-I tetramer assay of blood samples from treated mice on day 15, one day after they had received the last treatment. This abled us to detect and quantify T cells specific for the OVA antigen epitope SIINFEKL. Monotherapy with either 3pRNA or anti-CTLA-4 resulted in strong systemic expansion of OVA-specific CTLs. In addition, tetramer frequencies were further increased in animals that received the combination of both treatments, suggesting a potential synergism by combining both therapeutic approaches **(Figure 3.6)**. Importantly, this effect was dependent on tumor intrinsic RIG-I signaling, as mice bearing RIG-I deficient tumors showed markedly reduced numbers of OVA-specific CTLs compared to mice bearing WT tumors.

Thus, we demonstrated that either treatment with 3pRNA or anti-CTLA-4 checkpoint blockade causes a distinct systemic expansion of tumor antigen specific CTLs in an RIG-I dependent manner. Moreover, this effect can be boosted by combining both therapeutic approaches.

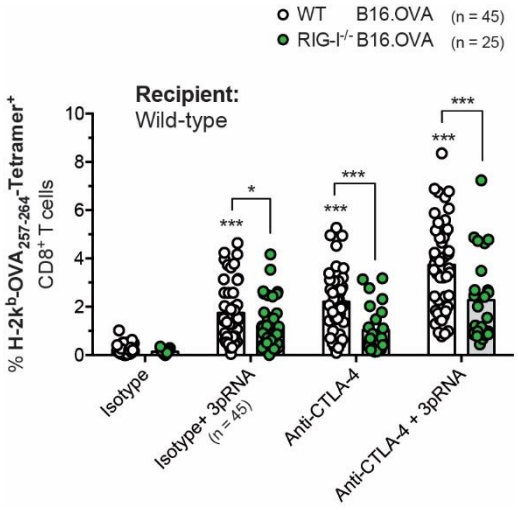

Figure 3.6: Effect of tumor intrinsic RIG-I signaling on the expansion of OVA specific CTLs. WT mice were bilaterally inoculated with either WT or RIG-I$^{-/-}$ B16.OVA cells and were repeatedly treated with anti-CTLA-4 +/- intratumoral 3pRNA. The frequency of H-2Kb-SIINFEKL Tetramer+ CD8+ T cells in peripheral blood was determined. All data give values of individual mice + group mean as bar that were pooled from at least four independent experiments.

To achieve their fully cytotoxic potential, tumor antigen-specific T cells need to overcome the immunosuppressive tumor microenvironment, infiltrate and accumulate in the tumor to ultimately identify and destroy tumor cells. Therefore, tumor-intrinsic RIG-I signaling might be substantial to break down these obstacles by facilitating apoptosis in malignant cells and the subsequent enhanced cross-priming by tumor resident DCs due to an increased antigen release.

Performing immunohistochemistry of whole tumor tissue revealed dense necrotic areas in local and distant tumors mainly in those injected with 3pRNA, whereas systemic administration of anti-CTLA-4 blocking antibodies revealed almost no necrotic lesions **(Figure 3.7 B+C)**. Nevertheless both therapeutic approaches lead to the accumulation of $CD8_+$ tumor-infiltrating leukocytes in a tumor intrinsic RIG-I dependent manner, predominantly in local tumors. **(Figure 3.7 A+C)** Combining both therapies slightly but not significantly enhanced T cell accumulation in the tumor, as this has been suggested by systemic tetramer frequencies.

In line with our previous results showing that intact tumor intrinsic RIG-I signaling is substantial for the expansion of antigen-specific T cells, these data demonstrate that expansion of CTLs is, furthermore, crucial for the development of a systemic immune response, the accumulation of antigen specific CTLs within the tumor and subsequent tumor eradication.

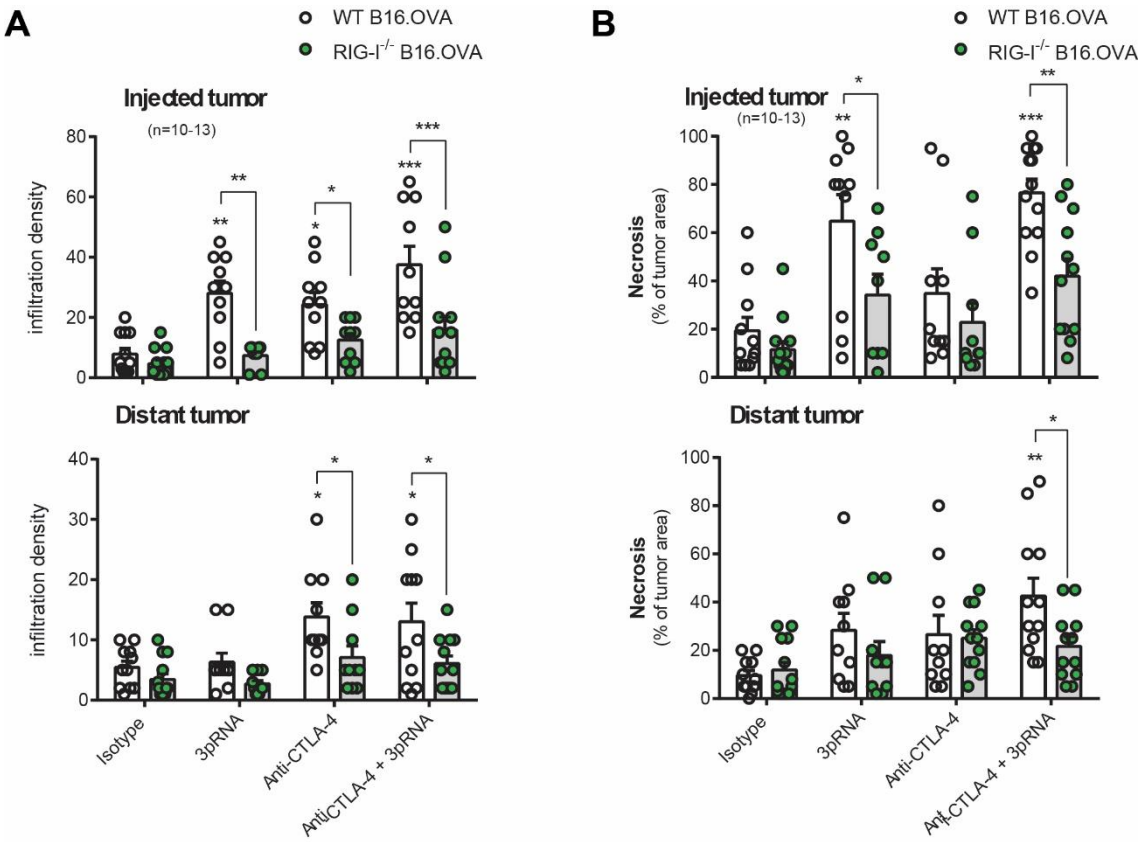
A
WT B16.OVA
RIG-I-/- B16.OVA
Injected tumor
(n=10-13)
infiltration density
Distant tumor
infiltration density
Isotype
3pRNA
Anti-CTLA-4
Anti-CTLA-4 + 3pRNA
B
WT B16.OVA
RIG-I-/- B16.OVA
Injected tumor
(n=10-13)
Necrosis
(% of tumor area)
Distant tumor
Necrosis
(% of tumor area)
Isotype
3pRNA
Anti-CTLA-4
Anti-CTLA-4 + 3pRNA

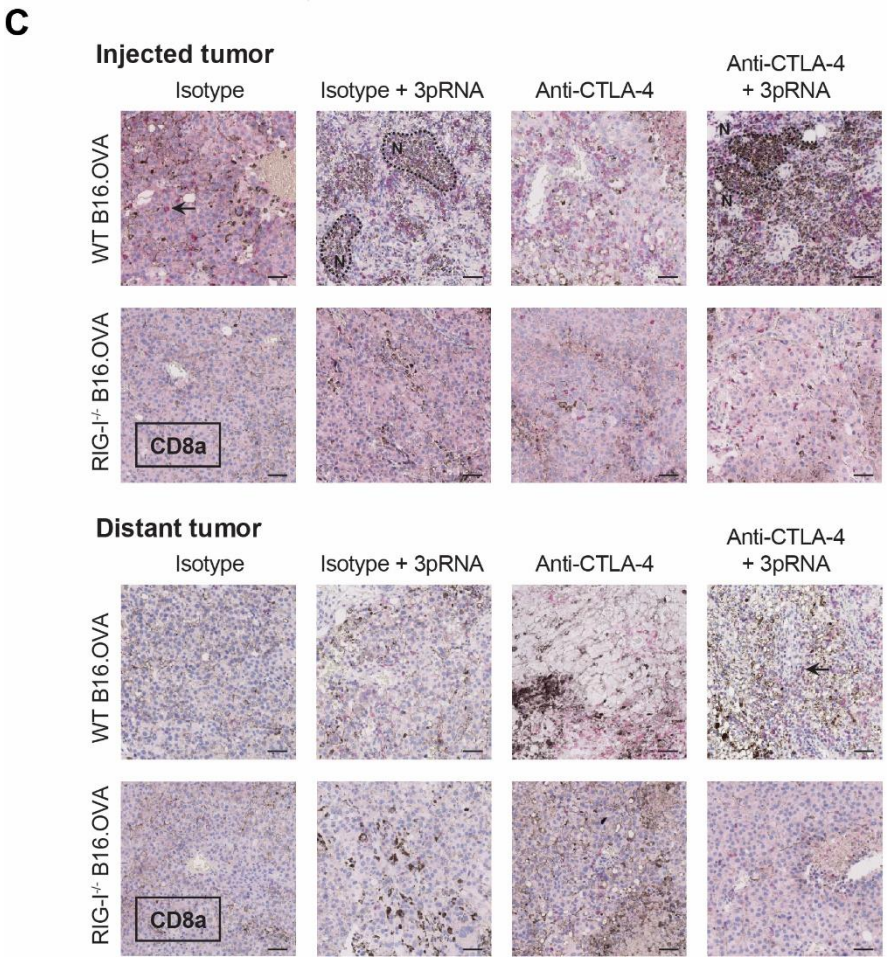
C
Injected tumor
Isotype
Isotype + 3pRNA
Anti-CTLA-4
Anti-CTLA-4
+ 3pRNA
WT B16.OVA
RIG-I-/- B16.OVA
CD8a
Distant tumor
Isotype
Isotype + 3pRNA
Anti-CTLA-4
Anti-CTLA-4
+ 3pRNA
WT B16.OVA
RIG-I-/- B16.OVA
CD8a

Figure 3.7: RIG-I dependent differences in the infiltration density of CTLs and development of necrosis. WT or RIG-I-/- B16.OVA cells were implanted in each flank of wilde type mice. The RIG-I ligand 3pRNA was injected into the right-sided tumor; anti-CTLA-4 antibody was administered ip. **(A)** The frequency of tumor-infiltrating CD8+ T cells and **(B)** histomorphologically necrotic tumor areas were analyzed with immunohistochemistry. **(C)** Shown are representative tumor sections after H&E and anti-CD8 (red, arrows) staining from one of three independent experiments (magnification 20x, scale bar 50 µm; N, highly necrotic area). All data were pooled from three independent experiments.

To further address possible underlying mechanisms, we performed gene expression analysis within whole tumor tissue lysates. By analyzing distant non-injected tumors we found that RIG-I deficient tumors displayed lower expression levels of genes encoding proteins involved in T cell lytic function such as granzyme B, IFN-γ and perforin **(Figure 3.8)**. Furthermore, CCL5 a chemokine involved in both recruitment of leukocytes into inflammatory sites and the proliferation and activation of NK cells as well as inducible T-cell co-stimulator (ICOS) - the expression of which has been shown to promote anti-CTLA-4 checkpoint blockade (Yoshinaga et al., 1999) - were upregulated dependent on tumor intrinsic RIG-I signaling. Moreover, we found increased expression levels of genes encoding inhibitory receptors including LAG3 and TIM-3 in $RIG^{-/-}$ tumors and of PDCD1, the gene encoding the inhibitory receptor PD-1 in WT B16.OVA tumors.

This data suggests that tumor intrinsic RIG-I signaling affects the gene expression profile of both TILs and tumor cells upon treatment. In addition, it appears that loss of tumor intrinsic RIG-I signaling impairs the expression of genes involved in lytic T cell function and furthermore favors the development of an exhaustion phenotype by upregulation of gene expression of inhibitory receptors.

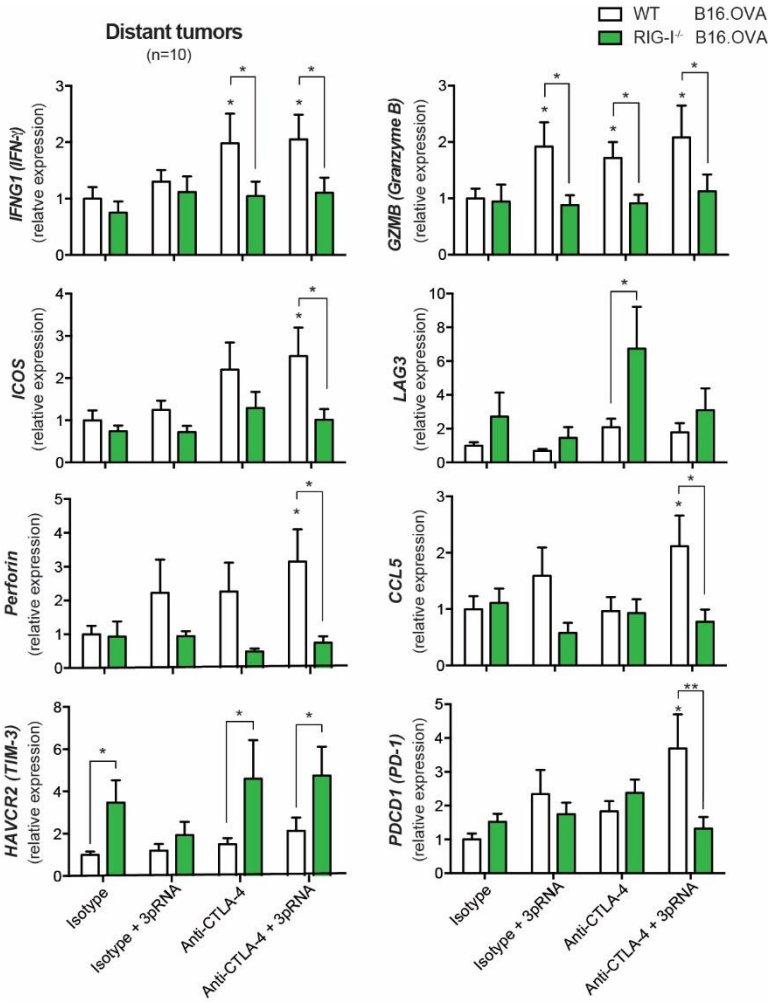

Figure 3.8: Tumor-intrinsic RIG-I signaling affects the gene expression profiles of TILs and tumor cells upon treatment. Gene expression analysis within lysates of distant, non-3pRNA-injected tumors was performed with real-time PCR. Data are normalized to gene expression in isotype-treated mice bearing WT B16.OVA tumors (control) and give mean ± S.E.M. of n = 10 individual mice that were pooled from two independent experiments. An asterisk without brackets indicates comparison to the WT control group.

3.3 Anti-CTLA-4-mediated immunotherapy is independent on tumor cell-derived IFN-I

3.3.1 RIG-I ligation promotes the induction of IFN-I and proinflammatory cytokines *in vivo*

Tumor intrinsic activation of RIG-I induces a rapid IFN-I response. DC-intrinsic IFN-I signaling has been demonstrated to be substantial for tumor specific T cell priming, intratumoral accumulation of DCs, effective antigen cross-presentation and the subsequent induction of antitumor immunity (Diamond et al., 2011; Fuertes et al., 2011). Our previous experiments have shown that DCs, in particular $CD103_+$ DCs, are key players in the induction of RIG-I dependent T cell-mediated antitumor immunity. Therefore, we wanted to investigate how tumor-derived IFN-I signaling impacts DC function in RIG-I-mediated immunity. Having observed a strong IFN-I release after transfection of WT B16.OVA tumor cells *in vitro* the question arose as to whether local administration of 3pRNA into pre-established tumors would induce the release of IFN-I or other proinflammatory cytokines *in vivo*.

A systemic induction of IFN-α and IFN-β in both injected and distant tumors was detected 24 hours after local RIG-I activation in the tumor microenvironment **(Figure 3.9)**. In addition, injection of 3pRNA induced the production of proinflammatory cytokines such as TNF-α, IL-6, IL-12p70 and IFN-γ whereas levels of IL-1β remained unchanged. Moreover, increased expression levels of proinflammatory cytokines were primarily found in lysates of the injected tumor whereas the levels in the distant tumor were less pronounced. However, IFN-I levels in the distant tumor were increased to an extent comparable to the injected tumor. Interestingly no significant differences in both the levels of IFN-I and proinflammatory cytokine release were observed between lysates of WT B16.OVA and RIG-$I^{-/-}$ B16.OVA tumors.

These data indicate that targeting of RIG-I in the tumor microenvironment with a specific ligand induces the production of IFN-I and several pyrogens independent of tumor intrinsic RIG-I signaling. Nevertheless, it appears that following RIG-I stimulation tumor cells are not the predominant source of IFN-I suggesting, the host as major source for IFN-I.

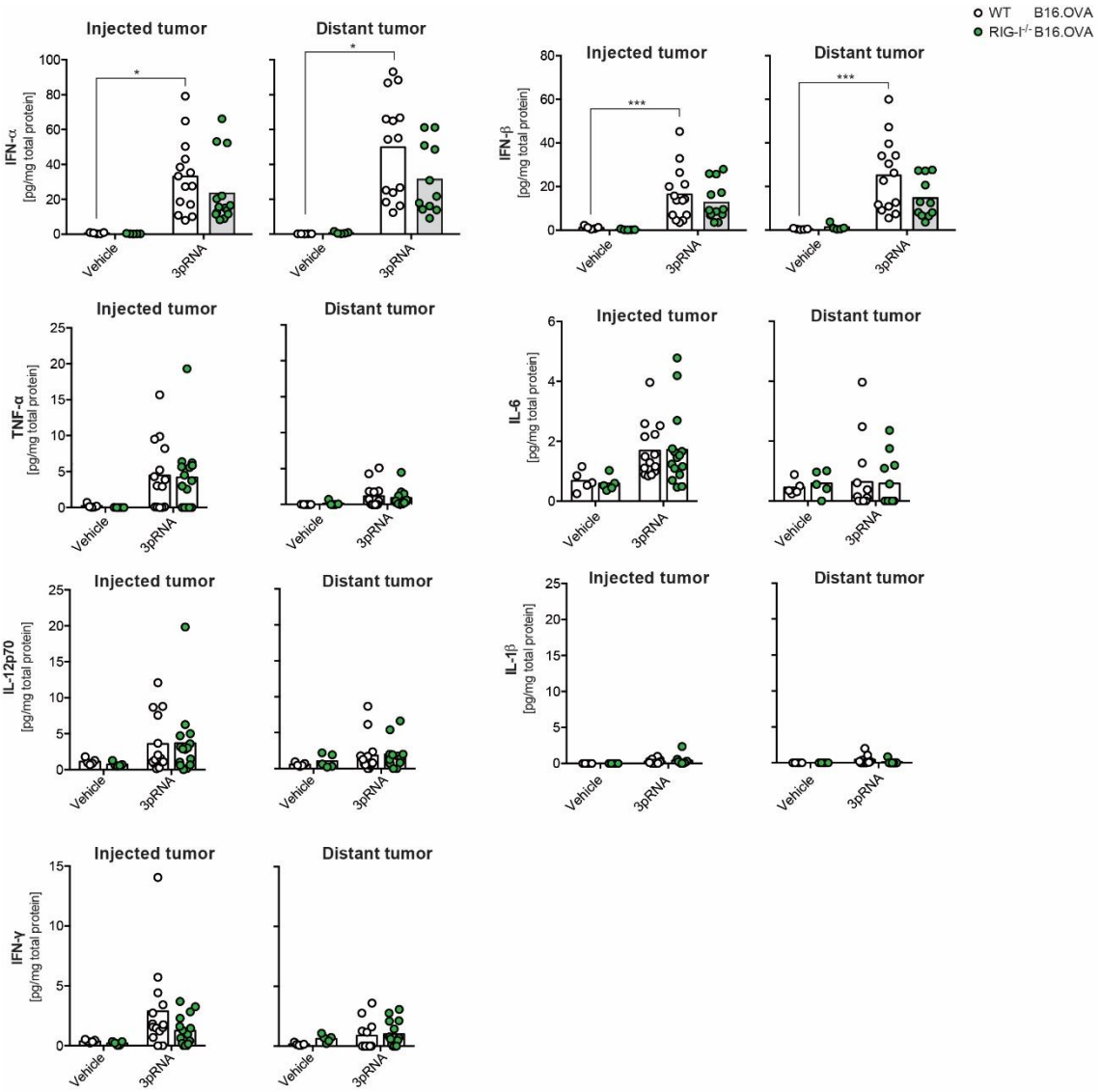

Figure 3.9: Effects of local immunostimulation on IFN-I and cytokine expression *in vivo*. Mice bearing bilateral WT or RIG-I-/- B16.OVA tumors were treated either with vehicle (jetPEI) or 3pRNA. 24 h later, the concentration of IFN-I and proinflammatory cytokines in local (3pRNA injected) and distant (untreated) tumor tissue were analyzed by ELISA. Data show values of n = 5 (vehicle) and n = 15 (3pRNA) individual mice with mean.

3.3.2 Host-derived IFN-I is vital for RIG-I-mediated tumor cell death and efficient anti-CTLA-4 checkpoint blockade

With our previous data suggesting the host as essential IFN-I source we went on by determining the role of host-IFN-I signaling on therapy efficiency. For this purpose, mice deficient in the interferon-α receptor subunit 1 (IFNaR1$^{-/-}$) were inoculated with WT B16.OVA cells. These animals lacking IFN-I signaling failed to induce an effective antitumor immune response upon treatment with 3pRNA as local and distant tumor control was not sufficient in keeping tumor growth in check **(Figure 3.10 A-B)**.

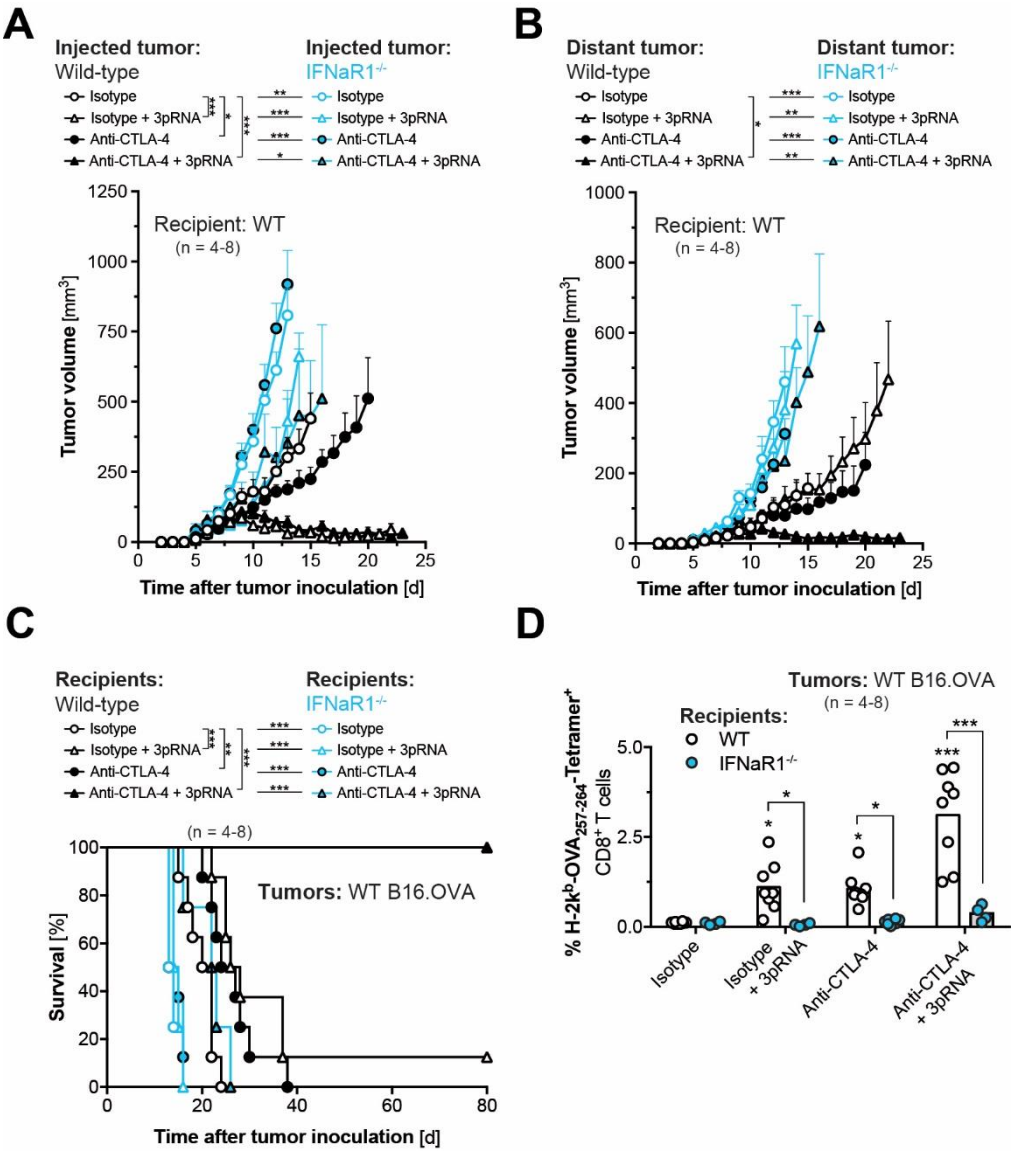

Figure 3.10: Role of host derived IFN-I signaling for efficient immunotherapy. (A-B) Tumor growth of WT and IFNaR1-deficient (IFNaR1-/-) mice bilaterally inoculated with WT B16.OVA cells. Mice were treated several times with anti-CTLA-4 +/- intratumoral 3pRNA. All tumor growth curves show mean tumor volume ± S.E.M. of n = 4 to 8 individual mice and were pooled from two independent experiments. **(C)** Overall

survival of tumor-bearing mice and **(D)** the frequency of H-2Kb-SIINFEKL Tetramer+ CD8+ T cells in peripheral blood on day 15 after tumor induction.

This resulted in a survival disadvantage of these mice **(Figure 3.10 C)** and was moreover reflected in clear IFNaR1 dependency of RIG-I-mediated expansion of OVA specific CTLs **(Figure 3.10 D)**. In accordance with previous studies, monotherapy with anti-CTLA-4 was compromised in mice lacking IFN-I signaling (Hannani et al., 2015). Nevertheless, the combination of both treatments significantly increased survival of IFNaR1$^{-/-}$ mice independent of OVA tetramer frequencies. However all knockout mice succumbed tumor outgrowth.

Preceding *in vitro* studies suggested IFN-I as important mediator in RIG-I-induced immunogenic tumor cell death as well as associated DC activation and subsequent T cell priming (Duewell et al., 2014). To test this assumption *in vivo* and to further examine the role of tumor cell-derived IFN-I in contrast to host-derived IFN-I, we generated a B16.OVA double KO cell line that genetically lacked the transcription factors IFN regulatory factor 3 and 7 (IRF3/7$^{-/-}$) which are considered as master regulators of IFN-I induction and subsequent IFN stimulated gene (ISG) expression.

As a first step, we started by evaluating the effects of RIG-I ligation on our previously designed double KO cell line in comparison to wild-type B16.OVA cells and RIG-I$^{-/-}$ B16.OVA cells. To begin with, we transfected the cells with 3pRNA *in vitro.* Interestingly, IRF3/7$^{-/-}$ cells were susceptible to RIG-I-mediated tumor cell killing, at least up to a certain extent, but failed to induce IFN-I expression as neither IFN-α nor IFN-β could be detected **(Figure 3.11 A-C)**.

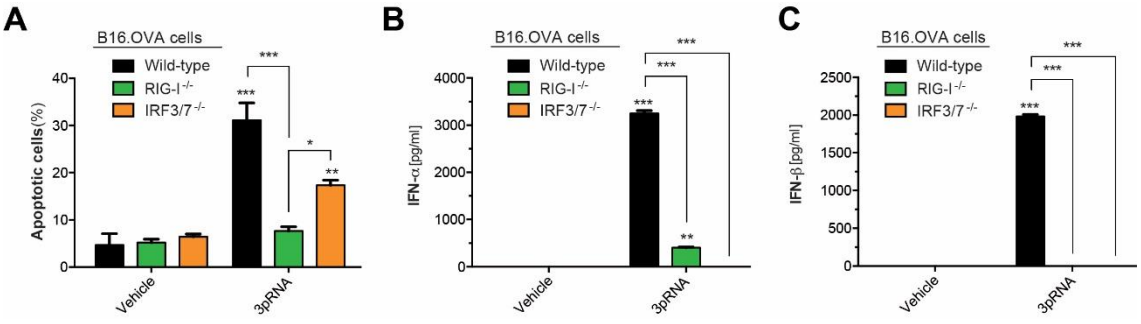

Figure 3.11: Effects of RIG-I ligation on IFN-I release and tumor cell death induction in various knock-out cell lines. Wild-type, RIG-I-/- and IRF3/7-/- B16.OVA clones were transfected with 3pRNA *in vitro* using Lipofectamin 2000. **(A)** After 48 h, apoptosis induction was assessed by Annexin V and 7-AAD staining. **(B, C)** Release of IFN-I was determined by ELISA. Error bars give the mean ± S.E.M. of at least quadruplicate samples. An asterisk without brackets indicates comparison to the appropriate ‚vehicle' control group.

To assess the effects of tumor intrinsic IFN-I deficiency *in vivo,* we performed our bilateral flank tumor model in wild-type mice. By comparing wild-type with IRF3/7$^{-/-}$ tumor cells, we observed that in contrast to RIG-I$^{-/-}$ tumor cells, IRF3/7$^{-/-}$ B16.OVA cells were less susceptible to RIG-I-mediated tumor cell death, unlike the findings suggested in our previous *in vitro* studies. Therefore, local tumor growth control was far less pronounced in 3pRNA treated animals bearing IRF3/7$^{-/-}$ B16.OVA tumors and, in addition, significantly impaired when compared to mice bearing B16.OVA WT tumors **(Figure 3.12 A)**. Tumor cell deficiency to release IFN-I did not result in significant differences in the systemic expansion of tumor antigen specific CTLs when we compared the levels in mice bearing WT tumors with mice inoculated with IRF3/7$^{-/-}$ cells **(Figure 3.12 D)**. This was further reflected in the tumor growth progression of mice bearing IRF3/7$^{-/-}$ tumors as these animals demonstrated a largely intact therapy response to either monotherapy with anti-CTLA-4 or its combination with 3pRNA **(Figure 3.12 A-B)**. In line with our *in vitro* data, RIG-I-mediated tumor cell death of injected tumors appeared to be dependent on tumor intrinsic IFN-I signaling as we observed impaired local tumor growth control in mice bearing IRF3/7-deficient tumors.

These results indicate that RIG-I-mediated efficient anti-CTLA-4 checkpoint blockade is associated with intrinsic programmed tumor cell death but independent of tumor cell-derived IFN-I. This also supports our previously acquired *in vivo* data suggesting host-derived IFN-I to be substantial for local and systemic tumor growth control. Nevertheless, tumor intrinsic IFN-I signaling appears to be vital for the induction of RIG-I-mediated tumor cell death, at least in murine tumor cells.

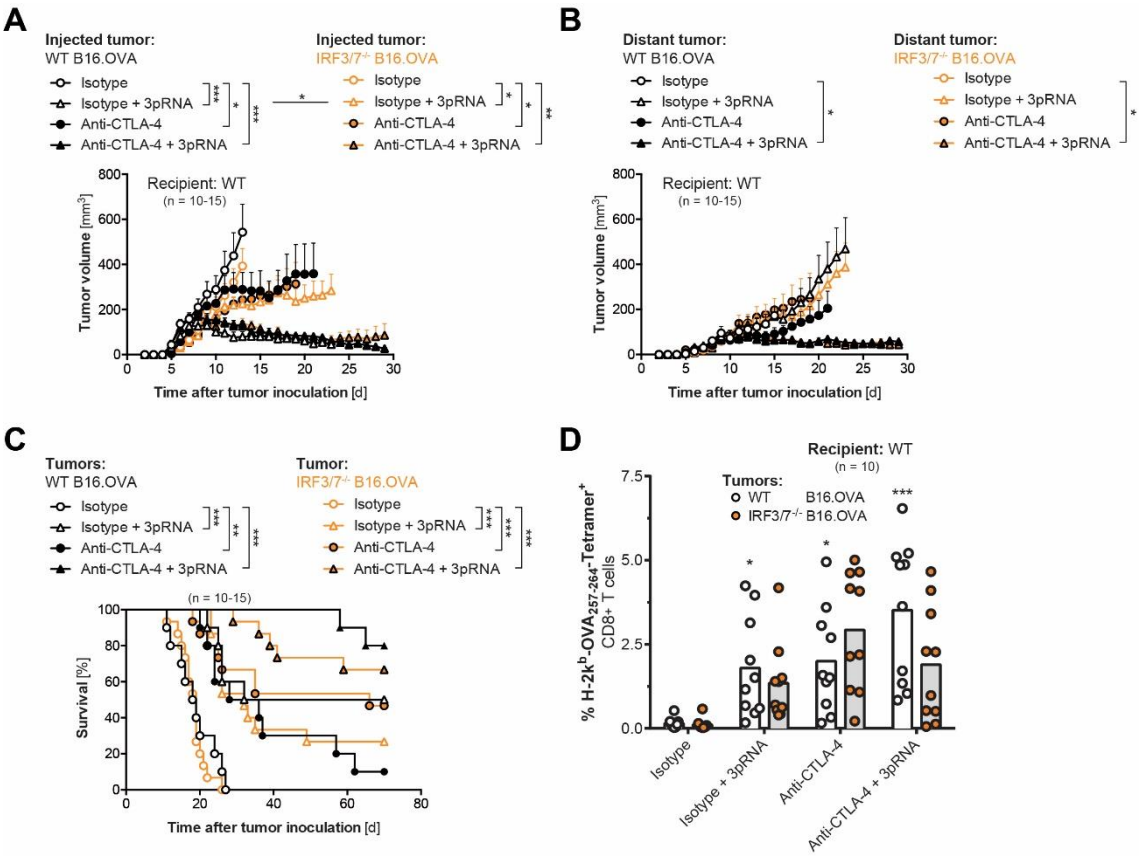

Figure 3.12: Effect of tumor intrinsic IFN-I signaling on therapy efficiency. WT mice were inoculated with either WT or IRF3/7-deficient (IRF3/7-/-) B16.OVA cells and repeatedly treated with anti-CTLA-4 +/- 3pRNA. **(A-B)** Tumor growth of 3pRNA-injected and distant tumors. **(C)** Overall survival of treated mice bearing WT or IRF3/7-/- B16.OVA tumors. **(D)** Frequency of H-2Kb-SIINFEKL Tetramer+ CD8+ T cells in peripheral blood on day 15 after tumor induction in WT mice bearing either WT or IRF3/7-/- B16.OVA tumors. All data were pooled from at least two independent experiments.

3.4 RIG-I-dependent induction of immunogenic tumor cell death

3.4.1 Tumor intrinsic RIG-I ligation induces apoptosis and activates different components of the necroptosis pathways

RIG-I-induced tumor cell death has been suggested to be mediated via tumor-intrinsic activation of the mitochondrial apoptosis pathway (Besch et al., 2009) and has been further shown to be immunogenic resulting in potent cross-priming of tumor-specific $CD8^+$ T cells (Duewell et al., 2014). In addition, a recent report demonstrates that RIG-I activation during viral infection triggers necroptosis in infected cells (Schock et al., 2017).

To characterize the underlying cell death pathways further, we performed western blot analysis of tumor lysates after transfecting wild type or RIG-I deficient B16.OVA tumor cells with 3pRNA **(Figure 3.13)**.

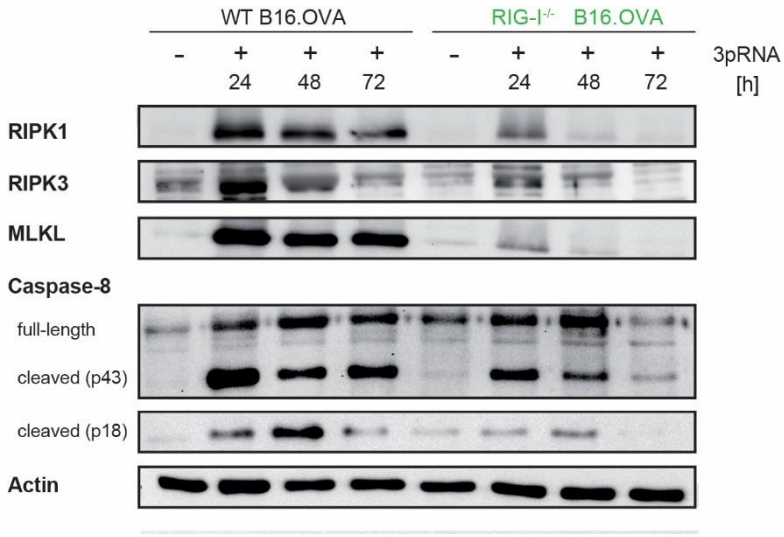

Figure 3.13: RIG-I ligation induced expression of components of both the apoptosis and the necroptosis pathway. Protein extracts of WT and RIG-I-/- B16.OVA cells, transfected with 3pRNA *in vitro*, were collected at the indicated time points and expression of cell death pathway proteins was analyzed by western blot. Actin served as loading control.

Consistent with the previous published data we found that tumor cell-intrinsic RIG-I ligation led to an upregulation of several proteins involved in distinct cell death pathways. One of these was the cleaved form of the apoptosis initiator caspase-8 with its key role in intrinsic apoptosis. RIPK3 and MLKL, both contributors to necrotic programmed cell death also known as necroptosis, as well as RIPK1, due to its function in both apoptosis and the proinflammatory necroptosis pathway, were upregulated upon tumor cell intrinsic RIG-I activation in an RIG-I dependent fashion.

This data suggests that tumor cell-intrinsic RIG-I activation induces apoptosis and proinflammatory forms of regulated cell death including necroptosis and furthermore that both apoptotic and necroptotic pathways might be involved in the immunogenic form of RIG-I induced tumor cell death.

3.4.2 Anti-CTLA-4-mediated systemic antitumor immunity depends on caspase-3-mediated tumor cell death

Consistent with our previous data showing an upregulation of genes involved in intrinsic apoptosis, and recent studies that highlighted the important role of RIG-I mediated activation of the mitochondrial apoptosis pathway in malignant cells, we found that tumor cell-intrinsic RIG-I ligation by 3pRNA *in vitro* resulted in the induction of apoptotic cell death as evidenced by enhanced cleavage of the apoptosis executioner caspase-3 and exposure of phosphatidylserine in the outer plasma membrane leaflet **(Figure 3.14 A-B).** Cell death appeared to be apoptotic rather than necroptotic as activation of RIG-I did not result in the phosphorylation of the necroptosis executioner protease MLKL in wild-type B16.OVA cells. Nonetheless**,** by using a series of known inducers of necroptosis, including the combination of TNF-α, SMAC mimetics and the pan-caspase inhibitor Z-VAD-FMK we were unable to see induction of pMLKL in B16.OVA melanoma, suggesting that this pathway may be suppressed in this melanoma cell line **(Figure 3.14 C).** Moreover, RIG-I-mediated apoptosis was suspended in B16.OVA cells harboring a stable caspase-3 deficiency (Caspase $3^{-/-}$ B16.OVA). In contrast, cell death induction by 3pRNA transfection was still intact in MLKL deficient melanoma cells ($MLKL^{-/-}$ B16.OVA) **(Figure 3.14 A-B)**. To assess caspase-3 activity *in vivo* we performed our bilateral flank tumor model in wild-type mice and analyzed tumor cells for the expression of activated caspase-3, 24 hours after 3pRNA administration. Local RIG-I activation led to a rapid RIG-I-dependent cleavage of caspase-3 and subsequent tumor cell death **(Figure 3.14 D)**. Consistent with this, monotherapy by intratumoral 3pRNA administration in pre-established caspase-$3^{-/-}$ B16.OVA tumors was incapable of developing a sufficient antigen specific T cell response in our bilateral flank tumor model. This was further accompanied by impaired local and systemic tumor control and resulted in rapid tumor outgrowth. Moreover, anti-CTLA-4-mediated antitumor immunity was also insufficient in keeping tumor growth in check. Consequently, the combination of anti-CTLA-4 and 3pRNA was significantly impaired in mice bearing caspase-$3^{-/-}$ tumors **(Figure 3.14 E-H)**. This was further reflected in reduced OVA tetramer frequencies and decreased survival.

Taken together, these data suggest RIG-I-dependent induction of tumor cell death in melanoma cells as a prerequisite for the efficiency of anti-CTLA-4-mediated immunotherapy that is mainly driven by the executioner caspase-3 with its central role in apoptosis.

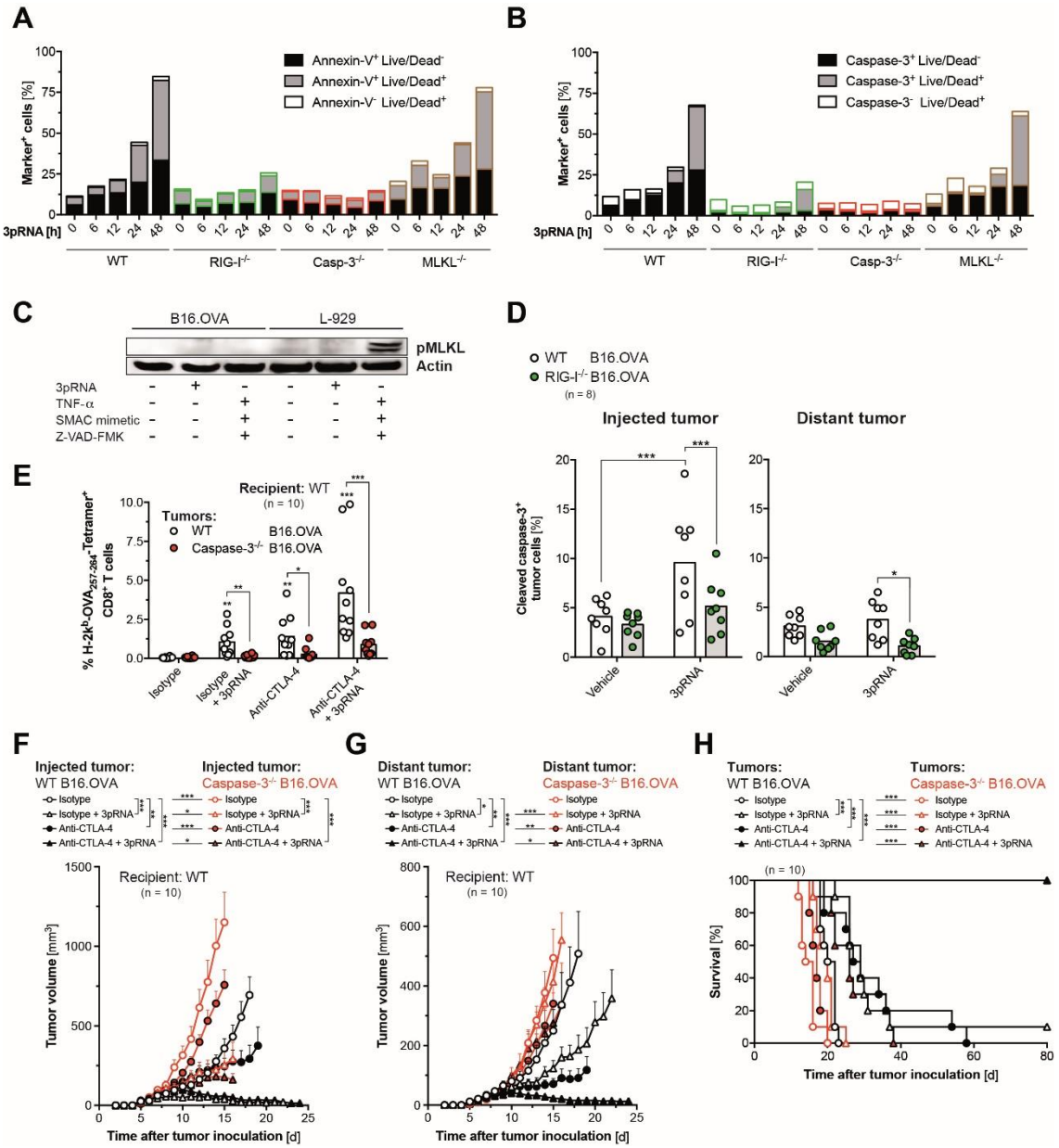

Figure 3.14: Anti-CTLA-4-mediated systemic antitumor immunity depends on caspase-3-mediated tumor cell death. (A-B) WT, RIG-I$^{-/-}$, caspase-3-deficient (caspase-3$^{-/-}$) and MLKL-deficient (MLKL$^{-/-}$) B16.OVA cells were transfected with 3RNA and were harvested at the indicated time points. Cells were stained **(A)** with Annexin-V and Live/Dead reagent or **(B)** cleaved caspase-3 and Live/Dead reagent and were analyzed by flow cytometry. Representative data are from one of three independent experiments. **(C)** WT B16.OVA and murine L-929 fibroblasts were transfected with 3pRNA and induction of necroptotic cell death with the presence of phosphorylated MLKL (pMLKL) was analyzed with western blot. The combination of TNF-α, SMAC mimetics and the pan-caspase inhibitor Z-VAD-FMK was used as a positive control to induce necroptosis. **(D)** WT mice bearing bilateral WT or RIG-I$^{-/-}$ B16.OVA tumors were treated with a single, one-sided intratumoral 3pRNA administration or its vehicle in vivo-jetPEI. 24 h later, the frequency of active-caspase-3 positive cells was analyzed by FACS. **(E-H)** WT recipient mice received B16.OVA WT or caspase-3$^{-/-}$ cells in each flank and were repeatedly treated with anti-CTLA-4 +/- intratumoral 3pRNA injections. Mean ± S.E.M. tumor growth of **(F)** 3pRNA-injected and **(G)** distant B16.OVA tumors. **(H)** Overall survival of treated mice bearing B16.OVA tumors. **(E)** The frequency of H-2Kb-SIINFEKL

Tetramer+ CD8+ T cells in peripheral blood was determined 15 days after tumor induction. All data show mean values of n = 10 individual mice pooled from two independent experiments.

3.4.3 Radiotherapy promotes anti-CTLA-4 checkpoint blockade in a RIG-I dependent manner

For a long time radiotherapy (RTx) - a therapeutic standard in cancer therapy – received little attention due to cytotoxicity issues. However, this perception is changing as new insights into the underlying mechanisms between radiation-invoked immune responses and tumor regression are emerging. RTx is, therefore, not only considered as a “killer” for tumor cells but rather a creator of endogenous anticancer vaccines (Golden & Apetoh, 2015). In this context, tumor irradiation and the subsequent release of DAMPs has previously been shown to result in host cGAS/STING-dependent maturation of intratumoral DCs, leading to T cell cross-priming (Deng, Liang, Xu, et al., 2014) and thus can serve as adjuvants for anticancer vaccines. In addition, irradiation of tumors and the subsequent tumor cell death have been shown to synergize with anti-CTLA-4 checkpoint blockade thus inducing an effective antitumor immune response (Vanpouille-Box, Pilones, Wennerberg, Formenti, & Demaria, 2015).

In order to investigate the role of tumor-intrinsic RIG-I signaling on anti-CTLA-4-enhanced antitumor immunity in connection with alternative cell death inducers apart from 3pRNA, we locally irradiated mice bearing either wild-type or RIG-I$^{-/-}$ B16.OVA tumors **(Figure 3.15 A)**. In keeping with the previously found data, we observed a synergism of local RTx in combination with anti-CTLA-4 therapy by performing this combined treatment in our bilateral flank tumor model **(Figure 3.15 C)**. Interestingly, these results were comparable to those achieved by combining local 3pRNA-induced RIG-I activation and anti-CTLA-4 treatment as RTx, on the one hand, resulted in local tumor growth control and, on the other hand, led to systemic tumor regression when combined with checkpoint blockade. Surprisingly, these synergistic effects crucially relied on tumor intrinsic RIG-I signaling. Even monotherapy with localized RTx achieved a survival benefit that was also dependent of tumor-intrinsic RIG-I signaling **(Figure 3.15 B)**.

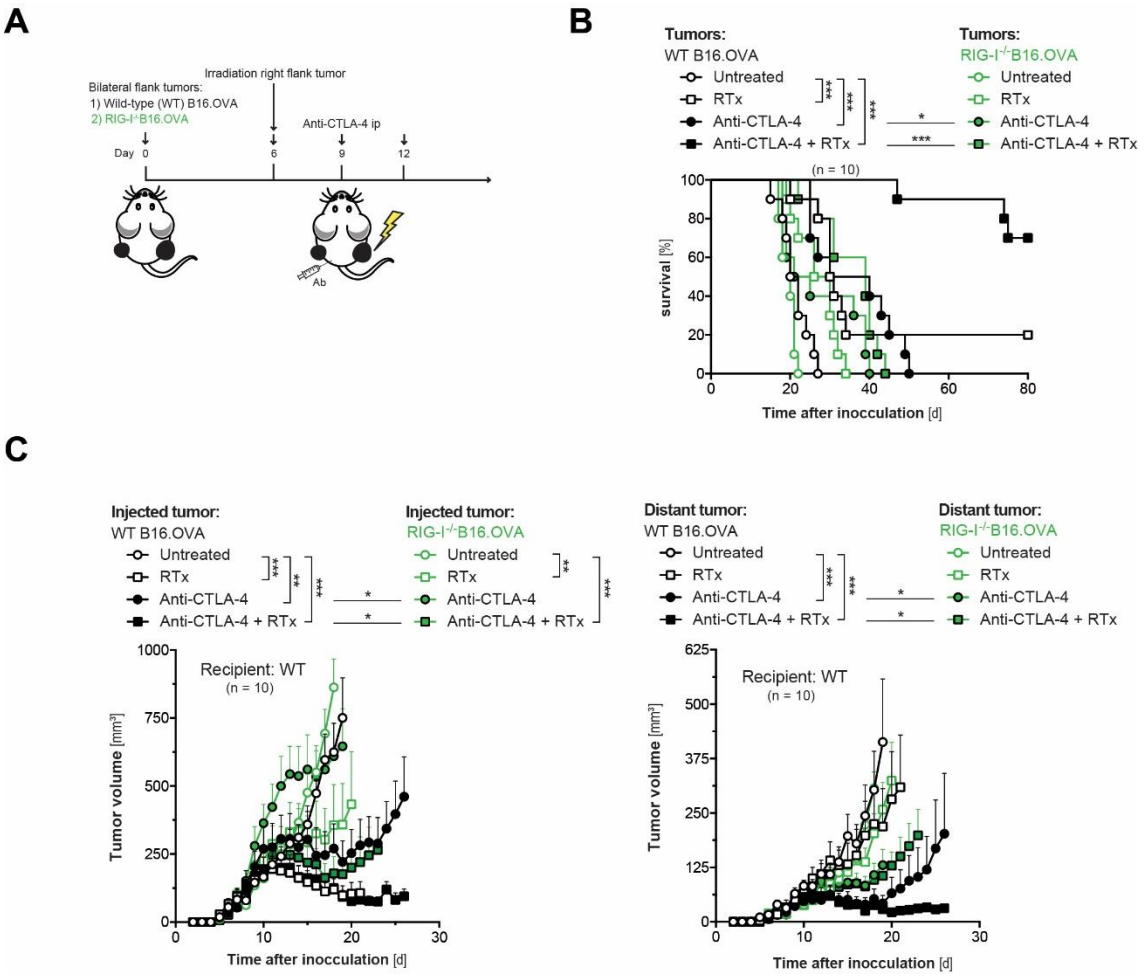

Figure 3.15: Radiotherapy promotes anti-CTLA-4 checkpoint blockade in a RIG-I dependent manner. **(A)** Mice were implanted with either WT or RIG-I-/- B16.OVA cells in each flank. On day 6, the right-sided tumor was irradiated with 20 Gy, followed by three consecutive anti-CTLA-4 injections. **(B)** Overall survival of tumor-bearing mice and **(C)** mean + S.E.M. tumor growth of irradiated and distant tumors were determined. Data of n = 10 mice are pooled from two independent experiments.

In accordance with a previous study, we found that RTx synergized with anti-CTLA-4 mediated checkpoint blockade in our tumor model (Vanpouille-Box et al., 2015). More striking was the discovery that this synergism depended on tumor cell intrinsic RIG-I signaling and therefore supported our previous data demonstrating that intact tumor intrinsic RIG-I signaling is required for the efficacy of anti-CTLA-4 checkpoint blockade. Thus, the induction of ICD via different modes of programmed tumor cell death appears to be a vital requirement for the generation of T cell mediated antitumor immune responses that have previously been shown to be substantial for effective anti-CTLA-4 mediated checkpoint blockade (Spranger et al., 2013).

3.4.4 Synergistic antitumor effects of DNA methyltransferase inhibitor 5-azacytidine and anti-CTLA-4 depend on tumor-intrinsic RIG-I activity

As reported in a previous study, melanoma patients with an upregulated viral defense signature in the tumor microenvironment particularly benefited from anti-CTLA-4-mediated immune checkpoint blockade and developed a durable clinical response (Chiappinelli et al., 2015). This was further supported by our finding that mice lacking tumor-intrinsic RIG-I signaling have a survival disadvantage due to sole anti-CTLA-4 checkpoint blockade, suggesting that basal RIG-I activation in tumor cells through a potential endogenous ligand might contribute to efficacy of anti-CTLA-4-mediated checkpoint blockade.

A possible explanation was provided by a recent study that identified tumor-derived endogenous retroviral elements (ERVs) as potential ligands for RIG-I-like helicases (Chiappinelli et al., 2015). ERVs constitute around 8 % of the human genome and can be detected by PRRs and therefore activate cytosolic RNA sensors. However, ERVs remain silenced by promoter DNA methylation in normal somatic cells but can also be overexpressed in distinct cancer entities (Hurst & Magiorkinis, 2015; Rycaj et al., 2015). Chiappinelli et al. enhanced ERV expression by treatment with the DNA methyltransferase inhibitor 5-azacytidine (Aza) which resulted in a RIG-I like helicase-dependent IFN-I response *in vitro.* Aza treatment further synergized with anti-CTLA-4 mediated checkpoint blockade, as was demonstrated in an effective antitumor response *in vivo*.

In accordance with their results, expression of distinct ERVs such as IAP and the spliced version of eMLV was increased up to 3-fold after treatment of the B16.OVA melanoma cells with Aza *in vitro*. This effect appeared to be independent of tumor-intrinsic RIG-I signaling **(Figure 3.16 A)**. By combining periodic low-dose Aza treatment with anti-CTLA-4 checkpoint blockade in our bilateral flank tumor model, we observed treatment effects of either Aza alone or in combination with anti-CTLA-4 checkpoint blockade. Monotherapy with Aza led to a delayed tumor growth of the injected tumor, largely independent on tumor cell-intrinsic RIG-I signaling **(Figure 3.16 B)**. In contrast, the systemic response to local Aza treatment appeared to rely on tumor intrinsic RIG-I signaling as we observed delayed tumor outgrowth in mice bearing wild-type tumors treated with the combination of Aza and anti-CTLA-4 checkpoint blockade **(Figure 3.16 C)**. Consistent with previously published data, we found synergistic effects by combining low dose Aza treatment with checkpoint blockade. Interestingly, this synergism was significantly impaired in mice bearing RIG-I$^{-/-}$ tumors and further reflected in the

prolonged survival of mice bearing WT tumors receiving either Aza monotherapy or both treatments **(Figure 3.16 D)**. In line with our *in vivo* data, we observed a dose-dependent induction of tumor cell death in different B16.OVA tumor cell lines *in vitro* **(Figure 3.16 E)**. Consistent with our previous data, RIG-I-deficient tumor cells were less susceptible to Aza-mediated cell death whereas IRF3/7-deficient cells appeared to be even more vulnerable to the induction of tumor cell death by Aza compared to wild-type B16.OVA cells.

These data suggest that continuous ERV expression within tumor cells and its microenvironment might facilitate basal activation of the RIG-I pathway and thus serve as an endogenous RIG-I ligand. Treatment with Aza can enhance ERV expression and subsequent RIG-I activation, thus promoting the efficacy of anti-CTLA-4 checkpoint blockade.

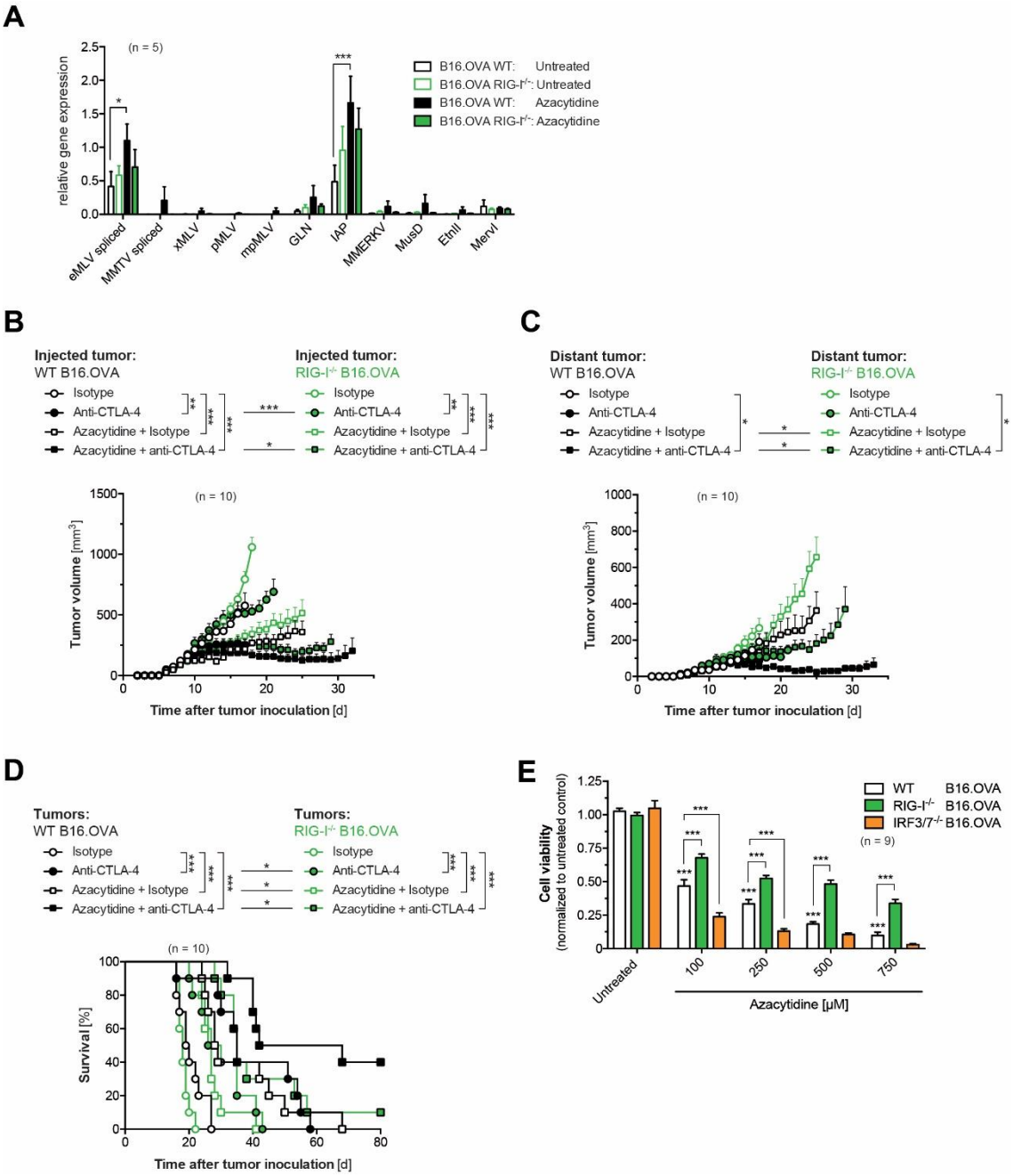

Figure 3.16: Synergistic antitumor effects of the DNA methyltransferase inhibitor 5-azacytidine and anti-CTLA-4 depend on tumor-intrinsic RIG-I activity. **(A)** WT and RIG-I$^{-/-}$ B16.OVA cells were treated with the DNA methyltransferase inhibitor 5-azacytidine. 24 h later, expression of endogenous retroviral (ERV) gene mRNA expression was determined by qRT-PCR. **(B-D)** Mice received either WT or RIG-I$^{-/-}$ B16.OVA cells in each flank and were repeatedly treated with anti-CTLA-4 +/- two cycles of intraturmoral 5-azacytidine administration. Tumor growth of **(B)** 5-azacytidine-injected and **(C)** distant B16.OVA tumors. **(D)** Overall survival of treated, tumor-bearing WT recipient mice. All figures give data of n = 10 individual mice per group that were pooled from two independent experiments. (E) WT, IRF3/7$^{-/-}$ and RIG-I$^{-/-}$ B16.OVA cells were treated with different concentrations of 5-azacytidine. 24 h later, apoptosis induction was assessed in an ATP release assay. Error bars give the mean ± S.E.M. of at least three independent experiments. An asterisk indicates comparison to the appropriate ‚untreated' control group.

3.5 RIG-I signaling in non-malignant host cells is required for durable and systemic tumor control after anti-CTLA-4 therapy

Our previous experiments have shown that efficient anti-CTLA-4 treatment crucially relies on tumor intrinsic RIG-I signaling which in turn triggers the release of host-derived IFN-I by DCs after 3pRNA mediated RIG-I activation. Therefore, we now wanted to investigate the role of the RIG-I pathway in non-malignant host cells for anti-CTLA-4 efficiency. Thus, we performed our bilateral flank tumor model in mice lacking MAVS (*Mavs*$^{-/-}$), the central adaptor protein in the RIG-I signaling pathway **(Figure 3.17 A)**.

In doing so, we found that Mavs$^{-/-}$ mice failed to mount a systemic antitumor immune response due to the lack of tumor antigen specific CTL expansion **(Figure 3.17 D)** which highlighted the importance of intact RIG-I signaling in non-malignant host cells. Even though *Mavs*$^{-/-}$ mice expressed low levels of tumor antigen specific CTLs following monotherapy or combined treatment, their systemic tumor control was impaired. The resulting rapid outgrowth of distant tumors was found in mice receiving either monotherapy with 3pRNA or anti-CTLA-4 and was further reflected in reduced survival of these animals **(Figure 3.17 C-E)**. Interestingly, local tumor rejection following 3pRNA application remained intact in *Mavs*$^{-/-}$ mice, suggesting other mechanisms were involved in local tumor growth control or the ability of tumor cell-intrinsic RIG-I signaling to facilitate antitumor immunity **(Figure 3.17 B)**. Although, anti-CLTA-4 treatment efficacy was impaired in *Mavs*$^{-/-}$ mice, this effect was less pronounced compared to the effect we had observed in mice bearing RIG-I deficient tumors that had received the anti-CTLA-4 blocking antibody. Moreover, and in contrast to deficiency of tumor cell-intrinsic RIG-I signaling, we observed no significantly reduced frequency of tumor-specific CD8$_+$ T cells in these mice.

Based on these data, we hypothesized that either intact tumor-intrinsic RIG-I signaling or intact host intrinsic RIG-I signaling can provoke a treatment response up to a certain extent. To challenge this model, we inoculated RIG-I-deficient B16.OVA melanoma cells into *Mavs*$^{-/-}$ recipients, thus entirely abrogating RIG-I signaling. Hereby we found that monotherapies and the combined treatment achieved no treatment response, resulting in a rapid outgrowth of both local and distant tumors, consequently, leading to a survival disadvantage of these mice **(Figure 3.17 F)**. Thus, our findings emphasize the distinct role of either tumor or host RIG-I/MAVS signaling since therapy otherwise completely lost its effectiveness.

Taken together, these data suggest that host intrinsic RIG-I signaling contributes to systemic antitumor immunity in response to both anti-CTLA-4 monotherapy and, in particular, the combination of checkpoint blockade with local RIG-I activation. Nevertheless, it seems that either intact tumor intrinsic or host intrinsic RIG-signaling can elicit a local immune response upon stimulation with 3pRNA and therefore compensate the loss of either.

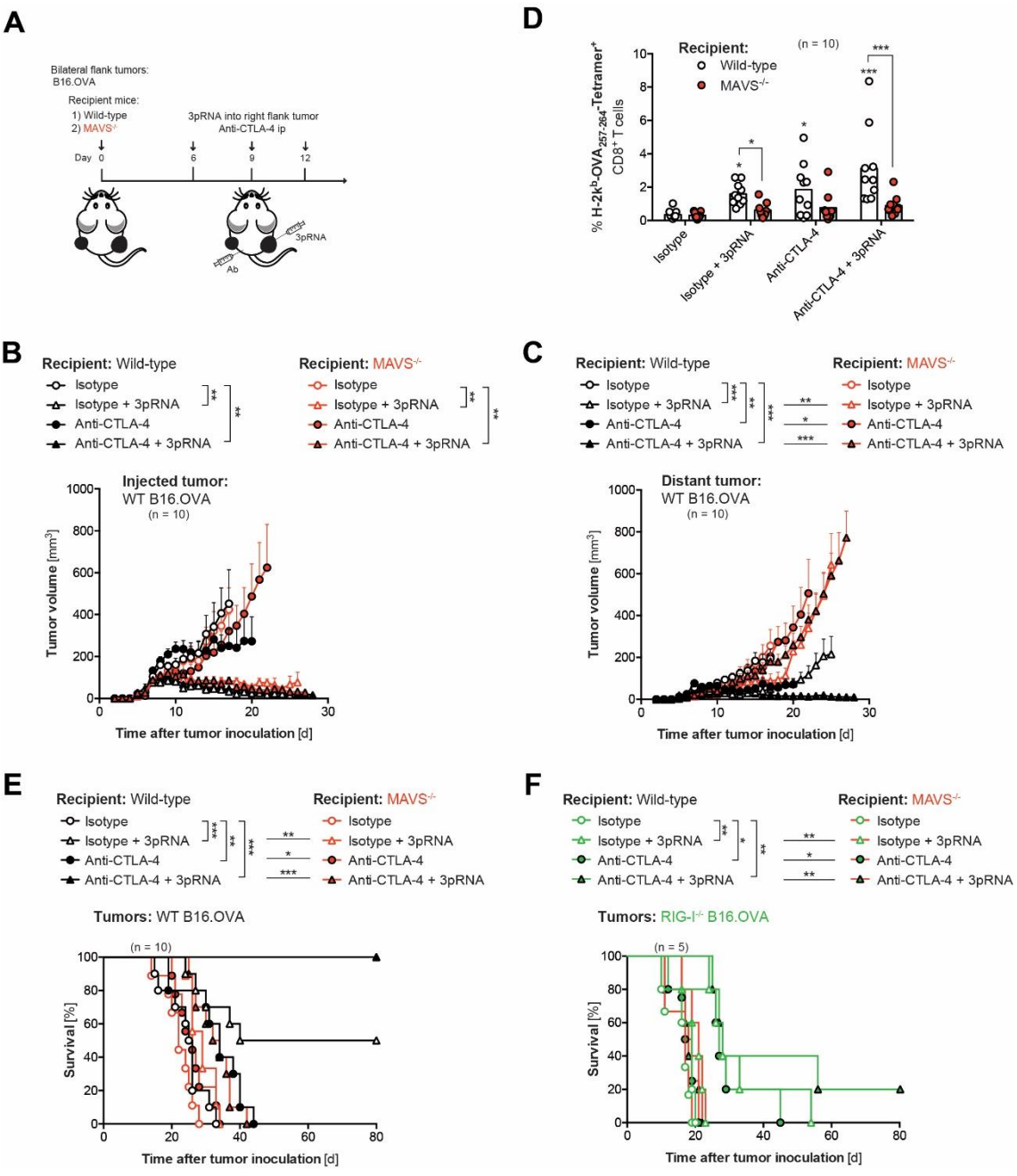

Figure 3.17: RIG-I signaling in non-malignant host cells is required for durable and systemic tumor control after anti-CTLA-4 therapy. (A) Treatment scheme: WT and MAVS-deficient (*Mavs*$^{-/-}$) mice were bilaterally inoculated with WT B16.OVA cells and repeatedly treated with anti-CTLA-4 +/- intraturmoral 3pRNA. **(B)** Tumor growth of 3pRNA-injected and **(C)** distant WT B16.OVA tumors. **(D)** Frequency of H-2Kb-SIINFEKL Tetramer+ CD8+ T cells in peripheral blood measured on day 15 after tumor induction. **(E)**

Overall survival of WT and *Mavs*$^{-/-}$ recipient mice bearing WT B16.OVA tumors. All figures give data of n = 10 individual mice per group that were pooled from two independent experiments. **(F)** WT and *Mavs*$^{-/-}$ mice were bilaterally inoculated with RIG-I$^{-/-}$ B16.OVA cells that were repeatedly treated with anti-CTLA-4 +/- intraturmoral 3pRNA. Overall survival of WT and *Mavs*$^{-/-}$ recipient mice bearing RIG-I$^{-/-}$ B16.OVA tumors.

3.6 Efficient anti-CTLA-4-mediated immunotherapy crucially relies on host but not tumor cell-intrinsic STING signaling

3.6.1 Tumor cell-intrinsic STING signaling is dispensable for efficient anti-CTLA-4-mediated checkpoint blockade

Cytosolic DNA is released upon tumor cell death, further sensed, and classified as a danger signal by the immune system that in turn can elicit a rapid antitumor immune response (Woo et al., 2014). In preceding experiments, we have elucidated the crucial role of cytosolic RNA sensing by tumor-intrinsic RIG-I signaling for augmenting the efficacy of anti-CTLA-4-mediated checkpoint blockade. Therefore, we next wanted to investigate the role of the cytosolic double stranded DNA sensing pathway cGAS/STING.

Even though genes encoding critical components of the cGAS/STING pathway have not been shown to be upregulated in tumor tissue of patients that benefited from checkpoint blockade (Chiappinelli et al., 2015), previous studies suggested the cGAS/STING pathway to be functional in different tumor cell lines (O. Demaria et al., 2015; Takashima et al., 2016). Hence, we generated a B16.OVA melanoma cell line deficient in tumor cell-intrinsic STING (STING$^{-/-}$) signaling and started by assessing STING activity following cGAS stimulation with interferon stimulatory DNA (ISD) (Stetson & Medzhitov, 2006). STING signaling in wild-type B16.OVA melanoma cells was intact and active as we observed IFN-I release upon ISD transfection in a time depended manner **(Figure 3.18 A)**. However, IFN-I induction was far less pronounced compared to the levels observed after stimulation with 3pRNA. In contrast to RIG-I activation, ISD-induced cGAS/STING failed to induce tumor cell death *in vitro* **(Figure 3.18 B)**.

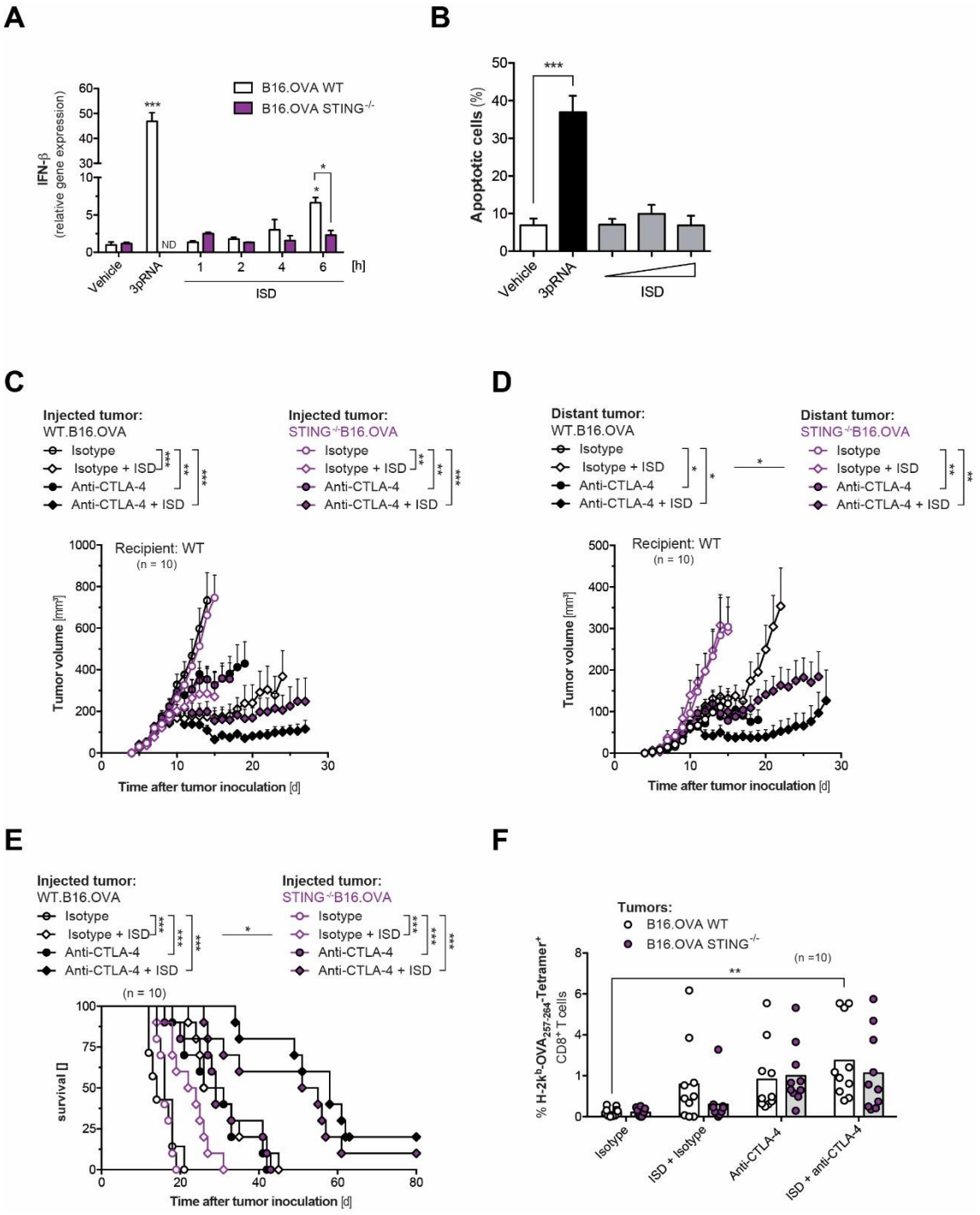

Figure 3.17: Tumor intrinsic STING signaling is dispensable for efficient anti-CTLA-4 mediated checkpoint blockade. (A-B) Wild-type (WT) or STING-deficient (STING$^{-/-}$) B16.OVA cells were transfected with 3pRNA or ISD *in vitro* using Lipofectamin 2000. **(A)** IFN-I release was determined by ELISA 48h later. **(B)** Apoptosis induction was assessed by Annexin V and 7-AAD staining. Error bars give the mean ± S.E.M. of triplicate samples. All data are representative for at least two independent experiments. **(C-F)** WT recipient mice were implanted with B16.OVA WT or STING$^{-/-}$ cells in each flank and repeatedly treated with anti-CTLA-4 +/- intratumoral ISD injections. Mean ± S.E.M. tumor growth of **(C)** ISD-injected and **(D)** distant B16.OVA tumors. **(E)** Overall survival of treated mice bearing B16.OVA tumors. **(F)** The frequency of H-2Kb-SIINFEKL Tetramer+ CD8+ T cells in peripheral blood was determined 15 days after tumor induction. All data show mean values of n = 10 individual mice pooled from two independent experiments.

To elucidate the role of tumor cell intrinsic STING deficiency in vivo, we inoculated wild-type mice with either B16.OVA WT or STING$^{-/-}$ cells. Consistent with the data derived from a previous study (Corrales et al., 2015), treatment of pre-established wild-type B16.OVA flank tumors by intratumoral application of ISD resulted in a delayed tumor outgrowth of both local and distant tumors. STING ligation synergized with anti-CTLA-4 checkpoint blockade as animals that received the combination of both treatments had a significant longer survival **(Figure 3.18 C-D)**. However, neither ISD monotherapy nor the combined treatment achieved complete tumor regression.

Apart from this, we observed identical therapy efficacy of anti-CTLA-4 monotherapy or the combined treatment in mice bearing either wild-type or STING$^{-/-}$ tumors. This similar therapy response was moreover reflected in both tumor growth and survival as mice bearing STING deficient tumors had neither an impaired tumor growth control nor a survival disadvantage when compared to animals bearing wild-type tumors **(Figure 3.18 E)**. In addition, the systemic expansion of tumor-specific circulating CD8^{+} T cells appeared to be independent of tumor cell-intrinsic STING signaling **(Figure 3.18 F)**. Nevertheless, we observed a trend towards reduced tumor-specific T cell frequencies in animals bearing STING$^{-/-}$ tumors that had been treated with ISD monotherapy. This, in turn, affected tumor growth control as these mice showed a faster outgrowth of systemic tumors compared to mice bearing wild-type B16.OVA tumors and resulted in a significant survival disadvantage following ISD treatment.

Thus, we demonstrated that in our model single agent anti-CTLA-4-mediated antitumor immunity does not require tumor cell intrinsic STING signaling. Nevertheless, intratumoral STING signaling seems to contribute to ISD-mediated systemic tumor control.

3.6.2 Host intrinsic STING signaling is crucial for efficient checkpoint blockade

Having demonstrated that tumor-intrinsic STING signaling is insignificant for anti-CTLA-4 checkpoint blockade, we went on by focusing our investigations on host intrinsic STING signaling. Previous studies suggested active STING signaling in host APCs as a basic requirement for efficient checkpoint blockade (Woo et al., 2014).

Therefore, we inoculated either wild-type mice or mice deficient in STING (*STING$^{gt/gt}$*) with B16.OVA WT cells and treated pre-established tumors with intratumoral injection of 3pRNA and systemic application of CTLA-4 blocking antibody. We found that the

RIG-I-mediated antitumor response remained intact in STING deficient mice since local 3pRNA application induced tumor regression in these animals leading to local tumor control and delayed systemic tumor outgrowth **(Figure 3.19 A-B)**. Consistent with the data of Woo et al., we observed that systemic anti-CTLA-4 checkpoint blockade was ineffective in *STING$_{gt/gt}$* mice and resulted in a rapid tumor outgrowth and a survival disadvantage of knockout mice **(Figure 3.19 C)**. Consequently, the synergistic effect of local RIG-I activation and systemic immune checkpoint blockade was lost in STING deficient animals.

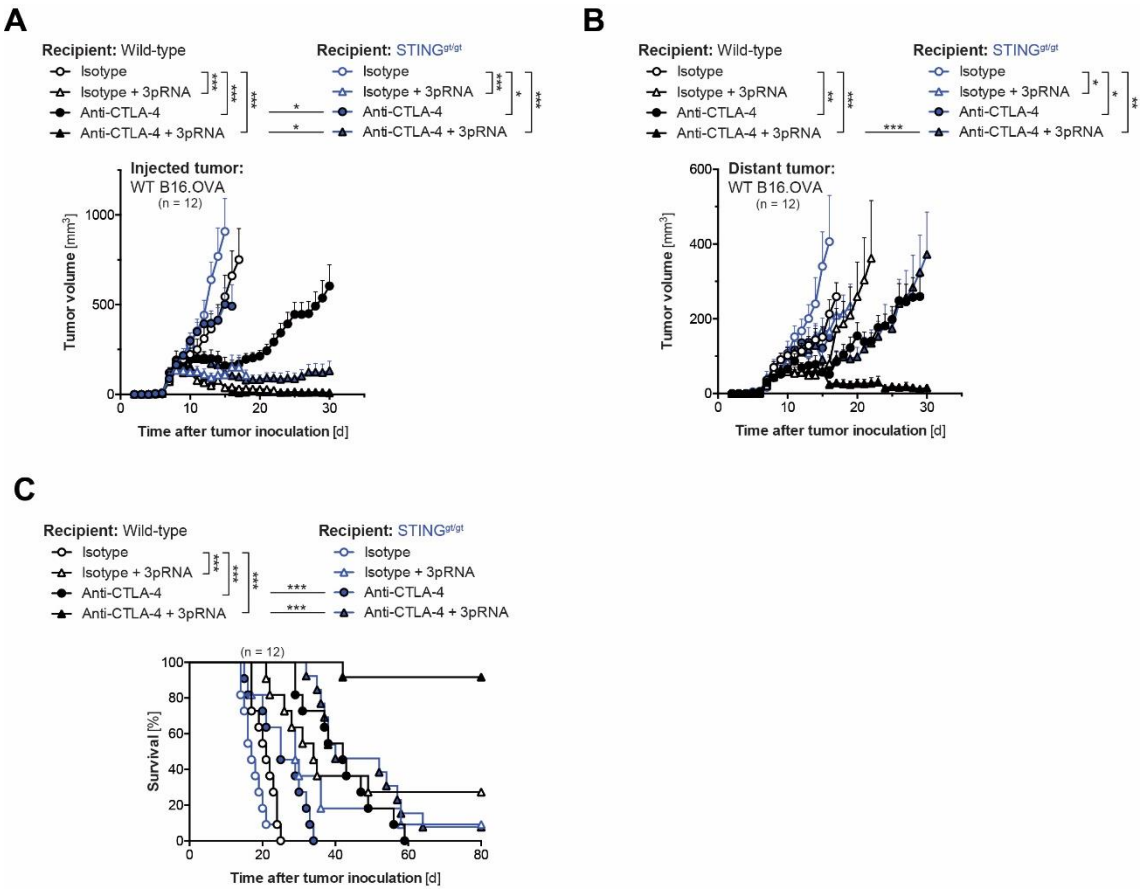

Figure 3.18: Host intrinsic STING signaling is mandatory for efficient checkpoint blockade. WT and STING-deficient (STINGgt/gt) mice were bilaterally inoculated with WT B16.OVA cells and repeatedly treated with anti-CTLA-4 +/- intratumoral 3pRNA. **(A)** Tumor growth of 3pRNA-injected and **(B)** distant wild-type B16.OVA tumors. **(C)** Overall survival in WT and STINGgt/gt recipient mice bearing WT B16.OVA tumors. All figures give data of n = 10-12 individual mice per group that were pooled from two independent experiments.

In contrast to our previous data, showing that tumor cell-intrinsic STING signaling is irrelevant for efficient anti-CTLA-4-mediated checkpoint blockade and in line with previously published data, we demonstrated that CTLA-4 immune checkpoint blockade lost its effect in mice lacking intact STING signaling which further influenced the synergistic effect of combined treatment in our model. We thus confirmed the important role of host but not tumor cell-intrinsic STING signaling for anti-CTLA-4-mediated antitumor responses.

3.7 Local RIG-I activation renders poorly immunogenic tumors susceptible to anti-CTLA-4 immunotherapy involving both CD8+ T cells and NK cells

3.7.1 Combination of local RIG-I activation and CTLA-4 checkpoint blockade synergized in a poorly immunogenic tumor model

So far, we studied the combination of selective RIG-I activation and anti-CTLA-4-mediated checkpoint blockade in an immunogenic tumor model as the B16 melanoma cell line we had been working with stably expressed the artificial tumor-associated antigen OVA. To investigate whether our synergistic therapy approach would be effective in a poorly immunogenic model, we treated mice inoculated with B16-F10 tumor cells with either 3pRNA and anti-CTLA-4 or the combination of both.

B16-F10 is a non-immunogenic B16 melanoma cell line that has previously been described to be resistant to anti-CTLA-4 monotherapy (van Elsas et al., 1999). Accordingly, anti-CTLA-4 monotherapy entirely failed to induce antitumor immunity as reflected in tumor growth and survival **(Figure 3.20 A-C)**. Nevertheless, local RIG-I activation led to delayed tumor growth of injected tumors; however, it was not capable of inducing a systemic antitumor response. Interestingly, 3pRNA administration rendered non-immunogenic B16-F10 tumors susceptible to anti-CTLA-4-mediated checkpoint blockade, as the combination of both therapeutic approaches resulted in a significantly delayed outgrowth of the opposing distant tumor **(Figure 3.20 B)**. Consequently, this growth delay led to prolonged survival. Moreover, mice receiving the combination of both selective RIG-I activation and anti-CTLA-4 blockade showed an expansion of cytotoxic T cells specific to the melanoma-associated tumor antigen tyrosinase-related protein 2 (TRP2) as shown by tetramer staining **(Figure 3.20 D)**.

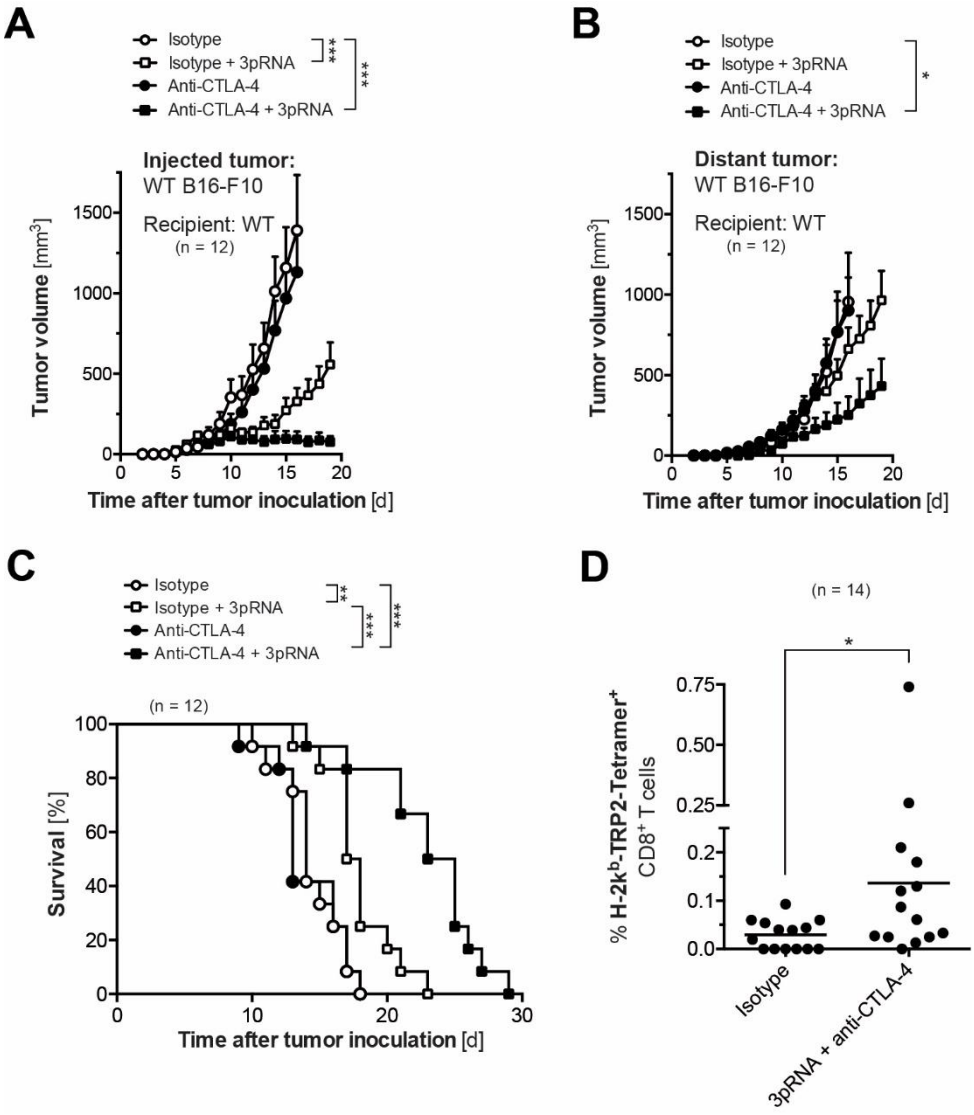

Figure 3.20: Combination of local RIG-I activation and CTLA-4 checkpoint blockade synergized in a poorly immunogenic tumor model. Wilde-type recipient mice received poorly immunogenic B16-F10 melanoma cells in each flank and were repeatedly treated with anti-CTLA-4 +/- intratumoral 3pRNA. **(A)** Tumor growth of local, 3pRNA-injected and **(B)** distant B16-F10 tumors and **(C)** overall survival of treated mice. **(D)** Frequency of TRP2 Tetramer+ CD8+ T cells in peripheral blood was determined on day 15 after tumor induction. All figures give data of n = 12-14 individual mice per group that were pooled from at least two independent experiments.

3.7.2 CD8+ T cells and NK cells are required for the formation of a systemic immune response against growing tumors

Our previous data revealed that both intact tumor-intrinsic and host-intrinsic RIG-I signaling is capable of facilitating local tumor growth control and thus indicated additional mechanisms involved in the rejection of local 3pRNA-injected tumors apart from selective tumor cell-intrinsic RIG-I activation and the resulting tumor cell death. In preceding experiments, we had investigated enhanced frequencies of systemic antigen-specific CTLs. In addition, a previous study demonstrated that RIG-I-mediated antitumor immunity is - at least in part - facilitated via IFN-I-mediated activation of NK cells (Poeck et al., 2008). Hence, we wanted to investigate if effector cells of innate and adaptive immunity would have an impact on systemic antitumor immunity in our model.

Therefore, we treated wild-type mice with either anti-CD8 or anti-CD4 antibodies to deplete these specific T cell subsets before we performed our bilateral flank tumor model. Our findings highlighted the crucial role of CTLs for systemic antitumor immunity as mice depleted for $CD8^+$ but not $CD4^+$ T cells failed to mount a systemic antitumor immune response following combined treatment with both 3pRNA and anti-CTLA-4 **(Figure 3.21 A-B)**. Compatible with the data obtained from previous studies (Ma et al., 2016), we observed that depletion of NK cells also abrogated the therapeutic effects of both monotherapies and the combined treatment and was followed by rapid outgrowth of injected and distant tumors **(Figure 3.21 A-B)**. However, it appeared that activation of tumor-infiltrating NK cells and the subsequent IFN-γ release were independent of tumor cell-intrinsic RIG-I signaling and further restricted to the local 3pRNA-injected tumor **(Figure 3.21 C-D)**. Thus, our findings suggest that activation of NK cells in the tumor microenvironment of local 3pRNA-injected tumors may induce tumor cell killing and contributes to subsequent T-cell priming and the resulting antitumor immune response.

Taken together, our data demonstrate that both NK cells and $CD8^+$ T cells are crucial for the development of synergistic therapy effects due to selective local RIG-I activation and anti-CTLA-4 blockade and the resulting systemic antitumor immune response in otherwise poorly immunogenic tumors.

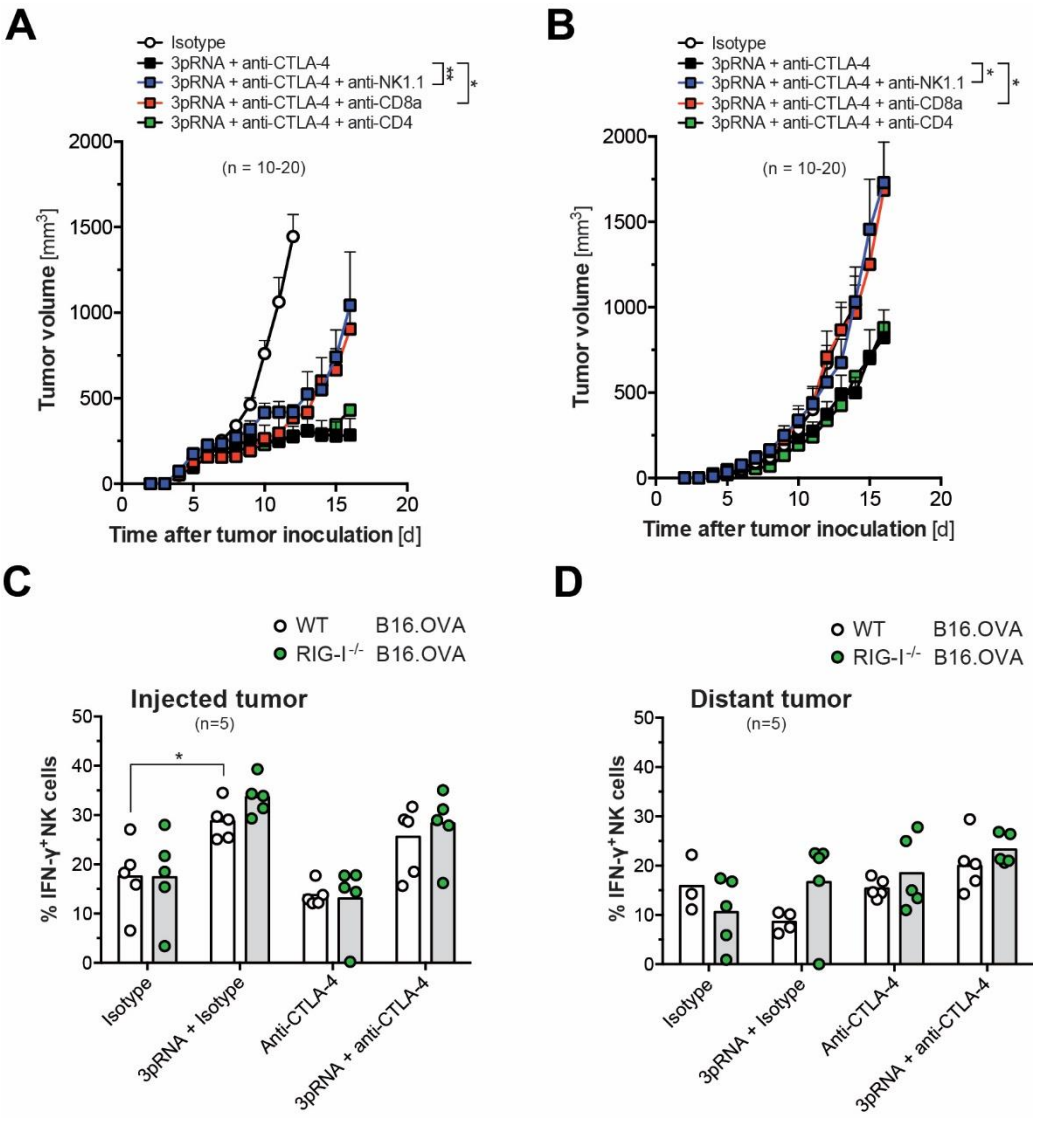

Figure 3.21: CD8+ T cells and NK cells are required for the formation of a systemic immune response. Mice were injected with poorly immunogenic B16-F10 melanoma cells in each flank and repeatedly treated with anti-CTLA-4 +/- intratumoral 3pRNA. Some mice were additionally pre-treated with anti-CD8α (cytotoxic T cells), anti-CD4 (helper T cells) or anti-NK1.1 (NK cells) depleting antibodies, beginning two days before tumor induction. Tumor growth of **(A)** 3pRNA-injected and **(B)** distant B16-F10 tumors in WT mice receiving additional depleting antibodies. Given data of n = 10-20 individual mice per group that were pooled from two independent experiments. **(C-D)** Mice bearing bilateral WT or RIG-I$^{-/-}$ B16.OVA tumors were treated with repeated intratumoral 3pRNA injections +/- anti-CTLA-4. Frequency of IFN-γ$_+$ tumor-infiltrating NK cells in **(C)** 3pRNA-injected and **(D)** distant tumors was determined by flow cytometry. The figures give data of n = 5 individual mice per group from one representative experiment.

3.7.3 Combined targeting of distinct immune checkpoints further enhances therapy efficiency

Other inhibitory checkpoints besides CTLA-4 such as PD-1 play an important role in regulating adaptive immunity. Their blockade has further been established in cancer immunotherapy. In contrast to the role of CTLA-4 in early T-cell activation, PD-1 contributes to T cell exhaustion and therefore compromises the antitumor efficacy of activated T cells (McClanahan et al., 2015). Previous studies have demonstrated that due to the expression of its ligand PD-L1 can occur on both tumor and infiltrating immune cells as direct response to IFN-γ release (Pardoll, 2012). With our previous experiments, showing a significant survival advantage of mice treated with anti-CTLA-4 monotherapy and its dependency on tumor intrinsic RIG-I signaling and associated IFN-γ release **(Figure 3.22 E-F)**, we were interested in the role of PD-1 in our experimental model.

Therefore, in a first experiment, we investigated expression levels of PD-L1 on both tumor-infiltrating $CD45^+$ cells and B16.OVA melanoma cells in response to 3pRNA treatment. Mice were inoculated with either B16.OVA wild-type cells or RIG-I deficient tumor cells and received a single intratumoral injection of either jetPEI as vehicle control or complexed 3pRNA. Here, we observed a rapid upregulation of PD-L1 expression on tumor-infiltrating immune cell subsets after local RIG-I activation **(Figure 3.22 C-D)**. However, it appeared that this effect was limited to tumor-infiltrating immune cells as PD-L1 levels on B16 melanoma cells were unaltered. In addition, it seemed that PD-L1 expression was unaffected by tumor intrinsic RIG-I signaling.

Several studies in preclinical models have demonstrated that combining blockade of PD-1 and CTLA-4 resulted in a more pronounced antitumor activity compared to the blockade of either pathway alone (Hodi et al., 2016). Therefore, as a next experiment, we investigated combined immune checkpoint blockade in our non-immunogenic tumor model. Combining anti-CTLA-4 checkpoint blockade with the blockade of the PD-1/PD-L1 axis further improved the efficacy of intratumoral 3pRNA by keeping tumor growth in check and prolonged survival of treated animals **(Figure 3.22 A-B)**.

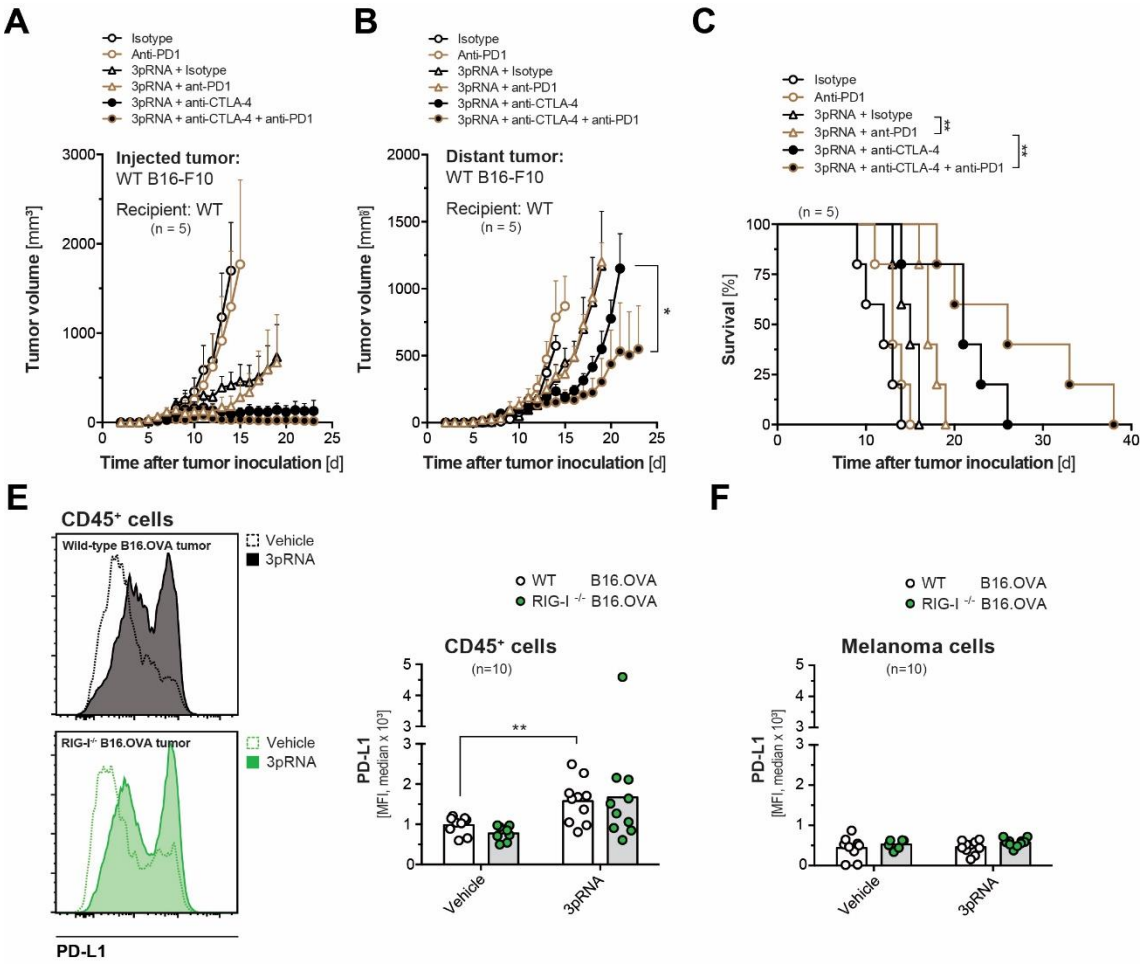

Figure 3.22: Combined targeting of distinct immune checkpoints further enhances therapy efficiency. B16-F10 tumor bearing wild-type mice were treated with anti-CTLA-4 +/- intratumoral 3pRNA and were additionally injected with anti-PD-1 antibodies. Tumor growth of **(A)** 3pRNA-injected, **(B)** distant B16-F10 tumors and **(C)** overall survival of WT recipient mice that were additionally treated with anti-PD1. Given data of n = 5 individual mice per group from a single representative experiment. **(E-F)** Mice bearing either WT or RIG-I$^{-/-}$ B16.OVA tumors were treated with a single intratumoral 3pRNA injection. After 24 h, the PD-L1 expression on **(E)** tumor-infiltrating CD45+ cells and **(F)** melanoma cells was analyzed by flow cytometry. Representative histograms show PD-L1 expression of CD45+ cells within wild-type (black) and RIG-I$^{-/-}$ (green) tumors.

3.8 Antitumor synergy between CTLA-4 blockade and local RIG-I activation is present in several different tumor models

3.8.1 RIG-I ligation induces cancer cell death and a pronounced IFN-I response in distinct tumor cell lines

Our previous experiments have shown that therapeutic targeting of RIG-I induces immunogenic cell death in a murine melanoma model *in vivo* and further augments therapy efficiency of anti-CTLA-4-mediated checkpoint blockade. A recent study confirmed that RIG-I-mediated immunogenic cell death is not limited to melanoma cells by demonstrating that RLH-induced cell death can induce efficient antitumor immunity in other malignancies such as pancreatic carcinoma (Duewell et al., 2014). Moreover, a modified siRNA with 5´-triphosphate ends targeting MDR-1 reduced drug resistance as well as immune and pro-apoptotic effects in various human leukemia cell lines. The mechanism-of-action involved IFN-I release, secretion of interferon-gamma-inducible protein 10 (IP-10), upregulation of MHC-I and caspase-mediated induction of apoptosis (D. Li et al., 2017). Therefore, we wanted to investigate whether local RIG-I activation and the subsequent associated immunogenic tumor cell death would enhance the treatment efficacy of anti-CTLA-4 checkpoint blockade in tumor entities other than melanoma.

As a first step, we tested different tumor cell lines for the release of IFN-I in response to RIG-I ligation *in vitro*. All cell lines revealed a consistent IFN-I release upon stimulation with 3pRNA as we observed significantly enhanced levels of both IFN-α and IFN-β **(Figure 3.23 A-B)**. Nevertheless, RIG-I-mediated cell death was less pronounced in pancreatic carcinoma (Panc02) and colon carcinoma (C26) cells in comparison to B16.OVA wild-type cells **(Figure 3.23 C)**. Moreover, the 4T1 mammary carcinoma (4T1) cell line appeared to be resistant to RIG-I-mediated cell death *in vitro*.

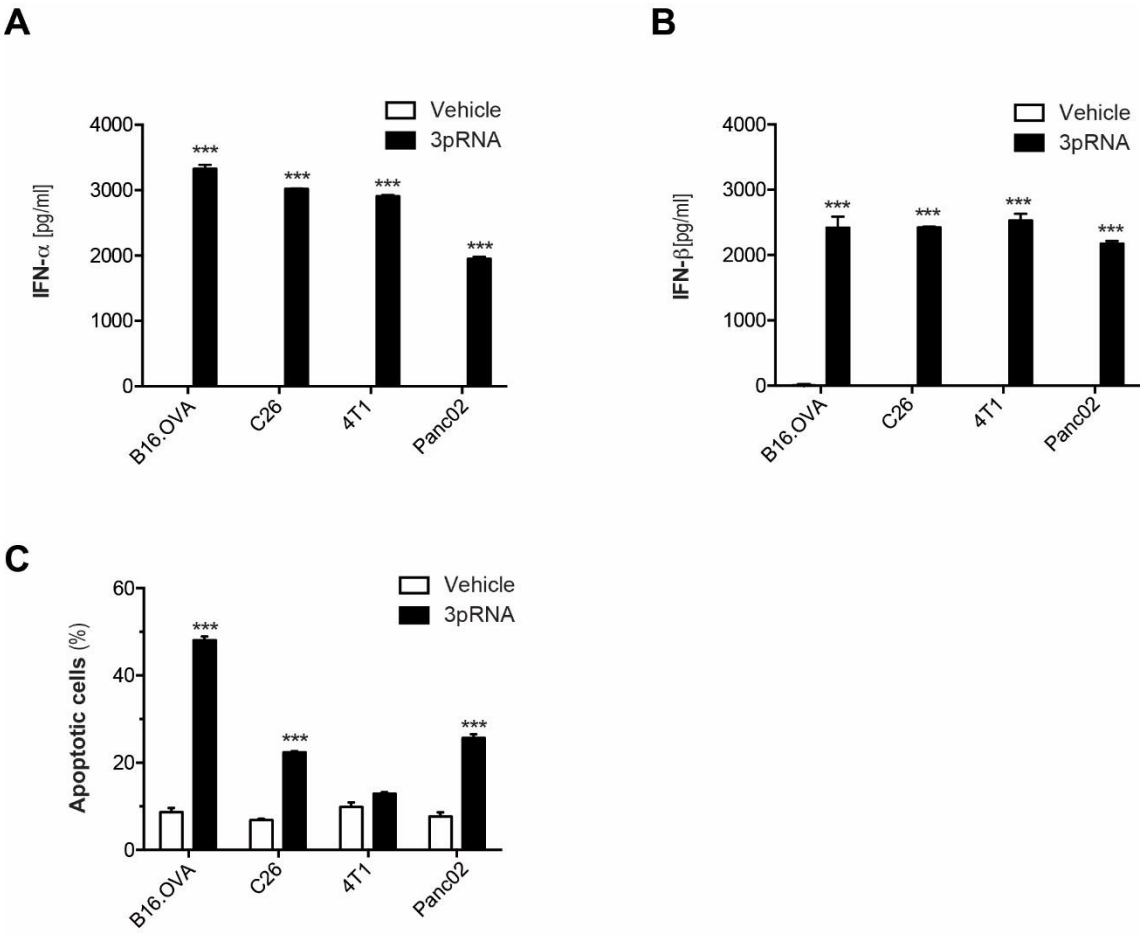

Figure 3.23: RIG-I ligation induces cancer cell death and a pronounced IFN-I response in distinct tumor cell lines. Different tumor cell lines were transfected with 3pRNA *in vitro* using Lipofectamin 2000. **(A-B)** Release of IFN-I was determined by ELISA. **(C)** Apoptosis induction was assessed by Annexin V and 7-AAD staining. Error bars give the mean ± S.E.M. of at least quadruplicate samples. An asterisk indicates comparison to the appropriate ‚vehicle' control group.

3.8.2 Antitumor synergy between CTLA-4 blockade and local RIG-I activation is present in several different tumor models

By performing our bilateral flank tumor model with Panc02 pancreatic carcinoma cells, we could observe synergistic effects by combining local 3pRNA application with anti-CTLA-4 blockade leading to complete regression of both local and distant tumors, resulting in long-term survival of these animals. However, this effect seemed to be mainly driven by anti-CTLA-4-mediated antitumor immunity, as monotherapy with 3pRNA achieved no substantial survival benefit whereas 60% of the mice that had received anti-CTLA-4 treatment survived. Even though subcutaneous colon carcinoma (C26) flank tumors showed delayed tumor growth upon RIG-I activation in local and distant tumors,

we could not asses any further synergistic effects as sole anti-CTLA-4 monotherapy led to a complete tumor regression independent of additional 3pRNA application. In contrast, by applying 4T1 mammary carcinoma cells in the bilateral flank tumor model, monotherapy with anti-CTLA-4 checkpoint blockade failed to induce an efficient antitumor immune response as tumor growth seemed to be unaffected. Nevertheless, 3pRNA treatment achieved tumor growth control at least up to a certain extent but did not synergize with checkpoint blockade which might be due to the inability of 3pRNA to induce RIG-I-mediated immunogenic cell death in this cell line *in vitro*.

Taken together, these data demonstrate that local targeting of RIG-I can enhance the efficacy of anti-CTLA-4 immunotherapy in different tumor models. However, RIG-I-mediated cell death appears to be decisive for therapy efficacy.

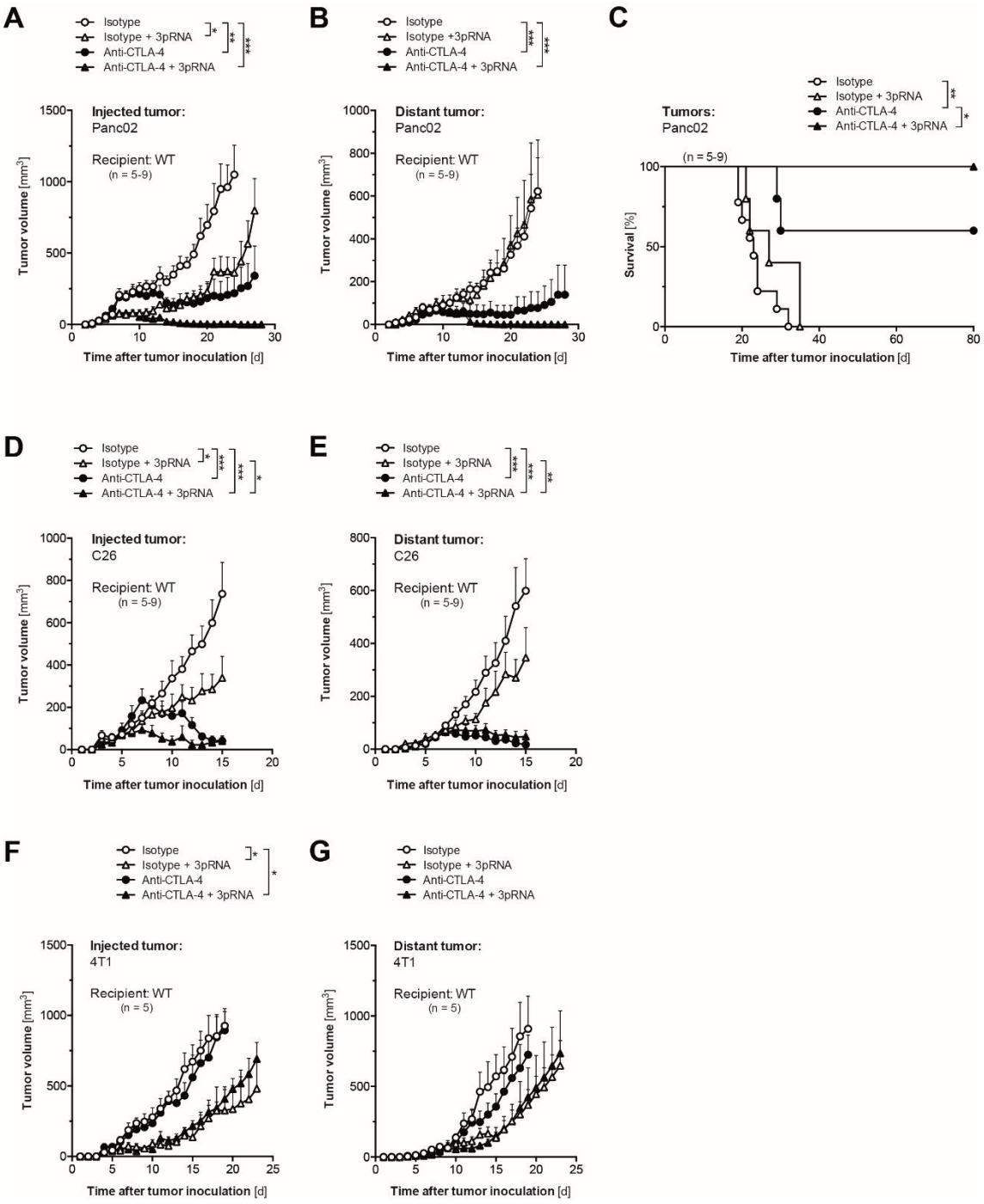

Figure 3.24: Antitumor synergy between CTLA-4 blockade and local RIG-I activation is present in several different tumor models. Using different tumor cell lines, mice received tumor cells in each flank and were repeatedly treated with anti-CTLA-4 +/- 3pRNA. **(A-B)** Tumor growth of 3pRNA-injected and distant Panc02 pancreatic carcinoma cell line tumors. **(C)** Overall survival in treated animals bearing bilateral Panc02 tumors. **(D-E)** Tumor growth of 3pRNA-injected and distant C26 colon carcinoma cell line tumors. **(F-G)** Tumor growth of 3pRNA-injected and distant 4T1 mammary carcinoma cell line tumors.

4 Discussion

4.1 PRR signaling in cancer immunotherapy

Novel immunotherapeutic approaches such as immune checkpoint blockade have been reshaping the treatment of cancer. However, a significant proportion of patients remains unaffected by therapy (Hodi et al., 2010). Its success has been associated with a pre-existing T cell response (Spranger et al., 2013; Tumeh et al., 2014). Hence, recent studies aim at designing seminal approaches to initiate a *de novo* antitumor immune response from within the tumor microenvironment. Previous reports have highlighted the particular role of PRR pathways in this context (Liu et al., 2016; C. K. Tang et al., 2013).

In the present study, we identified a so far unrecognized role of tumor-intrinsic RIG-I signaling for immune checkpoint blockade-mediated antitumor immune responses. Based on a previous study which suggested a connection between increased activity of antiviral defense genes in tumor biopsies and enhanced therapy responses to anti-CTLA-4 immunotherapy of melanoma patients (Chiappinelli et al., 2015), we now provide experimental evidence that RIG-I signaling in melanoma cells promotes the efficacy of anti-CTLA-4-mediated checkpoint blockade whereas STING signaling appeared to be dispensable. We identified distinct underlying mechanisms responsible for this synergism that comprise the induction of caspase-3-mediated apoptotic cancer cell death upon tumor cell-intrinsic RIG-I activation, the subsequent enhanced cross-presentation of tumor-associated antigens by CD103+ dendritic cells, which is spatially restricted to the tumor draining lymph nodes, as well as the systemic expansion of tumor-antigen-specific CTL and the subsequent infiltration of these cells into the tumor. Moreover, therapeutic targeting of RIG-I in the tumor microenvironment enhanced these effects potently and further increased efficacy of anti-CTLA-4 checkpoint blockade.

Preceding studies focused their therapeutic efforts on PRR signaling pathways in non-malignant host cells, whereas few of these studies addressed the impact of tumor-intrinsic nucleic acid receptor signaling on immune checkpoint inhibitor-mediated antitumor immunity and how it may converge with host-cell intrinsic antitumor immunity. By combining local tumor intrinsic RIG-I activation with systemic anti-CTLA-4-mediated immune checkpoint blockade, we identified a hitherto unrecognized role of tumor cell and host immune cell intrinsic RIG-I signaling to enhance checkpoint blockade-mediated antitumor responses. Both tumor- and host-intrinsic RIG-I signaling are fundamental

requirements for anti-CTLA-4-mediated antitumor immunity. Thus, targeting of RIG-I may serve as a basis for the development of new combination strategies to increase the response rate of checkpoint inhibitor-based immunotherapy, in particular in individuals without a sufficient spontaneous antitumor T-cell immune response. However, the endogenous ligand that could facilitate baseline activity of RIG-I in tumor cell and thus causes a beneficial condition for effective checkpoint-mediated antitumor immunity still remains unknown and therefore needs to be further evaluated in future studies.

4.1.1 Therapeutic targeting of RIG-I synergizes with immune checkpoint blockade

Cytosolic RNA sensing by RIG-I within host cells has previously been found to induce potent IFN-I release and the induction of an antiviral immune response upon activation (Goubau et al., 2014a). In addition, and in contrast to other cytosolic nucleic acid receptors, targeted activation of RIG-I within tumor cells can induce ICD that results in growth inhibition of pre-established tumors (Poeck et al., 2008). A follow-up study demonstrated that this cell-intrinsic pathway is particularly active in malignant cells as defective protection against apoptosis induction by the anti-apoptotic molecule Bcl-xL renders melanoma cells susceptible to this type of apoptotic stimulation. In contrast, non-malignant cells were found to evade cell death by upregulating of Bcl-xL (Besch et al., 2009). As RIG-I is ubiquitously expressed, both malignant and non-malignant cells respond with potent IFN-I release upon activation. The antitumor effects of RIG-I activation and combined anti-CTLA-4 blockade in this study were dependent on host-derived IFN-I signaling but did not rely on tumor-derived IFN-I. Thus, activation of RIG-I does indeed target different pathways in both malignant cells by induction of tumor intrinsic cell death and in non-malignant cells by facilitating IFN-I release.

IFN-I is of particular importance for the generation of antigen-specific T cell responses against growing tumors, facilitating the accumulation of $CD8\alpha^+$ DCs in the tumor and subsequent cross-priming of tumor antigen specific CTLs (Diamond et al., 2011; Fuertes et al., 2011). This might be facilitated by $CD103^+$ DCs as this Batf3-dependent DC subtype mainly mediates IFN-I-dependent antitumor immunity in melanoma (Salmon et al., 2016). In line with this, RIG-I activation by either therapeutic vaccination or adenovirus infection affects $CD11c^+$ cells, especially CD8α-like Batf3-dependent dendritic cells to cross-prime $CD8^+$ T cells (Hochheiser et al., 2016). Therefore, RIG-I ligation in the tumor and its microenvironment might enhance T cell-mediated immune responses due to antigen release by induction of tumor cell death, intratumoral

recruitment of DCs due to IFN-I release by host cells, cross-priming of CTLs by CD103+ DCs and subsequent eradication of preexisting tumors. Thus, therapeutic targeting of IFN-I inducing nucleic acid receptors in the tumor microenvironment is a promising therapeutic approach to generate T cell-mediated antitumor responses. Moreover, a previous study stressed the role of combining the immune stimulatory double-stranded RNA analogue poly(I:C), a TLR3 and RLH ligand, with antibody-mediated PD-1 blockade that in turn prolonged survival of mice bearing poorly immunogenic tumors (Bald et al., 2014). Therefore, PRRs, especially RLH agonists, might be a promising target for combination therapy allowing for the reduction of inter-individual variabilities in clinical response.

4.1.2 Induction of spontaneous antitumor immune response by sensing of cytosolic DNA

Previous studies have primarily investigated the role of DNA sensing pathways in non-malignant host cells and their influence on the generation of antitumor T-cell immunity in this context. For instance, activation of the cGAS/STING pathway in host DCs by tumor-derived DNA triggers IFN-I release and subsequently induces a spontaneous antitumor immune response (Woo et al., 2014). Consequently, activation of the cytosolic nucleic acid sensing pathway cGAS/STING with specific synthetic ligands such as ISD or cyclic dinucleotides has been successfully used to enhance antitumor immunity and to generate substantial systemic immune responses in preclinical models (Corrales et al., 2015). This effect was mediated by spontaneous tumor-initiated T cell priming that relied on IFN-β production by tumor resident DCs which further depended on host STING signaling. Furthermore, intratumoral targeting of STING synergized with systemic triple checkpoint modulation and promoted systemic tumor control in a preclinical prostate cancer model (Ager et al., 2017) suggesting STING as another promising target for the combination of immune checkpoint blockade and target PRR activation.

However, we found that anti-CTLA-4 efficacy is independent on tumor-intrinsic STING activity in B16-OVA melanoma cells whereas its effectiveness critically relied on STING signaling in host cells. This was in line with the data published by Wo et al.. Nevertheless, our data indicated an essential role of MAVS signaling in nonmalignant host cells for the efficacy of anti-CTLA-4, though the effect was less pronounced compared to STING signaling. However, this was in contrast to the results obtained by the above-mentioned study, as they postulated that MAVS signaling is dispensable for the spontaneous

development of T cell-mediated antitumor immune response in their B16.SIY melanoma model. Nonetheless, these findings might be explained by the more pronounced immunogenicity of B16.SIY cells and the subsequent potent spontaneous antitumor immune responses that result in tumor rejection. Based on our findings, we assume that anti-CTLA-4-mediated immunotherapy depends on tumor-intrinsic RIG-I signaling and subsequent activation of STING signaling in the host. We hypothesize that the induction of tumor cell death by activation of RIG-I can facilitate the release of tumor-derived DNA from dying tumor cells which could be transported by extracellular vesicles that in turn can be taken up by myeloid host cells and subsequently induce STING signaling.

Yet, stimulation of the cGAS/STING pathway by ISD enhanced anti-CTLA-4 efficacy. This enhancement was mainly mediated by STING signaling in the host, not in the tumor. However, ISD-mediated antitumor effects were less pronounced compared to tumor intrinsic RIG-I ligation suggesting induction of cancer cell death as an additional requirement for efficient anti-CTLA-4-mediated checkpoint blockade. Given the weak potency of ISD to induce cGAS/STING activation in our B16 cells, it is not excluded that other potential ligands such as 2`3-cGAMP may utilize both host and tumor-intrinsic STING signaling for effective tumor immunotherapy. This is further supported by data demonstrating that tumor irradiation and the subsequent release of DAMPs results in host cGAS/STING-dependent maturation of intratumoral DCs leading to T cell cross-priming (Deng, Liang, Xu, et al., 2014). Moreover, *in situ* vaccination by ionizing radiation has been demonstrated to enhance anti-CTLA-4-mediated immune responses (Vanpouille-Box et al., 2015).

Moreover, a recent report has highlighted the role of STING for anti-CTLA-4 immunotherapy under certain circumstances by demonstrating that the induction of double-stranded DNA breaks caused by either radiation or chemotherapy leads to the formation of micronuclei by mitosis that can be sensed via cGAS and thus activate tumor-intrinsic STING signaling which is required for abscopal tumor effects *in vivo* (Harding et al., 2017). In accordance with our data, this study also demonstrated that anti-CTLA-4-mediated effects in principal do not depend on tumor-intrinsic STING signaling. Instead, radiation-induced formation of micronuclei and the subsequent activation of cGAS/STING signaling augmented treatment efficacy in the specific scenario of a combined modality approach using genotoxic agents and immune checkpoint blocking antibodies.

4.1.3 Crosstalk between DNA and RNA sensing pathways

4.1.3.1 Interplay of cytosolic nucleic acid sensing pathways due to physical interaction and transactivation of mediators of the respective other pathway

There is evidence for a partial overlap of DNA and RNA sensing pathways independent of their different receptors and adaptor molecules. Recognition of AT-rich dsDNA and the subsequent induction of an IFN-I response has been shown to link DNA sensing with the RIG-I pathway. Cytosolic DNA can serve as a template for the RNA polymerase III-driven synthesis of dsRNA, harboring a 5´triphosphate moiety (Ablasser et al., 2009; Chiu, Macmillan, & Chen, 2009). Thus, RNA polymerase III can function as a cytosolic sensor for bacterial and viral DNA. Further interactions between RNA- and DNA sensing mechanisms have been implied from studies of different human retroviruses such as HIV-1 and T-lymphotrophic virus 1 (HTLV-1). In a multistep process, the retroviral RNA genome is reversely transcribed and forms DNA-RNA duplexes and ssDNA intermediates as well as dsDNA molecules as final products which in turn can activate cGAS/STING via the interferon-γ-inducible protein/IFI16 axis and thus counteract retroviral infection by induction of ISGs and apoptosis (Jakobsen, Olagnier, & Hiscott, 2015; van Montfoort, Olagnier, & Hiscott, 2014).

The critical role of STING signaling on antiviral immunity has been shown in distinct human cell lines as the lack of STING expression is accompanied by a significantly increased susceptibility to infection by RNA viruses due to reduced IFN-I production (Ishikawa & Barber, 2008; Mankan et al., 2014). A reason for that might be the inability of specific cell subsets to produce IFN-I upon dsRNA recognition in an RIG-I dependent manner in the absence of intact STING signaling (L. L. Chen, Yang, & Carmichael, 2010), suggesting a potential role for STING in potentiating RIG-I-mediated antiviral immunity. Consistent with this hypothesis, the ssRNA genome of the Japanese encephalitis virus (JEV), a flavivirus responsible for the induction of neuronal inflammation in humans, can be recognized by RIG-I which in turn recruits STING to initiate an antiviral immune response. The absence of intact STING signaling leads to an increased intracellular viral load due to missing activation of the IRF/IFN pathway and thus an inhibited release of cytokines and chemokines (Nazmi, Mukhopadhyay, Dutta, & Basu, 2012).

In addition, it appears that STING can interact with MAVS and RIG-I to form a complex which is stabilized upon viral infection (Ishikawa & Barber, 2008; Zhong et al., 2008) and

thus is involved in the transmission of RIG-I signals. Several viruses such as the hepatitis C virus have evolved strategies to inhibit STING-mediated innate immunity by competitively binding STING on the mitochondrial membrane which leads to the displacement of MAVS from the RIG-I/MAVS/STING complex and thus prevents the activation of downstream effector proteins (Nitta et al., 2013). Moreover, the dengue virus can interact with the N2SB3 protease that cleaves cytosolic STING and hence impedes STING-dependent IFN-I production (Aguirre et al., 2012). Thus it appears that STING is a central key player in the interaction between DNA and RNA sensing and further facilitates RIG-I-mediated antiviral immune responses.

Conversely, cytosolic RNA sensing has been shown to enhance the activity of host immune responses against non-self DNA. Upon DNA virus infection, TBK1 is phosphorylated in an MAVS dependent manner which results in IFN-β release after MAVS-TBK1 interaction due to co-localization (Suzuki et al., 2013). The recently discovered STING ligand G10, capable of activating the IFN-I and IFN-III pathway in human cells, stimulates the STING/IRF3 axis and therefore facilitates protection against alphavirus infection independent of RIG-I signaling. Nevertheless, G10-dependent induction of IFN is impaired in MAVS deficient follicular CD4+ helper T cells (Sali et al., 2015).

4.1.3.2 Co-regulation of cytosolic nucleic acid sensing pathway expression levels

Besides this pathway interaction, interplay between RIG-I and STING can further occur due to coordinated regulation of the respective receptor expression levels. Infection with RNA viruses as well as artificial stimulation with poly(I:C) or 3pRNA do not only activate the RIG-I signaling pathway but also upregulate STING expression levels in various preclinical models, thus suggesting a contribution of RIG-I activation on the protective properties of STING against DNA viruses (Huang, Chen, Yu, & Chen, 2012; Liu et al., 2016). Conversely, irradiation with gamma rays or exposure to the DNA-damaging agent etoposide cause a state of chronic stimulation of DNA immune sensing in BMDCs, which results in induction of modulators of the DNA-sensing cascade such as cGAS/STING or IFI16 but also RIG-I (Hartlova et al., 2015). Consequently, viral infected BMDCs treated with etoposide mount a potent IFN-I response capable of suppressing viral replication.

Although, cGAS is considered to exclusively bind cytosolic DNA (Sun et al., 2013) it has previously been found to bind a synthetic small dsRNA molecule, however, this interaction did not result in the production of cGAMP (Civril et al., 2013). Nevertheless, $cGAS^{-/-}$ mice are susceptible to infection by West Nile virus (WNV) though this effect

appeared to be mediated by a modulation of ISGs as well as reduced ISG expression levels in infected knock-out animals (Schoggins et al., 2014).

In return, silencing of the DNA sensor IFI16 mitigates IFN-I responses upon viral infection or transfection with 3pRNA. It is supposed that IFI16 facilitates its regulatory function by directly binding the IFN promoter and thus facilitates the recruitment of RNA polymerase II and subsequent activation of gene transcription (M. R. Thompson et al., 2014).

Thus, the function of both DNA and RNA sensing pathways appears to be closely inter-connected by a partial overlap. Intact signaling of the opposing signaling pathway seems to be a requirement for effective induction of immune responses and thus can further promote receptor function. Furthermore, these interactions rely on the direct interaction of components of both pathways and the co-regulation of their expression as well as the conversion of nucleic acid ligands by the host. Thus, this pathway interaction might be an explanation for synergistic therapy responses by combined treatment in STING-deficient animals as well as for RIG-I dependent antitumor effects after local radiotherapy. The targeted activation of both pathways has been successfully used in several preclinical therapy approaches such as vaccine adjuvants and cancer therapeutics against highly immunogenic tumors. Therefore, the generation of melanoma cells deficient in both RIG-I and STING signaling or the utilization of knock-out mice deficient in both RIG-I and STING signaling might be necessary to elucidate the interplay of both pathways and to further validate the respective contribution to therapy efficiency.

4.2 Impact of intact tumor and host-intrinsic RIG-I signaling on the induction of tumor cell death

4.2.2 RIG-I dependent induction of programmed tumor cell death

Targeting of tumor-intrinsic RIG-I by its specific ligand 3pRNA has previously been shown to trigger both IFN-I release and the induction of programmed cell death (Poeck et al., 2008). In human cells, 3pRNA application has been suggested to activate the mitochondrial apoptosis pathway and induces RIG-I dependent but IFN-I independent apoptosis of melanoma cells *in vitro* (Besch et al., 2009). Activation of both RIG-I and MDA-5 induces the pro-apoptotic protein Noxa which facilitates cancer cell apoptosis and ultimately decreases lung metastasis in mice (Poeck et al., 2008).

Moreover, activation of the STING pathway was shown to result in the production of IFN-I and the subsequent induction of ISGs that can further induce cell death. However, STING signaling can also induce cell death IFN-independently by mediating interaction of IRF-3 with Bcl2-associated X protein (Bax) which triggers mitochondrial apoptosis in a caspase-3 and caspase-9 dependent manner (C. H. Tang et al., 2016). Nevertheless, it has been demonstrated that apoptotic caspases can suppress STING-mediated IFN-I induction (White et al., 2014). Moreover, stimulation of TLR9 with CpG triggered tumor cell death in neuroblastoma cells (Brignole et al., 2010). The latter was attributable to apoptosis, as cell death involved caspase-3 and caspase-7 activity as well as mitochondrial apoptosis since CpG stimulation of tumor cells resulted in the depolarization of mitochondrial membrane potential, an event thought to contribute to cell death through the disruption of the normal mitochondria function (van Loo et al., 2002).

Besides its role in apoptosis induction in melanoma cells, preceding studies have highlighted the role of RIG-I for the induction of tumor cell death in several preclinical models, different tumor entities and human primary cancer cells. According to a previous study, RIG-I has been shown to be abundantly expressed in tumor biopsies of patients with head and neck squamous cell carcinoma when compared to normal adjacent cells. Nevertheless, activation of tumor-intrinsic RIG-I by high doses of 3pRNA led to cancer cell apoptosis and was further accompanied by decreased levels of Act activation in different cell lines *in vitro* (Hu et al., 2013). Moreover, RIG-I activation induces apoptosis in patient-derived primary ovarian cancer cells by upregulation of HLA class I as well as the secretion of proinflammatory cytokines such as CCL5, interleukin-6, TNF-α and IFN-

β by tumor cells (Kubler et al., 2010). Additionally, apoptotic tumor cells were phagocytosed by monocytes and dendritic cells which in turn upregulated both HLA class I and II and released costimulatory molecules CXCL10 and IFN-α. Consistent with these findings, activation of RIG-I and its downstream protein MAVS triggers apoptosis of human primary glioblastoma cells and further enhances the expression levels of CXCL10 (Glas et al., 2013).

In line with these data, we here demonstrate that 3pRNA-mediated tumor cell death is dependent on tumor-intrinsic RIG-I but was independent of tumor-intrinsic IFN-I signaling *in vivo*. Furthermore, tumor growth control by anti-CTLA-4 therapy crucially relies on tumor-intrinsic RIG-I signaling but is independent of tumor-derived IFN-I. Moreover, synergistic effects that occurred by combining local RIG-I activation with anti-CTLA-4 blockade were closely linked to RIG-I-mediated tumor cell death *in vivo*. These data correspond with our findings that tumor-intrinsic RIG-I signaling activates the expression of the apoptosis initiator caspase-8, triggers the release of activated executive caspase-3 and further causes apoptotic DNA fragmentation *in vitro*. Induction of intrinsic apoptosis requires the cleavage of procaspase-8 (Chang, Xing, Capacio, Peter, & Yang, 2003). Fully activated caspase-8 can subsequently cleave caspase-3 which results in the induction of extrinsic apoptosis whereas the cleavage of the pro-apoptotic Bcl-2 family member Bid by caspase-8 initiates the intrinsic mitochondrial apoptosis pathway leading to the release of cytochrome c, subsequent cleavage of caspase-9 and thus activation of downstream executioner caspase-3 that initiates apoptosis (Kantari & Walczak, 2011; H. Li, Zhu, Xu, & Yuan, 1998).

The crucial role of RIG-I-mediated apoptosis induction was further supported by our *in vivo* observations that emphasized the significance of active tumor-intrinsic caspase-3 signaling for both RIG-I-mediated tumor cell death and efficient anti-CTLA-4 checkpoint blockade.

Another kind of programmed cell death is pyroptosis, a highly inflammatory form of cell death that often occurs upon infection with intracellular pathogens and in antimicrobial responses. It is characterized by the recognition of PAMPs in immune cells such as macrophages by distinct PRRs and leads to the induction of proinflammatory cytokines and subsequent cell swelling, membrane rupture and cell death. In contrast to apoptosis, cell death induction by pyroptosis results in plasma-membrane rupture and the subsequent release of DAMPs and cytokines into the extracellular space, which further sustains the inflammatory cascade (Baroja-Mazo et al., 2014; Franklin et al., 2014). Furthermore, pyroptosis requires the activation of the inflammasome by caspase-1 which is facilitated by binding RIG-I to the adaptor protein ASC (apoptosis-associated speck

protein). This interaction crucially relies on the adaptor molecules CARD9 and Bcl-10 and results in the release of Interleukin 1β (IL-1β), a potent proinflammatory factor during viral infection by the inflammasome as well as IL-18 (Poeck et al., 2010). However, the predominant processes in pyroptotis are in marked contrast to the characteristic properties of apoptosis that include packaging of cellular content and non-inflammatory phagocytosis of membrane-bound apoptotic bodies.

A recent report has demonstrated that expression of RIPK1 and NF-κB activation during cell death are a requirement for efficient cross-priming and subsequent tumor immunity (Yatim et al., 2015). Furthermore, it was proposed that the release of inflammatory mediators such as DAMPs by dying tumor cells was insufficient in generating efficient $CD8^+$ T cell cross-priming. Moreover, necroptosis was postulated to be more efficient in the induction of cross-priming then apoptotic or necrotic cells, therefore suggesting that necroptotic cells bear a higher immunogenicity compared to necrotic or apoptotic cells. In addition, a hallmark of cancer is the blockade and/or evasion of apoptosis and thus is often considered as immunologically silent. Therefore, induction of necroptosis appears to be a promising target for cancer therapy. Nevertheless, induction of necroptosis and its immunogenic potential critically depend on both its activity in a distinct cancer cell line as well as its inducing stimulus (O. Krysko et al., 2017). Moreover, necroptotic cells do not necessarily have to be immunogenic. In this context, a previous study reported L-929 to be less inflammatory and to release lesser amounts of pro-inflammatory cytokines after induction of necroptosis *in vitro* (Kearney et al., 2015). However, additional studies are required to examine the immunogenicity of necroptosis further and how it affects the efficiency in cross-priming of $CD8^+$ T cells in different models.

Therefore, direct targeting of tumor intrinsic RIG-I signaling, and subsequent caspase-3-mediated cell death might initiate a *de novo* antitumor immune response by facilitating tumor antigen release which is the basis for promoting efficient antigen cross-presentation by $CD103_+$ dendritic cells and thus boost efficacy of anti-CTLA-4 mediated checkpoint blockade by facilitating a T cell-mediated immune response.

In this regard, a preceding study proposed that somatic mutations within malignant cells can potentially give rise to tumor-specific neoantigens which in turn can serve as major class T-cell rejection antigens and thus drive T-cell-mediated antitumor responses (Gubin et al., 2014). According to this study, apoptosis induction by tumor-intrinsic RIG-I ligation might enhance the ICD-dependent release of identified or unidentified tumor neoantigens and IFN-I-dependent processing and cross-priming of specific host antitumor immunity. This assumption was supported by another report that revealed a correlation between genetic mutations and therapy benefit by immune checkpoint

blockade (Rizvi et al., 2015; Snyder et al., 2014). Furthermore, CTLA-4 blockade has been demonstrated to enhance neoantigen-specific T-cell responses and also to broaden the melanoma antigen repertoire in human melanoma patients (Kvistborg et al., 2014).

Thus, induction of T cell-driven immune responses by tumor intrinsic RIG-I ligation and subsequent antigen release due to tumor cell apoptosis might be a potential approach to overcome interpatient heterogeneity and thus improve the efficacy of immune checkpoint blockade.

4.2.3 Necroptosis independent therapy responses

A recent report revealed that viral infection can trigger necroptosis in infected cells by activation of RIG-I (Schock et al., 2017). Consistent with this study, we found that the expression levels of RIPK1, RIPK3 and MLKL, all critical components of the proinflammatory necroptosis signaling cascade, were upregulated in an RIG-I dependent manner within tumor cells. A previous report indicated that activation of MLKL upon phosphorylation by the protein kinases RIPK3 is a prerequisite for the translocation of MLKL to the plasma and intracellular membranes where it triggers disruption of membrane integrity and induces subsequent programmed necroptotic cell death (Sun et al., 2012). Together with RIPK1 and RIPK3, MLKL can form a signaling complex, the so called necrosome that facilitates necroptosis. MLKL mediates protein aggregation and formation of this specific scaffold that is required for accurate signaling transduction (Wu et al., 2014).

However, MLKL signaling appeared to be inactive in B16 melanoma cells as neither TNF-induced necroptosis nor RIG-I ligation lead to phosphorylation of MLKL. Therefore, in our model, direct targeting of tumor-intrinsic RIG-I does not induce necroptosis in contrast to the induction of necroptosis by specific stimuli found in fibroblasts. Nevertheless, it remains unclear whether the MLKL pathway is active in B16 cells after all. Further studies are needed to investigate the role of MLKL signaling in B16 cells and whether it affects RIG-I signaling and the induction of tumor cell death.

These data further suggested that either MLKL- or necroptosis-independent mechanisms were involved in facilitating therapeutic effects of both 3pRNA application and checkpoint blockade. A possible explanation might be necroptosis-independent induction of inflammation by RIP kinases (Moriwaki & Chan, 2016). Previous studies

reported that activation of NF-κB signaling via RIPK1 within dying cells can initiate a $CD8^+$ T cell-driven antitumor immune response (Yatim et al., 2015) by facilitating efficient cross-priming and the generation of an inflammatory milieu. In contrast, RIPK3 has been shown to activate the NLRP3 inflammasome in a MLKL and thus in a necroptosis-independent manner (Lawlor et al., 2015). However, this was in contrast to our data that revealed only marginal levels of IL-1β in tumor tissue and its microenvironment after local 3pRNA application suggesting only a slight influence of inflammasome activation on therapy efficacy.

Additionally, a recent report associated MLKL with endosomal function by demonstrating its role for the controlled transport of endocytosed proteins, the concomitant modulation of receptor signaling by degradation as well as the generation of extracellular vesicles (Yoon, Kovalenko, Bogdanov, & Wallach, 2017). However, control of endosomal trafficking by MLKL was mediated independently of MLKL phosphorylation by RIPK3. In addition, it was further suggested that the release of phosphorylated MLKL within extracellular vesicles is a mechanism to limit the necroptotic activity of MLKL by itself.

Thus, loss of MLKL might compromise shuttling of nucleic acids and tumor-derived antigens by extracellular vesicles that could serve as ligands for PRR activation and therefore adversely affect RIG-I-mediated immune responses. However, further studies are needed to elucidate the role of MLKL signaling on RIG-I-mediated therapy responses when it is independent of necroptosis induction as well as the role of MLKL-dependent nucleic acid shuttling and its impact on PRR signaling.

4.3 Impact of RIG-I on synergistic effects of irradiation-mediated ICD and immune checkpoint blockade

Previous studies have revealed that induction of tumor cell death by RT can trigger immunogenic cell death which is a prerequisite for efficient T-cell priming and thus capable of eradicating established distant tumors through the generation of a $CD8^+$ T-cell-driven antitumor immune response (Obeid et al., 2007). Moreover, tumor irradiation promotes a pro-immunogenic tumor microenvironment. These effects are exerted by tumor and stromal cells that survived irradiation and thus facilitated the effector phase of antitumor immune responses by upregulating specific chemokines, cell surface receptors and mediation of vascular changes (S. Demaria & Formenti, 2007).

These data and further preclinical studies implyed that combining immunotherapeutic strategies with RT could enhance local and systemic antitumor effects. By combining RT with anti-CTLA-4-mediated immune checkpoint blockade, a promising report demonstrated abscopal antitumor effects reflected in significant growth inhibition and enhanced frequencies of $CD8^+$ T cells in a preclinical mouse model (Dewan et al., 2009). These findings were further supported by a recent study that observed systemic antitumor immunity and subsequent prolonged survival in patients with advanced melanoma that had been irradiated after tumor progression under anti-CTLA-4 treatment with ipilimumab (Grimaldi et al., 2014) and thus indicated that radiation directed to a single tumor lesion can increase tumor immunogenicity *in situ*. Moreover, the combination of tumor radiotherapy and anti-PD-1 checkpoint blockade rendered poorly immunogenic tumors susceptible to combined treatment and thus significantly increased tumor control and overall survival (Pike et al., 2017). This was primarily due to the upregulation of PDL1 on tumor cells, T cell infiltration into the tumor and the generation of a highly inflamed tumor. Similarly, combining radiotherapy with immune checkpoint blockade indeed showed synergistic effects as *in situ* vaccination of murine melanomas by irradiation enhanced therapy efficiency of anti-CTLA-4 checkpoint blockade which in turn critically depended on tumor-intrinsic RIG-I signaling. Early studies stressed the role of PRRs in RT-mediated antitumor effects by targeting TLR9 in the tumor and its microenvironment before tumor irradiation in an immunogenic mouse model (Milas et al., 2004). Subsequent tumor growth control and development of long lasting protective immune responses (Mason et al., 2005) suggested that RT enhances antitumor immunity through improved PRR signaling.

According to this assumption, activation of the tumor cell intrinsic RIG-I pathway by endogenous RNAs has been described previously (Ranoa et al., 2016). Irradiation of tumor cells resulted in translocation of small non-coding RNAs (sncRNAs) from the nucleus into the cytosol, the subsequent detection by RIG-I and activation of the IFN pathway. Furthermore, another recent report observed a link between host cGAS/STING signaling and irradiation-mediated antitumor effects (Deng, Liang, Xu, et al., 2014). According to these results, intact host intrinsic STING signaling was essential for the induction of IFN-I after irradiation and thus for sensing of irradiated tumor cells by intratumoral DCs and subsequent T-cell cross-priming. We, therefore, hypothesize that local radiation of primary tumors leads to the activation of tumor intrinsic RIG-I signaling by the release of double stranded sncRNAs from the nucleus into the cytosol. The combination of RIG-I activation and ionizing radiation then induced cancer cell death which is accompanied by the release of nuclear DNA that is identified as DAMP and therefore sensed by host intrinsic cGAS/STING. The subsequent activation of STING

induces a strong IFN-I release that in turn facilitates efficient T cell cross-priming and thus enhances T cell mediated antitumor immunity.

Tumor radiotherapy, therefore, appears to be another potential ICD inducer that synergizes with immune checkpoint blockade. In addition, it seems that cytosolic nucleic acid sensing receptors such as RIG-I and STING are a requirement for the mediation of therapy responses. Nevertheless, how host RIG-I/MAVS signaling influences sensing of DAMPs upon tumor irradiation has to be further investigated.

4.4 Mediation of local and systemic tumor growth control

4.4.2 Cellular mechanisms involved in RIG-I-mediated tumor control

We observed a RIG-I-dependent induction of tumor cell death *in vitro*, however, local tumor growth control and regression remained largely intact after therapeutic targeting of RIG-I in the absence of either functional tumor or host intrinsic RIG-I signaling *in vivo*. In contrast, systemic antitumor immunity appeared to be dependent on both intact tumor intrinsic RIG-I signaling and active MAVS signaling in the host.

We thus conclude that different aspects of immunity are responsible for both local and distant tumor growth control. Systemic immunity and the subsequent regression of distant tumors correlated with the expansion of tumor antigen specific $CD8^+$ T cells that in turn critically relied on both RIG-I signaling in tumor and host cells. However, the reduced frequency of systemic tumor antigen specific CTLs after treating $RIG\text{-}I^{-/-}$ tumors with 3pRNA and anti-CTLA-4 was still sufficient to control local directly injected tumors. Interestingly, either mechanism, tumor or host intrinsic RIG-I signaling, can obviously compensate the loss of the respective other and thereby facilitate local tumor control in the absence of functional RIG-I signaling within one cell subset. Thus, we hypothesize that local tumor growth control might be mediated by either RIG-I-induced intrinsic tumor cell death or by spatially restricted activation of RIG-I competent innate immune cells in the host tumor environment.

Therefore, it appears that the loss of host intrinsic RIG-I signaling can be compensated by efficient tumor cell killing mainly meditated by the induction of intrinsic apoptosis. In the absence of tumor intrinsic RIG-I signaling, activation of RIG-I competent innate immune cells in the tumor microenvironment including DCs and NK cells appears to create an inflammatory tumor hostile milieu that partly compensates the loss of RIG-I-

induced ICD which presumably involves host-derived IFN-I (Poeck et al., 2008). Consistent with this, depletion of $CD8^+$ cytotoxic T cells resulted in reduced local tumor growth control and absence of systemic antitumor immunity following combined treatment with 3pRNA and anti-CTLA-4. Therefore, persisting growth control of local 3pRNA-injected tumors appears to be primarily facilitated by antigen specific CTLs whose generation is significantly impaired in mice bearing $RIG\text{-}I^{-/-}$ tumors thus suggesting the crucial role of tumor intrinsic RIG-I for the long-term control of local tumors.

4.4.3 RIG-I independent NK cell recruitment and tumor cell killing

Although 3pRNA-enhanced tumor infiltration by activated NK cells was spatially restricted to local tumors, regression of distant tumors was diminished after depleting $NK1.1^+$ cells. These data suggest that local NK cell-mediated tumor cell killing might contribute to activation of dendritic cells by processing and cross-presentation of tumor-associated antigens and the subsequent induction of a systemic $CD8^+$ T cell response. This hypothesis was further supported by a previous study that demonstrated that recognition of viral nucleic acids by RIG-I upregulates the expression of natural killer group 2D (NKG2D) ligands on infected cells and thus enhances NK cell recruitment through IFN-I release (Esteso, Guerra, Vales-Gomez, & Reyburn, 2017). NKG2D has further been shown to be a major recognition receptor for the detection and the subsequent elimination of infected cells and was moreover found to be upregulated during cellular stress or genomic stress such as cancer (Gonzalez, Lopez-Soto, Suarez-Alvarez, Lopez-Vazquez, & Lopez-Larrea, 2008). Furthermore, it can serve as a co-stimulatory receptor that directly stimulates NK cells, macrophages and moreover co-stimulates activated $CD8^+$ T cells (Jamieson et al., 2002). Therefore, local RIG-I ligation could render tumor cells susceptible to NK cell-mediated tumor cell death due to enhanced recruitment and subsequent infiltration of NK cells into the tumor microenvironment and further facilitate T-cell-meditated immune responses.

In line with our data that revealed a RIG-I dependent upregulation of inhibitory receptors in melanoma cells deficient in tumor cell intrinsic RIG-I signaling, a previous study reported that NK cells become functionally exhausted in melanoma patients by upregulation of TIM-3. In clinical trials, this effect could be partially reversed by immune checkpoint blockade and further synergized with DC stimulation as well as several TLR agonists and melanoma antigens that served as tumor vaccines (Gonzalez-Gugel, Saxena, & Bhardwaj, 2016).

Therefore, the combination of distinct checkpoint blocking antibodies that could both enhance preexisting T cell immune responses and further target inhibitory receptors on additional innate immune cells might be a promising holistic approach in cancer immunotherapy. It has previously been shown that combining different immune checkpoint inhibitors is a promising approach in the treatment of melanoma in clinical trials (Hodi et al., 2016). However, the synergistic therapy advantages that arise from such a combination are just beginning to emerge and have to be further elucidated in future studies.

4.5 Activation of RIG-I by endogenous ligands

4.5.2 Microbial RNA as potential source of endogenous RIG-I ligands

The discovery that anti-CTLA-4 monotherapy was significantly less effective in mice bearing RIG-I$^{-/-}$ tumors suggested the existence of endogenous ligands that could facilitate basal pathway activation of tumor intrinsic RIG-I signaling and, therefore, might contribute to therapeutic efficacy of anti-CTLA-4.

In this regard, two independent reports stressed the role of environmental factors for efficient antitumor effects of CTLA-4 blockade (Sivan et al., 2015; Vetizou et al., 2015) by demonstrating that the composition of commensal microbiota influences therapy response to checkpoint blockade assuming that an intact microflora is a prerequisite for immune stimulatory effects. These studies further postulated that augmented DC function is mainly responsible for commensal-mediated enhanced antineoplastic activity by boosting CD8^{+} T cell priming and accumulation of these cells in the tumor microenvironment. However, the impact of commensal microbiota on tumor intrinsic nucleic acid sensing pathways was not addressed. Preceding studies showed that microbial nucleic acids can be detected within tumor cells (Duewell et al., 2014; Poeck et al., 2008) leading to the subsequent induction of an IFN-I-mediated immune response. Therefore, commensal microbiota species can be a potential source of RNA that can serve as endogenous ligands required for the activation of either the RIG-I, MAVS or IFN-I pathway in both tumor and host immune cells. This might enhance synergistic therapy responses as modulating the gut microbiome can improve therapeutic efficacy of checkpoint blockade (Pitt et al., 2016) and thus simultaneously reshape microbiota towards a favorable phenotype for PRR signaling. This could be further examined by

studying RIG-I-mediated therapy responses in germ free mice or mice depleted of defined commensals and subsequent sequencing of beneficial microbiota species.

4.5.3 MicroRNAs can selectively activate RIG-I signaling

Another potential endogenous RIG-I ligand might be microRNAs, as microRNAs have been found to be overexpressed in melanoma and various other types of cancer (O'Bryan, Dong, Mathis, & Alahari, 2017) and thus can interact with tumor or host intrinsic RIG-I. In view of their function in cellular processes like apoptosis, major signaling pathways and further post-transcriptional regulation of gene expression (Kloosterman & Plasterk, 2006), microRNAs might not only be potential RIG-I activators but moreover enhance its immunotherapeutic potential. On the one hand, several miRNAs have been shown to facilitate RIG-I activation and the subsequent induction of antiviral immune responses. miR-136 has been indicated to activate RIG-I in endothelial cells and to induce the expression of IFN-I and IL-6 which in turn inhibits viral replication (Zhao et al., 2015). Furthermore, miR-145 has been shown to trigger off-target immune responses by upregulating ISGs after interacting with RIG-I (Karlsen & Brinchmann, 2013). On the other hand, in contrast to the induction of unspecific immune responses, another miRNA, miR-34a, was found to upregulate the expression of RIG-I by binding to its 3´untranslatet region which resulted in enhanced apoptosis of cervical cancer cells (J. H. Wang et al., 2016). The activation of RIG-I has recently been demonstrated to be closely linked with several sncRNAs (Ranoa et al., 2016). However, how small RNA molecules that are restricted to the nucleus can translocate into the cytosol after irradiation was not further assessed.

One of these processes might involve active transport by the formation of nuclear pore complexes or the transport via shuttling proteins that could be upregulated upon irradiation. Furthermore, ionizing radiation induces cancer cell death accompanied by membrane disintegration and the release of DAMPs such as DNA or RNA molecules. These nucleic acids could be packed by exosomes and transported to neighboring cells where they can be engulfed and activate cytosolic PRRs. Furthermore, a previous study revealed that DNA damage or the loss of ATM (ataxia-telangiectasia mutated, a DNA repair apical kinase) results in the release of nuclear DNA into the cytosol (Hartlova et al., 2015).

Thus, miRNAs may act as endogenous ligands and enhance immunogenicity of RIG-I. However, further studies are needed to investigate the relationship between distinct

miRNAs and RIG-I signaling in various cancer entities. Therefore, computational transcriptomic small RNA and degradome analyses can be performed to characterize microRNA-mediated pathways of gene regulation in cancer cells and the tumor microenvironment.

4.5.4 Endogenous retroviral elements enhance checkpoint blockade

The DNA methyltransferase inhibitor 5-azacytidine upregulates the expression of ERV mRNA, triggers cytosolic RNA sensing and sensitizes mice to anti-CTLA-4 checkpoint blockade in a preclinical model (Chiappinelli et al., 2015). Following up on this study, we observed that the synergism of combining 5-azacytidine treatment with anti-CTLA-4 checkpoint depended on active tumor intrinsic RIG-I signaling *in vivo*. Another report supported our findings by demonstrating that endogenous retroelements, including ERVs and short interspersed elements (SINEs), could activate RIG-I and cGAS in B cells (Zeng et al., 2014). This was facilitated by T cell-independent B cell activation due to BCR engagement with TI-2 antigens and subsequent induction of ERV transcription through NF-κB activation. Moreover, SINEs could also function as endogenous RIG-I ligands when they are transcribed by polymerase III under cellular and environmental stress conditions (Mu, Ahmad, & Hur, 2016).Tumor cell intrinsic RIG-I pathway activation by endogenous RNAs has been described previously (Ranoa et al., 2016). Irradiation of tumor cells resulted in translocation of small non-coding RNAs from the nucleus into the cytosol, the subsequent detection by RIG-I and activation of the IFN pathway.

We therefore hypothesized that basal activity of the tumor intrinsic RIG-I pathway could be mediated by continuous detection of either retroviral elements, miRNAs or commensal RNA within tumor cells and thus facilitate anti-CTLA-4 efficacy in the absence of exogenous ligands.

4.6 Tumor intrinsic RIG-I signaling as a prognostic biomarker

In accordance to a previous study, RIG-I ligation induced ICD in pancreatic cancer cells (Duewell et al., 2014). Moreover, we observed that C26 cells, a colon cancer cell line, were also susceptible to RIG-I-mediated tumor cell death. In contrast, direct targeting of RIG-I in a murine breast cancer cell line failed to induce a therapeutic response. This data was further supported by a recent study that demonstrated that activation of RIG-I enhanced tumor growth, metastasis and therapy resistance in a preclinical breast cancer model (Nabet et al., 2017). Thus, it appears that tumor intrinsic RIG-I signaling can differentially affect therapy responses depending on the cancer entity. Interestingly, the therapeutic success of combined treatment with local RIG-I activation and systemic anti-CLTA-4 was limited to tumors that showed *in vitro* susceptibility to RIG-I-mediated ICD. We, therefore, presume that induction of ICD by intratumoral RIG-I ligation can function as an essential mediator for efficient anti-CTLA-4-mediated checkpoint blockade by inducing T cell immune responses. Thus, gene expression-based high-throughput screening and whole genome expression analysis could be performed on tumor biopsies to analyze gene expression profiles of distinct PRRs that can serve as biomarker to predict treatment outcome before targeting RIG-I in human patients. In this regard, targeting DCs by systemic application of immune-modulating RNAs for cancer therapy has recently proven to be feasible in a phase-I clinical trial (Kranz et al., 2016). However, tumor intrinsic RIG-I signaling might also address additional mechanisms to promote anti-CTLA-4 efficacy independently of RIG-I-mediated programmed tumor cell death. Thus, how tumor intrinsic RIG-I signaling affects cancer progression has to be further elucidated as overexpression of RIG-I has been demonstrated to negatively regulate intestinal bowel disease-induced CRC progression (Shu et al., 2017) while also being beneficial in controlling intestinal microbiota and therefore inhibiting colitis induced CRC (Zhu et al., 2017).

4.7 Combining oncolytic viral therapy with immune checkpoint blockade

Finally, our data may provide novel insights into the underlying mechanisms of therapeutic efficacy of oncolytic viruses (OV). Successful cancer immunotherapy using OVs is characterized by three major mechanisms of action. Firstly, the capacity of OVs to induce oncolysis of infected cancer cells and endothelial cells in the TME. Secondly,

the indirect effects of both apoptosis and necrosis of uninfected cells and associated endothelial cells in the tumor-associated vasculature resulting in decreased angiogenesis (Breitbach et al., 2013). Finally, OVs elicit and enhance antitumor and antiviral immunity by improving antigen cross-priming and subsequent recruitment of effector cells into the TME (Guo et al., 2017). However, oncolysis is not the only major mechanism responsible for tumor growth inhibition. Several preclinical studies have demonstrated that the therapeutic efficacy of OVs is not only conveyed by direct infection-mediated tumor cell cytotoxicity but critically depends on subsequent activation of both innate and adaptive immunity (Turnbull et al., 2015). This has been shown in several approaches including the use of tumor antigen encoding OV strains that effectively induced T cell-mediated antitumor responses (Diaz et al., 2007) as well as the depletion of $CD8^+$ T cells resulting in the inhibition of OV-based therapy efficiency (Sobol et al., 2011).

In a preclinical melanoma model, local intra-tumor application of Newcastle disease virus (NDV) resulted in the generation of an inflammatory response, lymphocytic infiltration and the subsequent induction of a systemic immune response by an apparent infiltration of tumor specific T cells (Zamarin et al., 2014). Furthermore, this localized OV therapy rendered poorly immunogenic tumors susceptible to anti-CTLA-4 immunotherapy which led to the rejection of pre-established distant tumors and immunological memory and depended on $CD8^+$ T cell, NK cell and IFN-I signaling. In addition, several oncolytic viral (OV) strains have been shown to activate the RIG-I / MAVS pathway (Kumar et al., 2015; Rahman, Bagdassarian, Ali, & McFadden, 2017). Moreover, loss of tumor intrinsic MAVS and IFN-I signaling results in diminished anticancer activity of NDV due to the suppression of tumor cell apoptosis via downregulation of TRAIL. Thus, combining RIG-I-mediated ICD and subsequent IFN-I induction with the infection-related cytolysis of tumor cells may account for the overall efficacy of OV immunotherapy.

4.8 Summary

Despite significant progress achieved by treatment of patients suffering from metastatic melanoma with immune checkpoint blockade, strong inter-patient heterogeneity in clinical response to checkpoint inhibitors such as anti-CTLA-4 and anti-PD-1 remains a major challenge. In addition, activation of innate nucleic acid receptor pathways such as RIG-I/MAVS and cGAS/STING in both immune and tumor cells are emerging as intriguing determinants of both anticancer immune responses as well as immune escape and resistance mechanisms. The fact that the majority of patients are either resistant to

therapy or relapse thereafter highlights the need to elucidate mechanisms that drive tumor resistance. Moreover, it is mandatory to gain detailed mechanistic insights into immune suppressive and stimulatory signaling in cancer to better understand carcinogenesis and to successfully develop combined therapies by interconnecting innate immune activation via pattern recognition receptors and immune checkpoint blockade to overcome interpatient heterogeneity.

Therefore, we focused our efforts on the effects of tumor intrinsic RIG-I signaling on the efficacy of anti-CTLA-4-mediated checkpoint blockade and possible synergistic effects by combining immune checkpoint blockade with local RIG-I activation. We demonstrated that the *in vivo* efficacy of anti-CTLA-4-mediated checkpoint blockade in mice crucially relied on intact tumor intrinsic RIG-I signaling, whereas tumor intrinsic STING and IFN-I signaling were dispensable. Mice bearing RIG-I-deficient tumors had an impaired systemic tumor growth control and failed to completely reject systemic immunogenic tumors. Furthermore, we demonstrated that following anti-CTLA-4 treatment, activation of tumor-intrinsic RIG-I signaling induces caspase-3-mediated tumor cell death that critically impacts on cross-presentation of tumor-associated antigens by $CD103^+$ dendritic cells, the subsequent expansion of tumor antigen-specific $CD8^+$ T cells and ultimately the accumulation of $CD8^+$ T cells within the tumor tissue. Consistently, therapeutic targeting of RIG-I with 5'-phosphorylated-RNA in both tumor and non-malignant host cells potently augmented the efficacy of CTLA-4 checkpoint blockade supporting our hypothesis of a potential synergism between these two distinct pathways. Additionally, these processes were also dependent on host STING, MAVS and type I interferon signaling and closely linked to RIG-I-mediated tumor cell death.

Several reports have shown that targeting tumor intrinsic RIG-I signaling in malignant cells induces a variant of ICD. A key factor in this process is the induction of apoptosis via activation of the intrinsic mitochondrial apoptosis pathway. However, it remains unclear whether additional cell death pathways are involved in RIG-I-mediated cell death. We demonstrated that tumor intrinsic RIG-I ligation induces enhanced caspase-3-mediated tumor cell death in melanoma cells *in vitro* and *in vivo*. However, RIG-I-mediated tumor cell death appeared to be primarily driven by apoptosis as RIG-I ligation failed to activate MLKL, a critical component of the necroptosome. Furthermore, mice bearing tumors deficient in caspase-3 signaling showed a markedly impaired therapy response to both local 3pRNA application and systemic checkpoint blockade, highlighting the significance of apoptosis induction in our experimental model. In addition, tumor cell death induction by radiotherapy also synergized with anti-CTLA-4 checkpoint blockade. Interestingly, this effect was also critically dependent on intact tumor cell

intrinsic RIG-I signaling, suggesting a decisive role of tumor intrinsic RIG-I for tumor immune surveillance.

Systemic administration of anti-CTLA-4 monoclonal antibodies induces tumor growth delay *in vivo* in the absence of exogenous 3pRNA suggesting the existence of an endogenous ligand that could facilitate basal pathway activation. Our data show that endogenous retroviruses (ERVs) can act as such a ligand for upregulation of ERV transcripts by treatment with demethylating agents causing tumor growth delay and inducing tumor cell death in an RIG-I-dependent manner that further synergizes with immune checkpoint blockade.

Further studies will need to specify the nature of possible endogenous ligands that facilitate synergistic effects by combining anti-CTLA-4 checkpoint blockade with local RIG-I activation. Solving this key issue should increase our understanding of the interplay between PRRs and inhibitory receptors in cancer immunotherapy and will make it possible to overcome inter-individual variations in clinical responses by creating a balance between co-stimulatory and inhibitory processes. Additionally, expression of tumor-intrinsic RIG-I could function as a biomarker and predictor of overall survival and therapeutic efficacy of immune checkpoint blockade.

5 Reference list

Aamdal, S. (2011). Current approaches to adjuvant therapy of melanoma. *Eur J Cancer, 47 Suppl 3*, S336-337. doi:10.1016/S0959-8049(11)70193-9

Ablasser, A., Bauernfeind, F., Hartmann, G., Latz, E., Fitzgerald, K. A., & Hornung, V. (2009). RIG-I-dependent sensing of poly(dA:dT) through the induction of an RNA polymerase III-transcribed RNA intermediate. *Nat Immunol, 10*(10), 1065-1072. doi:10.1038/ni.1779

Ager, C. R., Reilley, M. J., Nicholas, C., Bartkowiak, T., Jaiswal, A. R., & Curran, M. A. (2017). Intratumoral STING Activation with T-cell Checkpoint Modulation Generates Systemic Antitumor Immunity. *Cancer Immunol Res, 5*(8), 676-684. doi:10.1158/2326-6066.CIR-17-0049

Aguirre, S., Maestre, A. M., Pagni, S., Patel, J. R., Savage, T., Gutman, D., . . . Fernandez-Sesma, A. (2012). DENV inhibits type I IFN production in infected cells by cleaving human STING. *PLoS Pathog, 8*(10), e1002934. doi:10.1371/journal.ppat.1002934

Ahmadzadeh, M., Johnson, L. A., Heemskerk, B., Wunderlich, J. R., Dudley, M. E., White, D. E., & Rosenberg, S. A. (2009). Tumor antigen-specific CD8 T cells infiltrating the tumor express high levels of PD-1 and are functionally impaired. *Blood, 114*(8), 1537-1544. doi:10.1182/blood-2008-12-195792

Ahn, J., Xia, T., Konno, H., Konno, K., Ruiz, P., & Barber, G. N. (2014). Inflammation-driven carcinogenesis is mediated through STING. *Nat Commun, 5*, 5166. doi:10.1038/ncomms6166

Akira, S. (2009). Pathogen recognition by innate immunity and its signaling. *Proc Jpn Acad Ser B Phys Biol Sci, 85*(4), 143-156.

Altman, J. D., Moss, P. A., Goulder, P. J., Barouch, D. H., McHeyzer-Williams, M. G., Bell, J. I., . . . Davis, M. M. (1996). Phenotypic analysis of antigen-specific T lymphocytes. *Science, 274*(5284), 94-96.

Atianand, M. K., & Fitzgerald, K. A. (2013). Molecular basis of DNA recognition in the immune system. *J Immunol, 190*(5), 1911-1918. doi:10.4049/jimmunol.1203162

Atkins, M. B., Lotze, M. T., Dutcher, J. P., Fisher, R. I., Weiss, G., Margolin, K., . . . Rosenberg, S. A. (1999). High-dose recombinant interleukin 2 therapy for patients with metastatic melanoma: analysis of 270 patients treated between 1985 and 1993. *J Clin Oncol, 17*(7), 2105-2116. doi:10.1200/JCO.1999.17.7.2105

Azuma, M., Ito, D., Yagita, H., Okumura, K., Phillips, J. H., Lanier, L. L., & Somoza, C. (1993). B70 antigen is a second ligand for CTLA-4 and CD28. *Nature, 366*(6450), 76-79. doi:10.1038/366076a0

Bajetta, E., Del Vecchio, M., Bernard-Marty, C., Vitali, M., Buzzoni, R., Rixe, O., . . . Khayat, D. (2002). Metastatic melanoma: chemotherapy. *Semin Oncol, 29*(5), 427-445.

Bald, T., Landsberg, J., Lopez-Ramos, D., Renn, M., Glodde, N., Jansen, P., . . . Tuting, T. (2014). Immune cell-poor melanomas benefit from PD-1 blockade after

targeted type I IFN activation. *Cancer Discov, 4*(6), 674-687. doi:10.1158/2159-8290.CD-13-0458

Baroja-Mazo, A., Martin-Sanchez, F., Gomez, A. I., Martinez, C. M., Amores-Iniesta, J., Compan, V., . . . Pelegrin, P. (2014). The NLRP3 inflammasome is released as a particulate danger signal that amplifies the inflammatory response. *Nat Immunol, 15*(8), 738-748. doi:10.1038/ni.2919

Bastiaannet, E., Beukema, J. C., & Hoekstra, H. J. (2005). Radiation therapy following lymph node dissection in melanoma patients: treatment, outcome and complications. *Cancer Treat Rev, 31*(1), 18-26. doi:10.1016/j.ctrv.2004.09.005

Bedoui, S., Whitney, P. G., Waithman, J., Eidsmo, L., Wakim, L., Caminschi, I., . . . Heath, W. R. (2009). Cross-presentation of viral and self antigens by skin-derived CD103+ dendritic cells. *Nat Immunol, 10*(5), 488-495. doi:10.1038/ni.1724

Belardelli, F., & Ferrantini, M. (2002). Cytokines as a link between innate and adaptive antitumor immunity. *Trends Immunol, 23*(4), 201-208.

Beljanski, V., Chiang, C., Kirchenbaum, G. A., Olagnier, D., Bloom, C. E., Wong, T., . . . Hiscott, J. (2015). Enhanced Influenza Virus-Like Particle Vaccination with a Structurally Optimized RIG-I Agonist as Adjuvant. *J Virol, 89*(20), 10612-10624. doi:10.1128/JVI.01526-15

Berard, F., Blanco, P., Davoust, J., Neidhart-Berard, E. M., Nouri-Shirazi, M., Taquet, N., . . . Palucka, A. K. (2000). Cross-priming of naive CD8 T cells against melanoma antigens using dendritic cells loaded with killed allogeneic melanoma cells. *J Exp Med, 192*(11), 1535-1544.

Besch, R., Poeck, H., Hohenauer, T., Senft, D., Hacker, G., Berking, C., . . . Hartmann, G. (2009). Proapoptotic signaling induced by RIG-I and MDA-5 results in type I interferon-independent apoptosis in human melanoma cells. *J Clin Invest, 119*(8), 2399-2411. doi:10.1172/JCI37155

Blank, C., Brown, I., Peterson, A. C., Spiotto, M., Iwai, Y., Honjo, T., & Gajewski, T. F. (2004). PD-L1/B7H-1 inhibits the effector phase of tumor rejection by T cell receptor (TCR) transgenic CD8+ T cells. *Cancer Res, 64*(3), 1140-1145.

Bleyer, W. A. (2002). Cancer in older adolescents and young adults: epidemiology, diagnosis, treatment, survival, and importance of clinical trials. *Med Pediatr Oncol, 38*(1), 1-10.

Breitbach, C. J., Arulanandam, R., De Silva, N., Thorne, S. H., Patt, R., Daneshmand, M., . . . Kirn, D. H. (2013). Oncolytic vaccinia virus disrupts tumor-associated vasculature in humans. *Cancer Res, 73*(4), 1265-1275. doi:10.1158/0008-5472.CAN-12-2687

Brignole, C., Marimpietri, D., Di Paolo, D., Perri, P., Morandi, F., Pastorino, F., . . . Ponzoni, M. (2010). Therapeutic targeting of TLR9 inhibits cell growth and induces apoptosis in neuroblastoma. *Cancer Res, 70*(23), 9816-9826. doi:10.1158/0008-5472.CAN-10-1251

Brzostek, J., Gascoigne, N. R., & Rybakin, V. (2016). Cell Type-Specific Regulation of Immunological Synapse Dynamics by B7 Ligand Recognition. *Front Immunol, 7*, 24. doi:10.3389/fimmu.2016.00024

Burdette, D. L., Monroe, K. M., Sotelo-Troha, K., Iwig, J. S., Eckert, B., Hyodo, M., . . . Vance, R. E. (2011). STING is a direct innate immune sensor of cyclic di-GMP. *Nature, 478*(7370), 515-518. doi:10.1038/nature10429

Burkholder, B., Huang, R. Y., Burgess, R., Luo, S., Jones, V. S., Zhang, W., . . . Huang, R. P. (2014). Tumor-induced perturbations of cytokines and immune cell networks. *Biochim Biophys Acta, 1845*(2), 182-201. doi:10.1016/j.bbcan.2014.01.004

Chang, D. W., Xing, Z., Capacio, V. L., Peter, M. E., & Yang, X. (2003). Interdimer processing mechanism of procaspase-8 activation. *EMBO J, 22*(16), 4132-4142. doi:10.1093/emboj/cdg414

Chao, M. P., Alizadeh, A. A., Tang, C., Myklebust, J. H., Varghese, B., Gill, S., . . . Majeti, R. (2010). Anti-CD47 antibody synergizes with rituximab to promote phagocytosis and eradicate non-Hodgkin lymphoma. *Cell, 142*(5), 699-713. doi:10.1016/j.cell.2010.07.044

Chen, D. S., & Mellman, I. (2013). Oncology meets immunology: the cancer-immunity cycle. *Immunity, 39*(1), 1-10. doi:10.1016/j.immuni.2013.07.012

Chen, H., Sun, H., You, F., Sun, W., Zhou, X., Chen, L., . . . Jiang, Z. (2011). Activation of STAT6 by STING is critical for antiviral innate immunity. *Cell, 147*(2), 436-446. doi:10.1016/j.cell.2011.09.022

Chen, L., & Flies, D. B. (2013). Molecular mechanisms of T cell co-stimulation and co-inhibition. *Nat Rev Immunol, 13*(4), 227-242. doi:10.1038/nri3405

Chen, L. L., Yang, L., & Carmichael, G. G. (2010). Molecular basis for an attenuated cytoplasmic dsRNA response in human embryonic stem cells. *Cell Cycle, 9*(17), 3552-3564. doi:10.4161/cc.9.17.12792

Chiappinelli, K. B., Strissel, P. L., Desrichard, A., Li, H., Henke, C., Akman, B., . . . Strick, R. (2015). Inhibiting DNA Methylation Causes an Interferon Response in Cancer via dsRNA Including Endogenous Retroviruses. *Cell, 162*(5), 974-986. doi:10.1016/j.cell.2015.07.011

Chiu, Y. H., Macmillan, J. B., & Chen, Z. J. (2009). RNA polymerase III detects cytosolic DNA and induces type I interferons through the RIG-I pathway. *Cell, 138*(3), 576-591. doi:10.1016/j.cell.2009.06.015

Civril, F., Deimling, T., de Oliveira Mann, C. C., Ablasser, A., Moldt, M., Witte, G., . . . Hopfner, K. P. (2013). Structural mechanism of cytosolic DNA sensing by cGAS. *Nature, 498*(7454), 332-337. doi:10.1038/nature12305

Corrales, L., Glickman, L. H., McWhirter, S. M., Kanne, D. B., Sivick, K. E., Katibah, G. E., . . . Gajewski, T. F. (2015). Direct Activation of STING in the Tumor Microenvironment Leads to Potent and Systemic Tumor Regression and Immunity. *Cell Rep, 11*(7), 1018-1030. doi:10.1016/j.celrep.2015.04.031

Curran, M. A., Montalvo, W., Yagita, H., & Allison, J. P. (2010). PD-1 and CTLA-4 combination blockade expands infiltrating T cells and reduces regulatory T and myeloid cells within B16 melanoma tumors. *Proc Natl Acad Sci U S A, 107*(9), 4275-4280. doi:10.1073/pnas.0915174107

Dalod, M., Chelbi, R., Malissen, B., & Lawrence, T. (2014). Dendritic cell maturation: functional specialization through signaling specificity and transcriptional programming. *EMBO J, 33*(10), 1104-1116. doi:10.1002/embj.201488027

Delneste, Y., Beauvillain, C., & Jeannin, P. (2007). [Innate immunity: structure and function of TLRs]. *Med Sci (Paris), 23*(1), 67-73. doi:10.1051/medsci/200723167

Demaria, O., De Gassart, A., Coso, S., Gestermann, N., Di Domizio, J., Flatz, L., . . . Gilliet, M. (2015). STING activation of tumor endothelial cells initiates spontaneous and therapeutic antitumor immunity. *Proc Natl Acad Sci U S A, 112*(50), 15408-15413. doi:10.1073/pnas.1512832112

Demaria, S., & Formenti, S. C. (2007). Sensors of ionizing radiation effects on the immunological microenvironment of cancer. *Int J Radiat Biol, 83*(11-12), 819-825. doi:10.1080/09553000701481816

Dempke, W. C. M., Fenchel, K., Uciechowski, P., & Dale, S. P. (2017). Second- and third-generation drugs for immuno-oncology treatment-The more the better? *Eur J Cancer, 74*, 55-72. doi:10.1016/j.ejca.2017.01.001

den Haan, J. M., Arens, R., & van Zelm, M. C. (2014). The activation of the adaptive immune system: cross-talk between antigen-presenting cells, T cells and B cells. *Immunol Lett, 162*(2 Pt B), 103-112. doi:10.1016/j.imlet.2014.10.011

Deng, L., Liang, H., Burnette, B., Beckett, M., Darga, T., Weichselbaum, R. R., & Fu, Y. X. (2014). Irradiation and anti-PD-L1 treatment synergistically promote antitumor immunity in mice. *J Clin Invest, 124*(2), 687-695. doi:10.1172/JCI67313

Deng, L., Liang, H., Xu, M., Yang, X., Burnette, B., Arina, A., . . . Weichselbaum, R. R. (2014). STING-Dependent Cytosolic DNA Sensing Promotes Radiation-Induced Type I Interferon-Dependent Antitumor Immunity in Immunogenic Tumors. *Immunity, 41*(5), 843-852. doi:10.1016/j.immuni.2014.10.019

Dewan, M. Z., Galloway, A. E., Kawashima, N., Dewyngaert, J. K., Babb, J. S., Formenti, S. C., & Demaria, S. (2009). Fractionated but not single-dose radiotherapy induces an immune-mediated abscopal effect when combined with anti-CTLA-4 antibody. *Clin Cancer Res, 15*(17), 5379-5388. doi:10.1158/1078-0432.CCR-09-0265

Dhodapkar, M. V., Steinman, R. M., Krasovsky, J., Munz, C., & Bhardwaj, N. (2001). Antigen-specific inhibition of effector T cell function in humans after injection of immature dendritic cells. *J Exp Med, 193*(2), 233-238.

Diamond, M. S., Kinder, M., Matsushita, H., Mashayekhi, M., Dunn, G. P., Archambault, J. M., . . . Schreiber, R. D. (2011). Type I interferon is selectively required by dendritic cells for immune rejection of tumors. *J Exp Med, 208*(10), 1989-2003. doi:10.1084/jem.20101158

Diaz, R. M., Galivo, F., Kottke, T., Wongthida, P., Qiao, J., Thompson, J., . . . Vile, R. G. (2007). Oncolytic immunovirotherapy for melanoma using vesicular stomatitis virus. *Cancer Res, 67*(6), 2840-2848. doi:10.1158/0008-5472.CAN-06-3974

Drake, C. G., Jaffee, E., & Pardoll, D. M. (2006). Mechanisms of immune evasion by tumors. *Adv Immunol, 90*, 51-81. doi:10.1016/S0065-2776(06)90002-9

Duewell, P., Steger, A., Lohr, H., Bourhis, H., Hoelz, H., Kirchleitner, S. V., . . . Schnurr, M. (2014). RIG-I-like helicases induce immunogenic cell death of pancreatic cancer cells and sensitize tumors toward killing by CD8(+) T cells. *Cell Death Differ, 21*(12), 1825-1837. doi:10.1038/cdd.2014.96

Dunn, G. P., Bruce, A. T., Sheehan, K. C., Shankaran, V., Uppaluri, R., Bui, J. D., . . . Schreiber, R. D. (2005). A critical function for type I interferons in cancer immunoediting. *Nat Immunol, 6*(7), 722-729. doi:10.1038/ni1213

Esteso, G., Guerra, S., Vales-Gomez, M., & Reyburn, H. T. (2017). Innate Immune Recognition of Double-stranded RNA Triggers Increased Expression of NKG2D Ligands After Virus Infection. *J Biol Chem*. doi:10.1074/jbc.M117.818393

Fehervari, Z., & Sakaguchi, S. (2004). CD4+ Tregs and immune control. *J Clin Invest, 114*(9), 1209-1217. doi:10.1172/JCI23395

Fernandes-Alnemri, T., Yu, J. W., Datta, P., Wu, J., & Alnemri, E. S. (2009). AIM2 activates the inflammasome and cell death in response to cytoplasmic DNA. *Nature, 458*(7237), 509-513. doi:10.1038/nature07710

Floros, T., & Tarhini, A. A. (2015). Anticancer Cytokines: Biology and Clinical Effects of Interferon-alpha2, Interleukin (IL)-2, IL-15, IL-21, and IL-12. *Semin Oncol, 42*(4), 539-548. doi:10.1053/j.seminoncol.2015.05.015

Franchi, L., Eigenbrod, T., Munoz-Planillo, R., Ozkurede, U., Kim, Y. G., Chakrabarti, A., . . . Nunez, G. (2014). Cytosolic double-stranded RNA activates the NLRP3 inflammasome via MAVS-induced membrane permeabilization and K+ efflux. *J Immunol, 193*(8), 4214-4222. doi:10.4049/jimmunol.1400582

Francisco, L. M., Salinas, V. H., Brown, K. E., Vanguri, V. K., Freeman, G. J., Kuchroo, V. K., & Sharpe, A. H. (2009). PD-L1 regulates the development, maintenance, and function of induced regulatory T cells. *J Exp Med, 206*(13), 3015-3029. doi:10.1084/jem.20090847

Franklin, B. S., Bossaller, L., De Nardo, D., Ratter, J. M., Stutz, A., Engels, G., . . . Latz, E. (2014). The adaptor ASC has extracellular and 'prionoid' activities that propagate inflammation. *Nat Immunol, 15*(8), 727-737. doi:10.1038/ni.2913

Freeman, G. J., Long, A. J., Iwai, Y., Bourque, K., Chernova, T., Nishimura, H., . . . Honjo, T. (2000). Engagement of the PD-1 immunoinhibitory receptor by a novel B7 family member leads to negative regulation of lymphocyte activation. *J Exp Med, 192*(7), 1027-1034.

Fu, J., Kanne, D. B., Leong, M., Glickman, L. H., McWhirter, S. M., Lemmens, E., . . . Kim, Y. (2015). STING agonist formulated cancer vaccines can cure established tumors resistant to PD-1 blockade. *Sci Transl Med, 7*(283), 283ra252. doi:10.1126/scitranslmed.aaa4306

Fuertes Marraco, S. A., Neubert, N. J., Verdeil, G., & Speiser, D. E. (2015). Inhibitory Receptors Beyond T Cell Exhaustion. *Front Immunol, 6*, 310. doi:10.3389/fimmu.2015.00310

Fuertes, M. B., Kacha, A. K., Kline, J., Woo, S. R., Kranz, D. M., Murphy, K. M., & Gajewski, T. F. (2011). Host type I IFN signals are required for antitumor CD8+ T cell responses through CD8{alpha}+ dendritic cells. *J Exp Med, 208*(10), 2005-2016. doi:10.1084/jem.20101159

Gandini, S., Sera, F., Cattaruzza, M. S., Pasquini, P., Picconi, O., Boyle, P., & Melchi, C. F. (2005). Meta-analysis of risk factors for cutaneous melanoma: II. Sun exposure. *Eur J Cancer, 41*(1), 45-60. doi:10.1016/j.ejca.2004.10.016

Gao, D., Wu, J., Wu, Y. T., Du, F., Aroh, C., Yan, N., . . . Chen, Z. J. (2013). Cyclic GMP-AMP synthase is an innate immune sensor of HIV and other retroviruses. *Science, 341*(6148), 903-906. doi:10.1126/science.1240933

Garg, A. D., Martin, S., Golab, J., & Agostinis, P. (2014). Danger signalling during cancer cell death: origins, plasticity and regulation. *Cell Death Differ, 21*(1), 26-38. doi:10.1038/cdd.2013.48

Glas, M., Coch, C., Trageser, D., Dassler, J., Simon, M., Koch, P., . . . Scheffler, B. (2013). Targeting the cytosolic innate immune receptors RIG-I and MDA5 effectively counteracts cancer cell heterogeneity in glioblastoma. *Stem Cells, 31*(6), 1064-1074. doi:10.1002/stem.1350

Glimcher, L. H., & Murphy, K. M. (2000). Lineage commitment in the immune system: the T helper lymphocyte grows up. *Genes Dev, 14*(14), 1693-1711.

Golden, E. B., & Apetoh, L. (2015). Radiotherapy and immunogenic cell death. *Semin Radiat Oncol, 25*(1), 11-17. doi:10.1016/j.semradonc.2014.07.005

Goldszmid, R. S., Idoyaga, J., Bravo, A. I., Steinman, R., Mordoh, J., & Wainstok, R. (2003). Dendritic cells charged with apoptotic tumor cells induce long-lived protective CD4+ and CD8+ T cell immunity against B16 melanoma. *J Immunol, 171*(11), 5940-5947.

Gonzalez-Gugel, E., Saxena, M., & Bhardwaj, N. (2016). Modulation of innate immunity in the tumor microenvironment. *Cancer Immunol Immunother, 65*(10), 1261-1268. doi:10.1007/s00262-016-1859-9

Gonzalez, S., Lopez-Soto, A., Suarez-Alvarez, B., Lopez-Vazquez, A., & Lopez-Larrea, C. (2008). NKG2D ligands: key targets of the immune response. *Trends Immunol, 29*(8), 397-403. doi:10.1016/j.it.2008.04.007

Goubau, D., Schlee, M., Deddouche, S., Pruijssers, A. J., Zillinger, T., Goldeck, M., . . . Reis, E. S. C. (2014a). Antiviral immunity via RIG-I-mediated recognition of RNA bearing 5'-diphosphates. *Nature, 514*(7522), 372-375. doi:10.1038/nature13590

Goubau, D., Schlee, M., Deddouche, S., Pruijssers, A. J., Zillinger, T., Goldeck, M., . . . Reis, E. S. C. (2014b). Antiviral immunity via RIG-I-mediated recognition of RNA bearing 5'-diphosphates. *Nature*. doi:10.1038/nature13590

Grimaldi, A. M., Simeone, E., Giannarelli, D., Muto, P., Falivene, S., Borzillo, V., . . . Ascierto, P. A. (2014). Abscopal effects of radiotherapy on advanced melanoma patients who progressed after ipilimumab immunotherapy. *Oncoimmunology, 3*, e28780. doi:10.4161/onci.28780

Gubin, M. M., Zhang, X., Schuster, H., Caron, E., Ward, J. P., Noguchi, T., . . . Schreiber, R. D. (2014). Checkpoint blockade cancer immunotherapy targets tumour-specific mutant antigens. *Nature, 515*(7528), 577-581. doi:10.1038/nature13988

Guo, Z. S., Liu, Z., Kowalsky, S., Feist, M., Kalinski, P., Lu, B., . . . Bartlett, D. L. (2017). Oncolytic Immunotherapy: Conceptual Evolution, Current Strategies, and Future Perspectives. *Front Immunol, 8*, 555. doi:10.3389/fimmu.2017.00555

Handgretinger, R., Lang, P., & Andre, M. C. (2016). Exploitation of natural killer cells for the treatment of acute leukemia. *Blood, 127*(26), 3341-3349. doi:10.1182/blood-2015-12-629055

Hannani, D., Vetizou, M., Enot, D., Rusakiewicz, S., Chaput, N., Klatzmann, D., . . . Zitvogel, L. (2015). Anticancer immunotherapy by CTLA-4 blockade: obligatory contribution of IL-2 receptors and negative prognostic impact of soluble CD25. *Cell Res, 25*(2), 208-224. doi:10.1038/cr.2015.3

Harding, S. M., Benci, J. L., Irianto, J., Discher, D. E., Minn, A. J., & Greenberg, R. A. (2017). Mitotic progression following DNA damage enables pattern recognition within micronuclei. *Nature, 548*(7668), 466-470. doi:10.1038/nature23470

Harrington, K. J., Ferris, R. L., Blumenschein, G., Jr., Colevas, A. D., Fayette, J., Licitra, L., . . . Guigay, J. (2017). Nivolumab versus standard, single-agent therapy of investigator's choice in recurrent or metastatic squamous cell carcinoma of the head and neck (CheckMate 141): health-related quality-of-life results from a randomised, phase 3 trial. *Lancet Oncol, 18*(8), 1104-1115. doi:10.1016/S1470-2045(17)30421-7

Harrington, L. E., Hatton, R. D., Mangan, P. R., Turner, H., Murphy, T. L., Murphy, K. M., & Weaver, C. T. (2005). Interleukin 17-producing CD4+ effector T cells develop via a lineage distinct from the T helper type 1 and 2 lineages. *Nat Immunol, 6*(11), 1123-1132. doi:10.1038/ni1254

Hartlova, A., Erttmann, S. F., Raffi, F. A., Schmalz, A. M., Resch, U., Anugula, S., . . . Gekara, N. O. (2015). DNA damage primes the type I interferon system via the cytosolic DNA sensor STING to promote anti-microbial innate immunity. *Immunity, 42*(2), 332-343. doi:10.1016/j.immuni.2015.01.012

Hatfield, P., Merrick, A. E., West, E., O'Donnell, D., Selby, P., Vile, R., & Melcher, A. A. (2008). Optimization of dendritic cell loading with tumor cell lysates for cancer immunotherapy. *J Immunother, 31*(7), 620-632. doi:10.1097/CJI.0b013e31818213df

Hildner, K., Edelson, B. T., Purtha, W. E., Diamond, M., Matsushita, H., Kohyama, M., . . . Murphy, K. M. (2008). Batf3 deficiency reveals a critical role for CD8alpha+ dendritic cells in cytotoxic T cell immunity. *Science, 322*(5904), 1097-1100. doi:10.1126/science.1164206

Hochheiser, K., Klein, M., Gottschalk, C., Hoss, F., Scheu, S., Coch, C., . . . Kurts, C. (2016). Cutting Edge: The RIG-I Ligand 3pRNA Potently Improves CTL Cross-Priming and Facilitates Antiviral Vaccination. *J Immunol, 196*(6), 2439-2443. doi:10.4049/jimmunol.1501958

Hodi, F. S., Chesney, J., Pavlick, A. C., Robert, C., Grossmann, K. F., McDermott, D. F., . . . Postow, M. A. (2016). Combined nivolumab and ipilimumab versus ipilimumab alone in patients with advanced melanoma: 2-year overall survival outcomes in a multicentre, randomised, controlled, phase 2 trial. *Lancet Oncol, 17*(11), 1558-1568. doi:10.1016/S1470-2045(16)30366-7

Hodi, F. S., O'Day, S. J., McDermott, D. F., Weber, R. W., Sosman, J. A., Haanen, J. B., . . . Urba, W. J. (2010). Improved survival with ipilimumab in patients with metastatic melanoma. *N Engl J Med, 363*(8), 711-723. doi:10.1056/NEJMoa1003466

Horn, L., Spigel, D. R., Vokes, E. E., Holgado, E., Ready, N., Steins, M., . . . Eberhardt, W. E. E. (2017). Nivolumab Versus Docetaxel in Previously Treated Patients With Advanced Non-Small-Cell Lung Cancer: Two-Year Outcomes From Two Randomized, Open-Label, Phase III Trials (CheckMate 017 and CheckMate 057). *J Clin Oncol, 35*(35), 3924-3933. doi:10.1200/JCO.2017.74.3062

Hornung, V., Ellegast, J., Kim, S., Brzozka, K., Jung, A., Kato, H., . . . Hartmann, G. (2006). 5'-Triphosphate RNA is the ligand for RIG-I. *Science, 314*(5801), 994-997. doi:10.1126/science.1132505

Hu, J., He, Y., Yan, M., Zhu, C., Ye, W., Zhu, H., . . . Zhang, Z. (2013). Dose dependent activation of retinoic acid-inducible gene-I promotes both proliferation and apoptosis signals in human head and neck squamous cell carcinoma. *PLoS One, 8*(3), e58273. doi:10.1371/journal.pone.0058273

Huang, Z., Chen, X., Yu, B., & Chen, D. (2012). Cloning and functional characterization of rat stimulator of interferon genes (STING) regulated by miR-24. *Dev Comp Immunol, 37*(3-4), 414-420. doi:10.1016/j.dci.2012.02.010

Hurst, T. P., & Magiorkinis, G. (2015). Activation of the innate immune response by endogenous retroviruses. *J Gen Virol, 96*(Pt 6), 1207-1218. doi:10.1099/jgv.0.000017

Hurwitz, A. A., Yu, T. F., Leach, D. R., & Allison, J. P. (1998). CTLA-4 blockade synergizes with tumor-derived granulocyte-macrophage colony-stimulating factor for treatment of an experimental mammary carcinoma. *Proc Natl Acad Sci U S A, 95*(17), 10067-10071.

Ishikawa, H., & Barber, G. N. (2008). STING is an endoplasmic reticulum adaptor that facilitates innate immune signalling. *Nature, 455*(7213), 674-678. doi:10.1038/nature07317

Jakobsen, M. R., Olagnier, D., & Hiscott, J. (2015). Innate immune sensing of HIV-1 infection. *Curr Opin HIV AIDS, 10*(2), 96-102. doi:10.1097/COH.0000000000000129

Jamieson, A. M., Diefenbach, A., McMahon, C. W., Xiong, N., Carlyle, J. R., & Raulet, D. H. (2002). The role of the NKG2D immunoreceptor in immune cell activation and natural killing. *Immunity, 17*(1), 19-29.

Joffre, O., Nolte, M. A., Sporri, R., & Reis e Sousa, C. (2009). Inflammatory signals in dendritic cell activation and the induction of adaptive immunity. *Immunol Rev, 227*(1), 234-247. doi:10.1111/j.1600-065X.2008.00718.x

Jung, S., Unutmaz, D., Wong, P., Sano, G., De los Santos, K., Sparwasser, T., . . . Lang, R. A. (2002). In vivo depletion of CD11c+ dendritic cells abrogates priming of CD8+ T cells by exogenous cell-associated antigens. *Immunity, 17*(2), 211-220.

Junt, T., & Barchet, W. (2015). Translating nucleic acid-sensing pathways into therapies. *Nat Rev Immunol, 15*(9), 529-544. doi:10.1038/nri3875

Kantari, C., & Walczak, H. (2011). Caspase-8 and bid: caught in the act between death receptors and mitochondria. *Biochim Biophys Acta, 1813*(4), 558-563. doi:10.1016/j.bbamcr.2011.01.026

Karlsen, T. A., & Brinchmann, J. E. (2013). Liposome delivery of microRNA-145 to mesenchymal stem cells leads to immunological off-target effects mediated by RIG-I. *Mol Ther, 21*(6), 1169-1181. doi:10.1038/mt.2013.55

Kato, H., Takeuchi, O., Sato, S., Yoneyama, M., Yamamoto, M., Matsui, K., . . . Akira, S. (2006). Differential roles of MDA5 and RIG-I helicases in the recognition of RNA viruses. *Nature, 441*(7089), 101-105. doi:10.1038/nature04734

Kawai, T., & Akira, S. (2010). The role of pattern-recognition receptors in innate immunity: update on Toll-like receptors. *Nat Immunol, 11*(5), 373-384. doi:10.1038/ni.1863

Kearney, C. J., Cullen, S. P., Tynan, G. A., Henry, C. M., Clancy, D., Lavelle, E. C., & Martin, S. J. (2015). Necroptosis suppresses inflammation via termination of TNF- or LPS-induced cytokine and chemokine production. *Cell Death Differ, 22*(8), 1313-1327. doi:10.1038/cdd.2014.222

Kepp, O., Senovilla, L., Vitale, I., Vacchelli, E., Adjemian, S., Agostinis, P., . . . Galluzzi, L. (2014). Consensus guidelines for the detection of immunogenic cell death. *Oncoimmunology, 3*(9), e955691. doi:10.4161/21624011.2014.955691

Kirkwood, J. M., Butterfield, L. H., Tarhini, A. A., Zarour, H., Kalinski, P., & Ferrone, S. (2012). Immunotherapy of cancer in 2012. *CA Cancer J Clin, 62*(5), 309-335. doi:10.3322/caac.20132

Kloosterman, W. P., & Plasterk, R. H. (2006). The diverse functions of microRNAs in animal development and disease. *Dev Cell, 11*(4), 441-450. doi:10.1016/j.devcel.2006.09.009

Kohrt, H. E., Thielens, A., Marabelle, A., Sagiv-Barfi, I., Sola, C., Chanuc, F., . . . Andre, P. (2014). Anti-KIR antibody enhancement of anti-lymphoma activity of natural killer cells as monotherapy and in combination with anti-CD20 antibodies. *Blood, 123*(5), 678-686. doi:10.1182/blood-2013-08-519199

Kroemer, G., Galluzzi, L., Kepp, O., & Zitvogel, L. (2013). Immunogenic cell death in cancer therapy. *Annu Rev Immunol, 31*, 51-72. doi:10.1146/annurev-immunol-032712-100008

Krysko, D. V., Garg, A. D., Kaczmarek, A., Krysko, O., Agostinis, P., & Vandenabeele, P. (2012). Immunogenic cell death and DAMPs in cancer therapy. *Nat Rev Cancer, 12*(12), 860-875. doi:10.1038/nrc3380

Krysko, O., Aaes, T. L., Kagan, V. E., D'Herde, K., Bachert, C., Leybaert, L., . . . Krysko, D. V. (2017). Necroptotic cell death in anti-cancer therapy. *Immunol Rev, 280*(1), 207-219. doi:10.1111/imr.12583

Kubler, K., Gehrke, N., Riemann, S., Bohnert, V., Zillinger, T., Hartmann, E., . . . Barchet, W. (2010). Targeted activation of RNA helicase retinoic acid-inducible gene-I induces proimmunogenic apoptosis of human ovarian cancer cells. *Cancer Res, 70*(13), 5293-5304. doi:10.1158/0008-5472.CAN-10-0825

Kumar, S., Ingle, H., Mishra, S., Mahla, R. S., Kumar, A., Kawai, T., . . . Kumar, H. (2015). IPS-1 differentially induces TRAIL, BCL2, BIRC3 and PRKCE in type I interferons-dependent and -independent anticancer activity. *Cell Death Dis, 6*, e1758. doi:10.1038/cddis.2015.122

Kvistborg, P., Philips, D., Kelderman, S., Hageman, L., Ottensmeier, C., Joseph-Pietras, D., . . . Schumacher, T. N. (2014). Anti-CTLA-4 therapy broadens the melanoma-reactive CD8+ T cell response. *Sci Transl Med, 6*(254), 254ra128. doi:10.1126/scitranslmed.3008918

Kwon, E. D., Hurwitz, A. A., Foster, B. A., Madias, C., Feldhaus, A. L., Greenberg, N. M., . . . Allison, J. P. (1997). Manipulation of T cell costimulatory and inhibitory signals for immunotherapy of prostate cancer. *Proc Natl Acad Sci U S A, 94*(15), 8099-8103.

Langer, C. J., Gadgeel, S. M., Borghaei, H., Papadimitrakopoulou, V. A., Patnaik, A., Powell, S. F., . . . investigators, K.-. (2016). Carboplatin and pemetrexed with or without pembrolizumab for advanced, non-squamous non-small-cell lung cancer: a randomised, phase 2 cohort of the open-label KEYNOTE-021 study. *Lancet Oncol, 17*(11), 1497-1508. doi:10.1016/S1470-2045(16)30498-3

Larkin, J., Hodi, F. S., & Wolchok, J. D. (2015). Combined Nivolumab and Ipilimumab or Monotherapy in Untreated Melanoma. *N Engl J Med, 373*(13), 1270-1271. doi:10.1056/NEJMc1509660

Latchman, Y., Wood, C. R., Chernova, T., Chaudhary, D., Borde, M., Chernova, I., . . . Freeman, G. J. (2001). PD-L2 is a second ligand for PD-1 and inhibits T cell activation. *Nat Immunol, 2*(3), 261-268. doi:10.1038/85330

Lawlor, K. E., Khan, N., Mildenhall, A., Gerlic, M., Croker, B. A., D'Cruz, A. A., . . . Vince, J. E. (2015). RIPK3 promotes cell death and NLRP3 inflammasome activation in the absence of MLKL. *Nat Commun, 6*, 6282. doi:10.1038/ncomms7282

Leach, D. R., Krummel, M. F., & Allison, J. P. (1996). Enhancement of antitumor immunity by CTLA-4 blockade. *Science, 271*(5256), 1734-1736.

LeibundGut-Landmann, S., Gross, O., Robinson, M. J., Osorio, F., Slack, E. C., Tsoni, S. V., . . . Reis e Sousa, C. (2007). Syk- and CARD9-dependent coupling of innate immunity to the induction of T helper cells that produce interleukin 17. *Nat Immunol, 8*(6), 630-638. doi:10.1038/ni1460

Lettau, M., Kabelitz, D., & Janssen, O. (2015). Lysosome-Related Effector Vesicles in T Lymphocytes and NK Cells. *Scand J Immunol, 82*(3), 235-243. doi:10.1111/sji.12337

Levy, D. E., Marie, I. J., & Durbin, J. E. (2011). Induction and function of type I and III interferon in response to viral infection. *Curr Opin Virol, 1*(6), 476-486. doi:10.1016/j.coviro.2011.11.001

Li, B., VanRoey, M., Wang, C., Chen, T. H., Korman, A., & Jooss, K. (2009). Anti-programmed death-1 synergizes with granulocyte macrophage colony-stimulating factor--secreting tumor cell immunotherapy providing therapeutic benefit to mice with established tumors. *Clin Cancer Res, 15*(5), 1623-1634. doi:10.1158/1078-0432.CCR-08-1825

Li, D., Gale, R. P., Liu, Y., Lei, B., Wang, Y., Diao, D., & Zhang, M. (2017). 5'-Triphosphate siRNA targeting MDR1 reverses multi-drug resistance and activates RIG-I-induced immune-stimulatory and apoptotic effects against human myeloid leukaemia cells. *Leuk Res, 58*, 23-30. doi:10.1016/j.leukres.2017.03.010

Li, H., Zhu, H., Xu, C. J., & Yuan, J. (1998). Cleavage of BID by caspase 8 mediates the mitochondrial damage in the Fas pathway of apoptosis. *Cell, 94*(4), 491-501.

Li, X. D., Wu, J., Gao, D., Wang, H., Sun, L., & Chen, Z. J. (2013). Pivotal roles of cGAS-cGAMP signaling in antiviral defense and immune adjuvant effects. *Science, 341*(6152), 1390-1394. doi:10.1126/science.1244040

Linardakis, E., Bateman, A., Phan, V., Ahmed, A., Gough, M., Olivier, K., . . . Vile, R. (2002). Enhancing the efficacy of a weak allogeneic melanoma vaccine by viral fusogenic membrane glycoprotein-mediated tumor cell-tumor cell fusion. *Cancer Res, 62*(19), 5495-5504.

Linsley, P. S., Brady, W., Urnes, M., Grosmaire, L. S., Damle, N. K., & Ledbetter, J. A. (1991). CTLA-4 is a second receptor for the B cell activation antigen B7. *J Exp Med, 174*(3), 561-569.

Linsley, P. S., Greene, J. L., Brady, W., Bajorath, J., Ledbetter, J. A., & Peach, R. (1994). Human B7-1 (CD80) and B7-2 (CD86) bind with similar avidities but distinct kinetics to CD28 and CTLA-4 receptors. *Immunity, 1*(9), 793-801.

Liontos, M., Anastasiou, I., Bamias, A., & Dimopoulos, M. A. (2016). DNA damage, tumor mutational load and their impact on immune responses against cancer. *Ann Transl Med, 4*(14), 264. doi:10.21037/atm.2016.07.11

Liu, Y., Goulet, M. L., Sze, A., Hadj, S. B., Belgnaoui, S. M., Lababidi, R. R., . . . Lin, R. (2016). RIG-I-Mediated STING Upregulation Restricts Herpes Simplex Virus 1 Infection. *J Virol, 90*(20), 9406-9419. doi:10.1128/JVI.00748-16

Luke, J. J., Flaherty, K. T., Ribas, A., & Long, G. V. (2017). Targeted agents and immunotherapies: optimizing outcomes in melanoma. *Nat Rev Clin Oncol*. doi:10.1038/nrclinonc.2017.43

Ma, Z., Li, W., Yoshiya, S., Xu, Y., Hata, M., El-Darawish, Y., . . . Okamura, H. (2016). Augmentation of Immune Checkpoint Cancer Immunotherapy with IL18. *Clin Cancer Res, 22*(12), 2969-2980. doi:10.1158/1078-0432.CCR-15-1655

Mackiewicz, J. (2012). What is new in the treatment of advanced melanoma? State of the art. *Contemp Oncol (Pozn), 16*(5), 363-370. doi:10.5114/wo.2012.31763

Mankan, A. K., Schmidt, T., Chauhan, D., Goldeck, M., Honing, K., Gaidt, M., . . . Hornung, V. (2014). Cytosolic RNA:DNA hybrids activate the cGAS-STING axis. *EMBO J, 33*(24), 2937-2946. doi:10.15252/embj.201488726

Marzec, M., Zhang, Q., Goradia, A., Raghunath, P. N., Liu, X., Paessler, M., . . . Wasik, M. A. (2008). Oncogenic kinase NPM/ALK induces through STAT3 expression of immunosuppressive protein CD274 (PD-L1, B7-H1). *Proc Natl Acad Sci U S A, 105*(52), 20852-20857. doi:10.1073/pnas.0810958105

Mason, K. A., Ariga, H., Neal, R., Valdecanas, D., Hunter, N., Krieg, A. M., . . . Milas, L. (2005). Targeting toll-like receptor 9 with CpG oligodeoxynucleotides enhances tumor response to fractionated radiotherapy. *Clin Cancer Res, 11*(1), 361-369.

McClanahan, F., Hanna, B., Miller, S., Clear, A. J., Lichter, P., Gribben, J. G., & Seiffert, M. (2015). PD-L1 checkpoint blockade prevents immune dysfunction and leukemia development in a mouse model of chronic lymphocytic leukemia. *Blood, 126*(2), 203-211. doi:10.1182/blood-2015-01-622936

McGuire, S. (2016). World Cancer Report 2014. Geneva, Switzerland: World Health Organization, International Agency for Research on Cancer, WHO Press, 2015. *Adv Nutr, 7*(2), 418-419. doi:10.3945/an.116.012211

Medzhitov, R., & Janeway, C. A., Jr. (1997). Innate immunity: impact on the adaptive immune response. *Curr Opin Immunol, 9*(1), 4-9.

Medzhitov, R., Preston-Hurlburt, P., & Janeway, C. A., Jr. (1997). A human homologue of the Drosophila Toll protein signals activation of adaptive immunity. *Nature, 388*(6640), 394-397. doi:10.1038/41131

Milas, L., Mason, K. A., Ariga, H., Hunter, N., Neal, R., Valdecanas, D., . . . Whisnant, J. K. (2004). CpG oligodeoxynucleotide enhances tumor response to radiation. *Cancer Res, 64*(15), 5074-5077. doi:10.1158/0008-5472.CAN-04-0926

Moriwaki, K., & Chan, F. K. (2016). Necroptosis-independent signaling by the RIP kinases in inflammation. *Cell Mol Life Sci, 73*(11-12), 2325-2334. doi:10.1007/s00018-016-2203-4

Mu, X., Ahmad, S., & Hur, S. (2016). Endogenous Retroelements and the Host Innate Immune Sensors. *Adv Immunol, 132*, 47-69. doi:10.1016/bs.ai.2016.07.001

Muller, U., Steinhoff, U., Reis, L. F., Hemmi, S., Pavlovic, J., Zinkernagel, R. M., & Aguet, M. (1994). Functional role of type I and type II interferons in antiviral defense. *Science, 264*(5167), 1918-1921.

Nabet, B. Y., Qiu, Y., Shabason, J. E., Wu, T. J., Yoon, T., Kim, B. C., . . . Minn, A. J. (2017). Exosome RNA Unshielding Couples Stromal Activation to Pattern Recognition Receptor Signaling in Cancer. *Cell, 170*(2), 352-366 e313. doi:10.1016/j.cell.2017.06.031

Nakanishi, K., Yoshimoto, T., Tsutsui, H., & Okamura, H. (2001). Interleukin-18 regulates both Th1 and Th2 responses. *Annu Rev Immunol, 19*, 423-474. doi:10.1146/annurev.immunol.19.1.423

Nazmi, A., Mukhopadhyay, R., Dutta, K., & Basu, A. (2012). STING mediates neuronal innate immune response following Japanese encephalitis virus infection. *Sci Rep, 2*, 347. doi:10.1038/srep00347

Nitta, S., Sakamoto, N., Nakagawa, M., Kakinuma, S., Mishima, K., Kusano-Kitazume, A., . . . Watanabe, M. (2013). Hepatitis C virus NS4B protein targets STING and abrogates RIG-I-mediated type I interferon-dependent innate immunity. *Hepatology, 57*(1), 46-58. doi:10.1002/hep.26017

O'Bryan, S., Dong, S., Mathis, J. M., & Alahari, S. K. (2017). The roles of oncogenic miRNAs and their therapeutic importance in breast cancer. *Eur J Cancer, 72*, 1-11. doi:10.1016/j.ejca.2016.11.004

Obeid, M., Panaretakis, T., Joza, N., Tufi, R., Tesniere, A., van Endert, P., . . . Kroemer, G. (2007). Calreticulin exposure is required for the immunogenicity of gamma-irradiation and UVC light-induced apoptosis. *Cell Death Differ, 14*(10), 1848-1850. doi:10.1038/sj.cdd.4402201

Ott, P. A., Hodi, F. S., Kaufman, H. L., Wigginton, J. M., & Wolchok, J. D. (2017). Combination immunotherapy: a road map. *J Immunother Cancer, 5*, 16. doi:10.1186/s40425-017-0218-5

Ott, P. A., Hu, Z., Keskin, D. B., Shukla, S. A., Sun, J., Bozym, D. J., . . . Wu, C. J. (2017). An immunogenic personal neoantigen vaccine for patients with melanoma. *Nature, 547*(7662), 217-221. doi:10.1038/nature22991

Pardoll, D. M. (2012). The blockade of immune checkpoints in cancer immunotherapy. *Nat Rev Cancer, 12*(4), 252-264. doi:10.1038/nrc3239

Parry, R. V., Chemnitz, J. M., Frauwirth, K. A., Lanfranco, A. R., Braunstein, I., Kobayashi, S. V., . . . Riley, J. L. (2005). CTLA-4 and PD-1 receptors inhibit T-cell activation by distinct mechanisms. *Mol Cell Biol, 25*(21), 9543-9553. doi:10.1128/MCB.25.21.9543-9553.2005

Peggs, K. S., Quezada, S. A., Korman, A. J., & Allison, J. P. (2006). Principles and use of anti-CTLA4 antibody in human cancer immunotherapy. *Curr Opin Immunol, 18*(2), 206-213. doi:10.1016/j.coi.2006.01.011

Pike, L. R. G., Bang, A., Ott, P., Balboni, T., Taylor, A., Catalano, P., . . . Schoenfeld, J. D. (2017). Radiation and PD-1 inhibition: Favorable outcomes after brain-directed radiation. *Radiother Oncol, 124*(1), 98-103. doi:10.1016/j.radonc.2017.06.006

Pitt, J. M., Vetizou, M., Daillere, R., Roberti, M. P., Yamazaki, T., Routy, B., . . . Zitvogel, L. (2016). Resistance Mechanisms to Immune-Checkpoint Blockade in Cancer: Tumor-Intrinsic and -Extrinsic Factors. *Immunity, 44*(6), 1255-1269. doi:10.1016/j.immuni.2016.06.001

Poeck, H., Besch, R., Maihoefer, C., Renn, M., Tormo, D., Morskaya, S. S., . . . Hartmann, G. (2008). 5'-Triphosphate-siRNA: turning gene silencing and Rig-I activation against melanoma. *Nat Med, 14*(11), 1256-1263. doi:10.1038/nm.1887

Poeck, H., Bscheider, M., Gross, O., Finger, K., Roth, S., Rebsamen, M., . . . Ruland, J. (2010). Recognition of RNA virus by RIG-I results in activation of CARD9 and inflammasome signaling for interleukin 1 beta production. *Nat Immunol, 11*(1), 63-69. doi:10.1038/ni.1824

Pollack, L. A., Li, J., Berkowitz, Z., Weir, H. K., Wu, X. C., Ajani, U. A., . . . Pollack, B. P. (2011). Melanoma survival in the United States, 1992 to 2005. *J Am Acad Dermatol, 65*(5 Suppl 1), S78-86. doi:10.1016/j.jaad.2011.05.030

Pothlichet, J., Meunier, I., Davis, B. K., Ting, J. P., Skamene, E., von Messling, V., & Vidal, S. M. (2013). Type I IFN triggers RIG-I/TLR3/NLRP3-dependent inflammasome activation in influenza A virus infected cells. *PLoS Pathog, 9*(4), e1003256. doi:10.1371/journal.ppat.1003256

Quezada, S. A., Peggs, K. S., Curran, M. A., & Allison, J. P. (2006). CTLA4 blockade and GM-CSF combination immunotherapy alters the intratumor balance of effector and regulatory T cells. *J Clin Invest, 116*(7), 1935-1945. doi:10.1172/JCI27745

Rahman, M. M., Bagdassarian, E., Ali, M. A. M., & McFadden, G. (2017). Identification of host DEAD-box RNA helicases that regulate cellular tropism of oncolytic Myxoma virus in human cancer cells. *Sci Rep, 7*(1), 15710. doi:10.1038/s41598-017-15941-1

Ranoa, D. R., Parekh, A. D., Pitroda, S. P., Huang, X., Darga, T., Wong, A. C., . . . Khodarev, N. N. (2016). Cancer therapies activate RIG-I-like receptor pathway

through endogenous non-coding RNAs. *Oncotarget, 7*(18), 26496-26515. doi:10.18632/oncotarget.8420

Rathinam, V. A., & Fitzgerald, K. A. (2011). Cytosolic surveillance and antiviral immunity. *Curr Opin Virol, 1*(6), 455-462. doi:10.1016/j.coviro.2011.11.004

Ravichandran, K. S. (2011). Beginnings of a good apoptotic meal: the find-me and eat-me signaling pathways. *Immunity, 35*(4), 445-455. doi:10.1016/j.immuni.2011.09.004

Rizvi, N. A., Hellmann, M. D., Snyder, A., Kvistborg, P., Makarov, V., Havel, J. J., . . . Chan, T. A. (2015). Cancer immunology. Mutational landscape determines sensitivity to PD-1 blockade in non-small cell lung cancer. *Science, 348*(6230), 124-128. doi:10.1126/science.aaa1348

Robert, C., & Ghiringhelli, F. (2009). What is the role of cytotoxic T lymphocyte-associated antigen 4 blockade in patients with metastatic melanoma? *Oncologist, 14*(8), 848-861. doi:10.1634/theoncologist.2009-0028

Robert, C., Thomas, L., Bondarenko, I., O'Day, S., Weber, J., Garbe, C., . . . Wolchok, J. D. (2011). Ipilimumab plus dacarbazine for previously untreated metastatic melanoma. *N Engl J Med, 364*(26), 2517-2526. doi:10.1056/NEJMoa1104621

Rossi, M., & Young, J. W. (2005). Human dendritic cells: potent antigen-presenting cells at the crossroads of innate and adaptive immunity. *J Immunol, 175*(3), 1373-1381.

Rycaj, K., Plummer, J. B., Yin, B., Li, M., Garza, J., Radvanyi, L., . . . Wang-Johanning, F. (2015). Cytotoxicity of human endogenous retrovirus K-specific T cells toward autologous ovarian cancer cells. *Clin Cancer Res, 21*(2), 471-483. doi:10.1158/1078-0432.CCR-14-0388

Sahin, U., Derhovanessian, E., Miller, M., Kloke, B. P., Simon, P., Lower, M., . . . Tureci, O. (2017). Personalized RNA mutanome vaccines mobilize poly-specific therapeutic immunity against cancer. *Nature, 547*(7662), 222-226. doi:10.1038/nature23003

Sali, T. M., Pryke, K. M., Abraham, J., Liu, A., Archer, I., Broeckel, R., . . . DeFilippis, V. R. (2015). Characterization of a Novel Human-Specific STING Agonist that Elicits Antiviral Activity Against Emerging Alphaviruses. *PLoS Pathog, 11*(12), e1005324. doi:10.1371/journal.ppat.1005324

Salmon, H., Idoyaga, J., Rahman, A., Leboeuf, M., Remark, R., Jordan, S., . . . Merad, M. (2016). Expansion and Activation of CD103(+) Dendritic Cell Progenitors at the Tumor Site Enhances Tumor Responses to Therapeutic PD-L1 and BRAF Inhibition. *Immunity, 44*(4), 924-938. doi:10.1016/j.immuni.2016.03.012

Sauer, J. D., Sotelo-Troha, K., von Moltke, J., Monroe, K. M., Rae, C. S., Brubaker, S. W., . . . Vance, R. E. (2011). The N-ethyl-N-nitrosourea-induced Goldenticket mouse mutant reveals an essential function of Sting in the in vivo interferon response to Listeria monocytogenes and cyclic dinucleotides. *Infect Immun, 79*(2), 688-694. doi:10.1128/IAI.00999-10

Schadendorf, D., Hodi, F. S., Robert, C., Weber, J. S., Margolin, K., Hamid, O., . . . Wolchok, J. D. (2015). Pooled Analysis of Long-Term Survival Data From Phase

II and Phase III Trials of Ipilimumab in Unresectable or Metastatic Melanoma. *J Clin Oncol, 33*(17), 1889-1894. doi:10.1200/JCO.2014.56.2736

Schimmer, A. D. (2004). Inhibitor of apoptosis proteins: translating basic knowledge into clinical practice. *Cancer Res, 64*(20), 7183-7190. doi:10.1158/0008-5472.CAN-04-1918

Schlee, M., Roth, A., Hornung, V., Hagmann, C. A., Wimmenauer, V., Barchet, W., . . . Hartmann, G. (2009). Recognition of 5' triphosphate by RIG-I helicase requires short blunt double-stranded RNA as contained in panhandle of negative-strand virus. *Immunity, 31*(1), 25-34. doi:10.1016/j.immuni.2009.05.008

Schmidt, A., Endres, S., & Rothenfusser, S. (2011). Pattern recognition of viral nucleic acids by RIG-I-like helicases. *J Mol Med (Berl), 89*(1), 5-12. doi:10.1007/s00109-010-0672-8

Schneider, H., Mandelbrot, D. A., Greenwald, R. J., Ng, F., Lechler, R., Sharpe, A. H., & Rudd, C. E. (2002). Cutting edge: CTLA-4 (CD152) differentially regulates mitogen-activated protein kinases (extracellular signal-regulated kinase and c-Jun N-terminal kinase) in CD4+ T cells from receptor/ligand-deficient mice. *J Immunol, 169*(7), 3475-3479.

Schock, S. N., Chandra, N. V., Sun, Y., Irie, T., Kitagawa, Y., Gotoh, B., . . . Winoto, A. (2017). Induction of necroptotic cell death by viral activation of the RIG-I or STING pathway. *Cell Death Differ, 24*(4), 615-625. doi:10.1038/cdd.2016.153

Schoggins, J. W., MacDuff, D. A., Imanaka, N., Gainey, M. D., Shrestha, B., Eitson, J. L., . . . Rice, C. M. (2014). Pan-viral specificity of IFN-induced genes reveals new roles for cGAS in innate immunity. *Nature, 505*(7485), 691-695. doi:10.1038/nature12862

Schoggins, J. W., & Rice, C. M. (2011). Interferon-stimulated genes and their antiviral effector functions. *Curr Opin Virol, 1*(6), 519-525. doi:10.1016/j.coviro.2011.10.008

Schwartzentruber, D. J., Lawson, D. H., Richards, J. M., Conry, R. M., Miller, D. M., Treisman, J., . . . Hwu, P. (2011). gp100 peptide vaccine and interleukin-2 in patients with advanced melanoma. *N Engl J Med, 364*(22), 2119-2127. doi:10.1056/NEJMoa1012863

Seth, R. B., Sun, L., Ea, C. K., & Chen, Z. J. (2005). Identification and characterization of MAVS, a mitochondrial antiviral signaling protein that activates NF-kappaB and IRF 3. *Cell, 122*(5), 669-682. doi:10.1016/j.cell.2005.08.012

Shortman, K., & Heath, W. R. (2001). Immunity or tolerance? That is the question for dendritic cells. *Nat Immunol, 2*(11), 988-989. doi:10.1038/ni1101-988

Shu, X. S., Zhao, Y., Sun, Y., Zhong, L., Cheng, Y., Zhang, Y., . . . Ying, Y. (2017). PBRM1 restricts the basal activity of innate immune system through repressing RIG-I-like receptor signaling and is a potential prognostic biomarker for colon cancer. *J Pathol*. doi:10.1002/path.4986

Siegel, R. L., Miller, K. D., & Jemal, A. (2017). Cancer Statistics, 2017. *CA Cancer J Clin, 67*(1), 7-30. doi:10.3322/caac.21387

Simpson, T. R., Li, F., Montalvo-Ortiz, W., Sepulveda, M. A., Bergerhoff, K., Arce, F., . . . Quezada, S. A. (2013). Fc-dependent depletion of tumor-infiltrating regulatory T cells co-defines the efficacy of anti-CTLA-4 therapy against melanoma. *J Exp Med, 210*(9), 1695-1710. doi:10.1084/jem.20130579

Sivan, A., Corrales, L., Hubert, N., Williams, J. B., Aquino-Michaels, K., Earley, Z. M., . . . Gajewski, T. F. (2015). Commensal Bifidobacterium promotes antitumor immunity and facilitates anti-PD-L1 efficacy. *Science, 350*(6264), 1084-1089. doi:10.1126/science.aac4255

Snyder, A., Makarov, V., Merghoub, T., Yuan, J., Zaretsky, J. M., Desrichard, A., . . . Chan, T. A. (2014). Genetic basis for clinical response to CTLA-4 blockade in melanoma. *N Engl J Med, 371*(23), 2189-2199. doi:10.1056/NEJMoa1406498

Sobol, P. T., Boudreau, J. E., Stephenson, K., Wan, Y., Lichty, B. D., & Mossman, K. L. (2011). Adaptive antiviral immunity is a determinant of the therapeutic success of oncolytic virotherapy. *Mol Ther, 19*(2), 335-344. doi:10.1038/mt.2010.264

Spranger, S., Spaapen, R. M., Zha, Y., Williams, J., Meng, Y., Ha, T. T., & Gajewski, T. F. (2013). Up-regulation of PD-L1, IDO, and T(regs) in the melanoma tumor microenvironment is driven by CD8(+) T cells. *Sci Transl Med, 5*(200), 200ra116. doi:10.1126/scitranslmed.3006504

Stetson, D. B., & Medzhitov, R. (2006). Recognition of cytosolic DNA activates an IRF3-dependent innate immune response. *Immunity, 24*(1), 93-103. doi:10.1016/j.immuni.2005.12.003

Sun, L., Wang, H., Wang, Z., He, S., Chen, S., Liao, D., . . . Wang, X. (2012). Mixed lineage kinase domain-like protein mediates necrosis signaling downstream of RIP3 kinase. *Cell, 148*(1-2), 213-227. doi:10.1016/j.cell.2011.11.031

Sun, L., Wu, J., Du, F., Chen, X., & Chen, Z. J. (2013). Cyclic GMP-AMP synthase is a cytosolic DNA sensor that activates the type I interferon pathway. *Science, 339*(6121), 786-791. doi:10.1126/science.1232458

Suzuki, T., Oshiumi, H., Miyashita, M., Aly, H. H., Matsumoto, M., & Seya, T. (2013). Cell type-specific subcellular localization of phospho-TBK1 in response to cytoplasmic viral DNA. *PLoS One, 8*(12), e83639. doi:10.1371/journal.pone.0083639

Swann, J. B., & Smyth, M. J. (2007). Immune surveillance of tumors. *J Clin Invest, 117*(5), 1137-1146. doi:10.1172/JCI31405

Swann, J. B., Vesely, M. D., Silva, A., Sharkey, J., Akira, S., Schreiber, R. D., & Smyth, M. J. (2008). Demonstration of inflammation-induced cancer and cancer immunoediting during primary tumorigenesis. *Proc Natl Acad Sci U S A, 105*(2), 652-656. doi:10.1073/pnas.0708594105

Takashima, K., Takeda, Y., Oshiumi, H., Shime, H., Okabe, M., Ikawa, M., . . . Seya, T. (2016). STING in tumor and host cells cooperatively work for NK cell-mediated tumor growth retardation. *Biochem Biophys Res Commun, 478*(4), 1764-1771. doi:10.1016/j.bbrc.2016.09.021

Takeuchi, O., & Akira, S. (2007). [Pathogen recognition by innate immunity]. *Arerugi, 56*(6), 558-562.

Takeuchi, O., & Akira, S. (2010). Pattern recognition receptors and inflammation. *Cell, 140*(6), 805-820. doi:10.1016/j.cell.2010.01.022

Tanaka, Y., & Chen, Z. J. (2012). STING specifies IRF3 phosphorylation by TBK1 in the cytosolic DNA signaling pathway. *Sci Signal, 5*(214), ra20. doi:10.1126/scisignal.2002521

Tang, C. H., Zundell, J. A., Ranatunga, S., Lin, C., Nefedova, Y., Del Valle, J. R., & Hu, C. C. (2016). Agonist-Mediated Activation of STING Induces Apoptosis in Malignant B Cells. *Cancer Res, 76*(8), 2137-2152. doi:10.1158/0008-5472.CAN-15-1885

Tang, C. K., Aoshi, T., Jounai, N., Ito, J., Ohata, K., Kobiyama, K., . . . Ishii, K. J. (2013). The chemotherapeutic agent DMXAA as a unique IRF3-dependent type-2 vaccine adjuvant. *PLoS One, 8*(3), e60038. doi:10.1371/journal.pone.0060038

Taube, J. M., Anders, R. A., Young, G. D., Xu, H., Sharma, R., McMiller, T. L., . . . Chen, L. (2012). Colocalization of inflammatory response with B7-h1 expression in human melanocytic lesions supports an adaptive resistance mechanism of immune escape. *Sci Transl Med, 4*(127), 127ra137. doi:10.1126/scitranslmed.3003689

Terme, M., Ullrich, E., Aymeric, L., Meinhardt, K., Desbois, M., Delahaye, N., . . . Zitvogel, L. (2011). IL-18 induces PD-1-dependent immunosuppression in cancer. *Cancer Res, 71*(16), 5393-5399. doi:10.1158/0008-5472.CAN-11-0993

Thompson, M. R., Sharma, S., Atianand, M., Jensen, S. B., Carpenter, S., Knipe, D. M., . . . Kurt-Jones, E. A. (2014). Interferon gamma-inducible protein (IFI) 16 transcriptionally regulates type i interferons and other interferon-stimulated genes and controls the interferon response to both DNA and RNA viruses. *J Biol Chem, 289*(34), 23568-23581. doi:10.1074/jbc.M114.554147

Thompson, R. H., Gillett, M. D., Cheville, J. C., Lohse, C. M., Dong, H., Webster, W. S., . . . Kwon, E. D. (2004). Costimulatory B7-H1 in renal cell carcinoma patients: Indicator of tumor aggressiveness and potential therapeutic target. *Proc Natl Acad Sci U S A, 101*(49), 17174-17179. doi:10.1073/pnas.0406351101

Tumeh, P. C., Harview, C. L., Yearley, J. H., Shintaku, I. P., Taylor, E. J., Robert, L., . . . Ribas, A. (2014). PD-1 blockade induces responses by inhibiting adaptive immune resistance. *Nature, 515*(7528), 568-571. doi:10.1038/nature13954

Turnbull, S., West, E. J., Scott, K. J., Appleton, E., Melcher, A., & Ralph, C. (2015). Evidence for Oncolytic Virotherapy: Where Have We Got to and Where Are We Going? *Viruses, 7*(12), 6291-6312. doi:10.3390/v7122938

Ueha, S., Yokochi, S., Ishiwata, Y., Ogiwara, H., Chand, K., Nakajima, T., . . . Matsushima, K. (2015). Robust Antitumor Effects of Combined Anti-CD4-Depleting Antibody and Anti-PD-1/PD-L1 Immune Checkpoint Antibody Treatment in Mice. *Cancer Immunol Res, 3*(6), 631-640. doi:10.1158/2326-6066.CIR-14-0190

Van Allen, E. M., Miao, D., Schilling, B., Shukla, S. A., Blank, C., Zimmer, L., . . . Garraway, L. A. (2015). Genomic correlates of response to CTLA-4 blockade in metastatic melanoma. *Science, 350*(6257), 207-211. doi:10.1126/science.aad0095

van Elsas, A., Hurwitz, A. A., & Allison, J. P. (1999). Combination immunotherapy of B16 melanoma using anti-cytotoxic T lymphocyte-associated antigen 4 (CTLA-4) and granulocyte/macrophage colony-stimulating factor (GM-CSF)-producing vaccines induces rejection of subcutaneous and metastatic tumors accompanied by autoimmune depigmentation. *J Exp Med, 190*(3), 355-366.

van Loo, G., Saelens, X., Matthijssens, F., Schotte, P., Beyaert, R., Declercq, W., & Vandenabeele, P. (2002). Caspases are not localized in mitochondria during life or death. *Cell Death Differ, 9*(11), 1207-1211. doi:10.1038/sj.cdd.4401101

van Montfoort, N., Olagnier, D., & Hiscott, J. (2014). Unmasking immune sensing of retroviruses: interplay between innate sensors and host effectors. *Cytokine Growth Factor Rev, 25*(6), 657-668. doi:10.1016/j.cytogfr.2014.08.006

Vanpouille-Box, C., Pilones, K. A., Wennerberg, E., Formenti, S. C., & Demaria, S. (2015). In situ vaccination by radiotherapy to improve responses to anti-CTLA-4 treatment. *Vaccine, 33*(51), 7415-7422. doi:10.1016/j.vaccine.2015.05.105

Velu, V., Titanji, K., Zhu, B., Husain, S., Pladevega, A., Lai, L., . . . Amara, R. R. (2009). Enhancing SIV-specific immunity in vivo by PD-1 blockade. *Nature, 458*(7235), 206-210. doi:10.1038/nature07662

Vetizou, M., Pitt, J. M., Daillere, R., Lepage, P., Waldschmitt, N., Flament, C., . . . Zitvogel, L. (2015). Anticancer immunotherapy by CTLA-4 blockade relies on the gut microbiota. *Science, 350*(6264), 1079-1084. doi:10.1126/science.aad1329

Vignali, D. A., Collison, L. W., & Workman, C. J. (2008). How regulatory T cells work. *Nat Rev Immunol, 8*(7), 523-532. doi:10.1038/nri2343

Vivier, E., Raulet, D. H., Moretta, A., Caligiuri, M. A., Zitvogel, L., Lanier, L. L., . . . Ugolini, S. (2011). Innate or adaptive immunity? The example of natural killer cells. *Science, 331*(6013), 44-49. doi:10.1126/science.1198687

Wada, S., Jackson, C. M., Yoshimura, K., Yen, H. R., Getnet, D., Harris, T. J., . . . Drake, C. G. (2013). Sequencing CTLA-4 blockade with cell-based immunotherapy for prostate cancer. *J Transl Med, 11*, 89. doi:10.1186/1479-5876-11-89

Wang, H., Hu, S., Chen, X., Shi, H., Chen, C., Sun, L., & Chen, Z. J. (2017). cGAS is essential for the antitumor effect of immune checkpoint blockade. *Proc Natl Acad Sci U S A, 114*(7), 1637-1642. doi:10.1073/pnas.1621363114

Wang, J. H., Zhang, L., Ma, Y. W., Xiao, J., Zhang, Y., Liu, M., & Tang, H. (2016). microRNA-34a-Upregulated Retinoic Acid-Inducible Gene-I Promotes Apoptosis and Delays Cell Cycle Transition in Cervical Cancer Cells. *DNA Cell Biol, 35*(6), 267-279. doi:10.1089/dna.2015.3130

Weber, J., Mandala, M., Del Vecchio, M., Gogas, H. J., Arance, A. M., Cowey, C. L., . . . CheckMate, C. (2017). Adjuvant Nivolumab versus Ipilimumab in Resected Stage III or IV Melanoma. *N Engl J Med, 377*(19), 1824-1835. doi:10.1056/NEJMoa1709030

White, M. J., McArthur, K., Metcalf, D., Lane, R. M., Cambier, J. C., Herold, M. J., . . . Kile, B. T. (2014). Apoptotic caspases suppress mtDNA-induced STING-mediated type I IFN production. *Cell, 159*(7), 1549-1562. doi:10.1016/j.cell.2014.11.036

Woo, S. R., Fuertes, M. B., Corrales, L., Spranger, S., Furdyna, M. J., Leung, M. Y., . . . Gajewski, T. F. (2014). STING-dependent cytosolic DNA sensing mediates innate immune recognition of immunogenic tumors. *Immunity, 41*(5), 830-842. doi:10.1016/j.immuni.2014.10.017

Wu, X. N., Yang, Z. H., Wang, X. K., Zhang, Y., Wan, H., Song, Y., . . . Han, J. (2014). Distinct roles of RIP1-RIP3 hetero- and RIP3-RIP3 homo-interaction in mediating necroptosis. *Cell Death Differ, 21*(11), 1709-1720. doi:10.1038/cdd.2014.77

Yatim, N., Jusforgues-Saklani, H., Orozco, S., Schulz, O., Barreira da Silva, R., Reis e Sousa, C., . . . Albert, M. L. (2015). RIPK1 and NF-kappaB signaling in dying cells determines cross-priming of CD8(+) T cells. *Science, 350*(6258), 328-334. doi:10.1126/science.aad0395

Yoon, S., Kovalenko, A., Bogdanov, K., & Wallach, D. (2017). MLKL, the Protein that Mediates Necroptosis, Also Regulates Endosomal Trafficking and Extracellular Vesicle Generation. *Immunity, 47*(1), 51-65 e57. doi:10.1016/j.immuni.2017.06.001

Yoshinaga, S. K., Whoriskey, J. S., Khare, S. D., Sarmiento, U., Guo, J., Horan, T., . . . Senaldi, G. (1999). T-cell co-stimulation through B7RP-1 and ICOS. *Nature, 402*(6763), 827-832. doi:10.1038/45582

Yu, H. B., & Finlay, B. B. (2008). The caspase-1 inflammasome: a pilot of innate immune responses. *Cell Host Microbe, 4*(3), 198-208. doi:10.1016/j.chom.2008.08.007

Zamarin, D., Holmgaard, R. B., Subudhi, S. K., Park, J. S., Mansour, M., Palese, P., . . . Allison, J. P. (2014). Localized oncolytic virotherapy overcomes systemic tumor resistance to immune checkpoint blockade immunotherapy. *Sci Transl Med, 6*(226), 226ra232. doi:10.1126/scitranslmed.3008095

Zeng, M., Hu, Z., Shi, X., Li, X., Zhan, X., Li, X. D., . . . Beutler, B. (2014). MAVS, cGAS, and endogenous retroviruses in T-independent B cell responses. *Science, 346*(6216), 1486-1492. doi:10.1126/science.346.6216.1486

Zhao, L., Zhu, J., Zhou, H., Zhao, Z., Zou, Z., Liu, X., . . . Jin, M. (2015). Identification of cellular microRNA-136 as a dual regulator of RIG-I-mediated innate immunity that antagonizes H5N1 IAV replication in A549 cells. *Sci Rep, 5*, 14991. doi:10.1038/srep14991

Zhong, B., Yang, Y., Li, S., Wang, Y. Y., Li, Y., Diao, F., . . . Shu, H. B. (2008). The adaptor protein MITA links virus-sensing receptors to IRF3 transcription factor activation. *Immunity, 29*(4), 538-550. doi:10.1016/j.immuni.2008.09.003

Zhu, H., Xu, W. Y., Hu, Z., Zhang, H., Shen, Y., Lu, S., . . . Wang, Z. G. (2017). RNA virus receptor Rig-I monitors gut microbiota and inhibits colitis-associated colorectal cancer. *J Exp Clin Cancer Res, 36*(1), 2. doi:10.1186/s13046-016-0471-3

Zou, W., & Chen, L. (2008). Inhibitory B7-family molecules in the tumour microenvironment. *Nat Rev Immunol, 8*(6), 467-477. doi:10.1038/nri2326

6 Appendix

6.1 Abbreviations

A

ALH	AIM-2-like-helicase
ALK	Anaplastic lymphoma kinase
APC	Antigen-presenting cell
APC	Allophycocyanin
ASC	Apoptosis-associated speck protein
ATP	Adenosintriphosphat
Aza	5-acazytidine

B

B16.OVA	B16 melanoma cell line expressing OVA
Batf3	Basic Leucine Zipper ATF-Like Transcription Factor 3
Bcl-2	B-cell lymphoma 2
BSA	Bovine serum albumin

C

CARD9	Caspase-recruitment-domain-protein 9
Caspase	Cysteinyl-aspartate specific protease
CD	Cluster of differentiation
cDNA	Copy-desoxyribonucleic acid
cGAMP	Cyclic guanosine monophosphate–adenosine monophosphate
cGAS	Cyclic GMP-AMP synthase
CLR	C-type lectin receptor
CpG	Oligonucleotide with cytosine-(phosphate)-guanine motifs
CRISPR	Clustered regularly interspaced short palindromic repeats

CTL	Cytotoxic T lymphocyte
CTLA-4	Cytotoxic T-lymphocyte-associated antigen-4

D

DAMP	Danger-associated molecular pattern
DC	Dendritic cell
DMEM	Dulbecco's modified Eagle´s medium
DMSO	Dimethyl sulfoxide
DNA	Desoxyribonucleid acid
ds	Double-stranded
DTT	Dithiothreitol

E

EDTA	Ethylenediaminetetraacetic acid
EGFR	Epidermal growth factor receptor
ELISA	Enzyme-linked immunosorbent assay
ER	Endoplasmatic reticulum
ERV	Endogenous retroviral element

F

FACS	Fluorescent-activated cell sorting
FBS	Filtrated Bovine serum albumine
FCS	Fetal calf serum
FDA	Food and Drug Administration
FITC	Fluorescein isocyanate
Foxp3	Forkhead box p3
FSC	Forward scatter

G

GM-CSF	Granulocyte-macrophage colony stimulating factor
gp100	Glycoprotein 100

H

HMGB1	High-mobility group box 1
HRP	Horseradish peroxidase
HSV-1	Herpes simplex virus 1

I

ICD	Immunogenic cell death
ICOS	Inducible T-cell co-stimulator
IF	Interferon
IFNaR	Interferon-α receptor
IL	Interleukin
IRF	Interferon regulatory factor
ISD	Interferon Stimulatory DNA
ISG	IFN-stimulated gene

L

Lgp2	Laboratory of genetics and physiology 2
LPS	Lipopolysaccharid

M

MAVS	Mitochondrial Antiviral Signaling Protein
MDA-5	Melanoma differentiation-associated protein 5
MFI	mean fluorescence intensity
MHC	Major histocompatibility complex
miRNA	micro RNA

MLKL	Mixed lineage kinase domain like pseudokinase
mRNA	Messenger ribonucleic acid
MyD88	Myeloid differentiation primary response gene 88

N

nd	Not determined
NF-kB	Nuclear factor-κB
NK cell	Natural killer cell
NKG2D	Natural killer group 2D
NLR	NOD-like receptor
ns	Not significant

O

ORR	objective response rate

P

PAMP	pathogen-associated molecular pattern
PBS	Phosphate buffered saline
PCR	Polymerase chain reaction
PD-1	Programmed cell-death protein 1
PD-L	PD-1 ligand
PE	Phycoerythrin
PerCP	Peridinin chlorophyll protein
PRR	Pattern-recognition receptor

Q

qRT-PCR	Quantitative real-time PCR

R

RIG-I	retinoic acid inducible gene I

RIPK	Receptor-interacting serine/threonine-protein kinase
RLH	RIG-I like helicase
RNA	Ribonucleic acid
ROS	Reactive oxygen species
RPMI	Roswell Park Memorial Institute
RT	Room temperature
RTx	Radiotherapy

S

SDS-PAGE	Sulfate polyacrylamide gel electrophoresis
SEM	Standard error of the mean
sgRNA	Single guide RNA
ss	Single-stranded
STING	stimulator of interferon gene

T

TBK1	TANK-binding kinase 1
TCR	T cell receptor
TGF	Tumor growth factor
Th cell	T-helper cell
TIL	Tumor infiltrating lymphocyte
TIM-3	T-cell immunoglobulin and mucin-domain containing-3
TLR	Toll-like receptor
TME	Tumor microenvironment
TNF	Tumor necrosis factor
Treg cell	Regulatory T cell
TRIF	TIR-containing adapter inducing IFN-β
TRP-2	Tyrosinase-related protein 2
TUNEL	Terminal deoxynucleotidyl transferase dUTP nick end labeling

6.2 Publications

Submitted

Simon Heidegger[*], **Alexander Wintges***, Sarah Bek, Martina Schmickl, Katja Steiger, Julius C. Fischer, Paul-Albert Koenig, Diana Kreppel, Juergen Ruland, Marcel R.M. van den Brink, Christian Peschel, Tobias Haas[#] and Hendrik Poeck[#]

Tumor-intrinsic RIG-I signaling is required for anti-CTLA-4 checkpoint inhibitor-mediated anticancer immunity

Published

Tobias Haas, Simon Heidegger, **Alexander Wintges**, Michael Bscheider, Sarah Bek, Julius C. Fischer, Gabriel Eisenkolb, Martina Schmickl, Silvia Spörl, Christian Peschel, Hendrik Poeck, Jürgen Ruland.
Card9 controls Dectin-1-induced T-cell cytotoxicity and prevention of tumor growth

Eur J Immunol. 2017 May;47(5):872-879.

Julius C. Fischer, **Alexander Wintges**, Tobias Haas and Hendrik Poeck.
Assessment of mucosal integrity by quantifying neutrophil granulocyte influx in murine models of acute intestinal injury
Cell Immunol. 2017 Jun;316:70-76.

Julius C. Fischer, Michael Bscheider, Gabriel Eisenkolb, Chia-Ching Lin, **Alexander Wintges**, Vera Otten, Caroline Lindemans, Simon Heidegger, Martina Rudelius, Sébastien Monette, Kori A. Porosnicu Rodriguez, Marco Calafiore, Sophie Liebermann, Chen Liu, Stefan Lienenklaus, Siegfried Weiss, Ulrich Kalinke, Jürgen Ruland, Christian Peschel, Yusuke Shono, Melissa Docampo, Enrico Velardi, Robert Jenq, Alan M. Hanash, Jarrod A. Dudakov, Tobias Haas, Marcel R.M. van den Brink and Hendrik Poeck.
Cytosolic nucleic acid sensors promote intestinal epithelial integrity during acute tissue damage and protect from graft-versus-host disease
Sci Transl Med. 2017 Apr 19;9(386). pii: eaag2513.

In preparation

Alexander Wintges*, Diana Kreppel*, Michael Bscheider, Sarah Bek, Martina Schmickl, Julius C. Fischer, Theresa Frenz, Ulrich Kalinke, Veit R. Buchholz, Dirk H. Busch, Jürgen Ruland, Christian Peschel, Tobias Haas†, Simon Heidegger†,and Hendrik Poeck†

Therapeutic targeting of RIG-I synergizes with checkpoint blockade to enhance the efficacy of anticancer vaccines

Manuscript in preparation 2018

Sarah Bek, Florian Stritzke, **Alexander Wintges**, Martina Schmickl, Christian Peschel, Tobias Haas, Simon Heidegger# and Hendrik Poeck#

Tumor-intrinsic RIG-I signaling initiates T cell-based antitumor immunity via transfer of immunogenic nucleic acids within extracellular vesicles

Manuscript in preparation 2018

6.3 Acknowledgments

First and foremost, my deepest gratitude goes to my supervisors PD Dr. Hendrik Poeck and Dr. Tobias Haas for providing me with the opportunity to work on my PhD thesis in their lab and for giving me the chance to work on such a highly competitive as well as timely and relevant field of research.

I am very grateful to PD Dr. Simon Heidegger for sharing with me such an interesting research project and letting me participate in planning and implementation. His constant personal encouragement and scientific challenging were truly inspiring and served as a role model. Thank you for the inspiring scientific discussions and the pleasurable cooperation. I think we complemented each other quite well and I will always remember our trip to Canada. In addition, I want to thank my fellow doctoral students and co-workers in the lab for such a pleasant atmosphere both inside and outside the laboratory and especially their active support in times of need.

Furthermore, I want to thank my friend Andreas Roth for providing me with Hendriks mobile phone number and for encouraging me to apply for a PhD position that did not exist at that time.

Last but not least, I thank my family, especially my wife Laura. You were always at my side and supported me in every phase of my thesis, whether good or bad. Your encouragement is one of the reasons that I was able to complete this thesis. I love you!